
***National Nanotechnology Coordinated
Infrastructure (NNCI)***

Research and Education Highlights

Year 6 (October 2020 – September 2021)



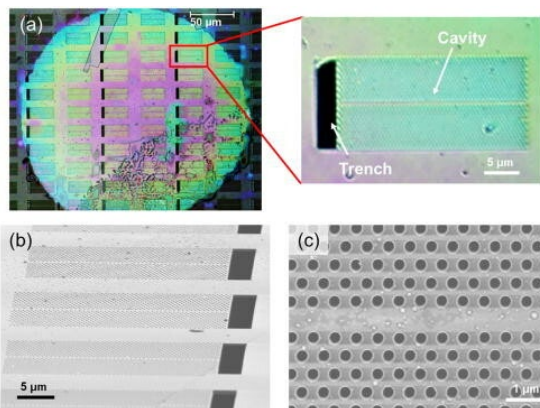
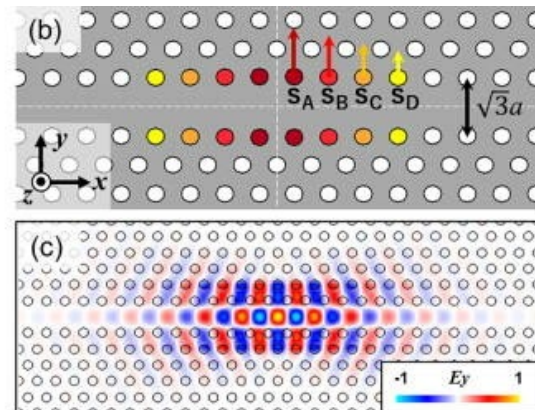
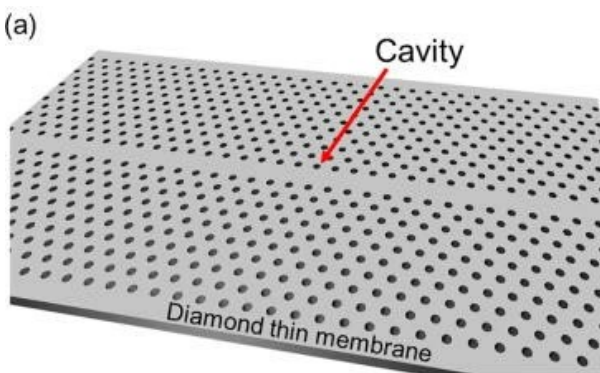
Table of Contents

Center for Nanoscale Systems (CNS)	3
Cornell Nanoscale Science and Engineering Facility (CNF)	9
Kentucky Multiscale	17
Mid-Atlantic Nanotechnology Hub (MANTH)	28
Midwest Nanotechnology Infrastructure Corridor (MiNIC)	35
Montana Nanotechnology Facility (MONT)	43
Nanotechnology Collaborative Infrastructure Southwest (NCI-SW)	54
Nebraska Nanoscale Facility (NNF)	66
NNCI Site @ Stanford (nano@stanford)	74
Northwest Nanotechnology Infrastructure (NNI)	78
Research Triangle Nanotechnology Network (RTNN)	97
San Diego Nanotechnology Infrastructure (SDNI)	104
Soft and Hybrid Nanotechnology Experimental (SHyNE) Resource	110
Southeastern Nanotechnology Infrastructure Corridor (SENIC)	122
Texas Nanofabrication Facility (TNF)	137
Virginia Tech National Center for Earth and Environmental Nanotechnology Infrastructure (NanoEarth)	143
Education and Outreach	148

Center for Nanoscale Systems (CNS)

Telecommunication-wavelength two-dimensional photonic crystal cavities in a thin single-crystal diamond membrane

The Loncar team demonstrated a two-dimensional photonic crystal cavities operating at telecommunication wavelengths in a single-crystal diamond membrane. We use a high-optical-quality and thin (similar to 300 nm) diamond membrane, supported by a polycrystalline diamond frame, to realize fully suspended two-dimensional photonic crystal cavities with a high theoretical quality factor of similar to 8×10^6 and a relatively small mode volume of similar to $2(\lambda/n)^3$. The cavities are fabricated in the membrane using electron-beam lithography and vertical dry etching. We observe cavity resonances over a wide wavelength range spanning the telecommunication O- and S-bands (1360-1470nm) with Q factors of up to 1800. This method paves the way for on-chip diamond nanophotonic applications in the telecommunication-wavelength range.



**New Materials/device
Processing developed
with Staff Support*

K. Kuruma, A.H. Piracha, D. Renaud, C. Chia, N. Sinclair, A. Nadarajah, A. Stacey, S. Prawer, M. Loncar, Harvard University. This work was performed at Harvard Center for Nanoscale Systems.

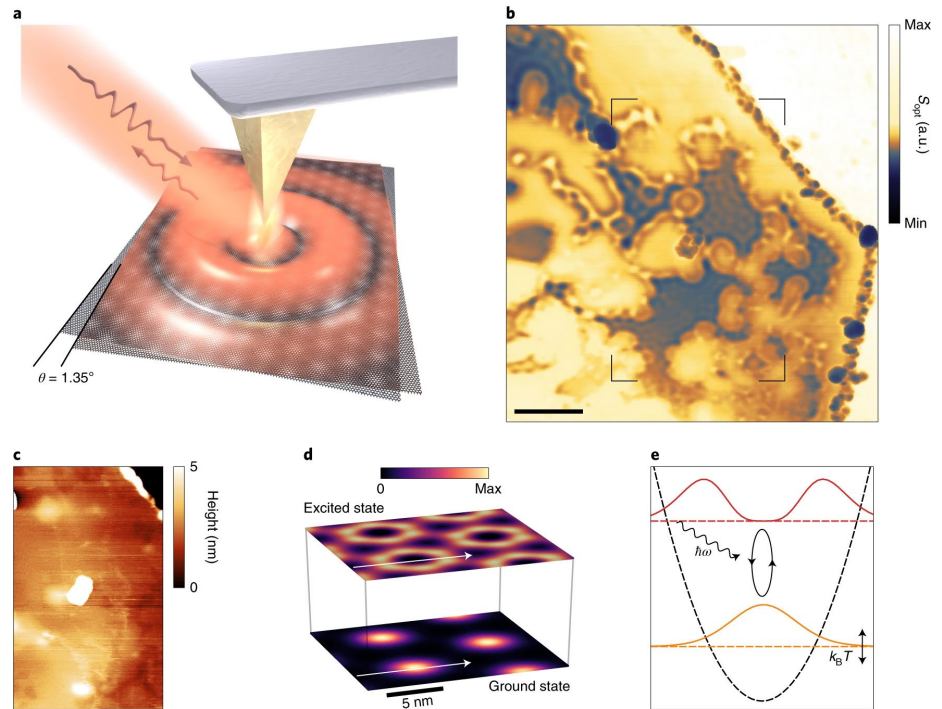
This work was supported by NSF RAISE TAQS (ECCS-1838976), NSF STC (DMR-1231319), NSF ERC (EEC-1941583). *Appl. Phys. Lett.* 119, 171106 (2021)

National Research Priority: NAE Grand Challenge—Engineer the Tools of Scientific Discovery

Observation of interband collective excitations in twisted bilayer graphene

Moire potentials substantially alter the electronic properties of twisted bilayer graphene at a magic twist angle. A propagating plasmon mode, which can be observed with optical nano-imaging, is associated with transitions between the moire minibands.

Here the team probes the collective excitations of TBG with a spatial resolution of 20nm, by applying mid-infrared near-field optical microscopy. They find a propagating plasmon mode in charge-neutral TBG for $\theta = 1.1$ - 1.7 degrees, which is different from the intraband plasmon in single-layer graphene. They interpret it as an interband plasmon associated with the optical transitions between minibands originating from the moire superlattice. The details of the plasmon dispersion are directly related to the motion of electrons in the moire superlattice and offer an insight into the physical properties of TBG, such as band nesting between the flat band and remote band, local interlayer coupling, and losses.



Hesp, Torre, Rodan-Legrain, Novelli Cao, Carr, Fang, Stepanov, Barcons-Ruiz, Herzig Sheinfux, Watanabe, Taniguchi, Efetov, Kaxiras, Jarillo-Herrero, Polini, Koppens, MIT. This work was performed at Harvard Center for Nanoscale Systems.

This work was supported by NSF (DMR-1809802), the Center for Integrated Quantum Materials under NSF (DMR-1231319). *Nature Phys.* 17, 1162–1168 (2021).

High-purity orbital angular momentum states from a visible metasurface laser

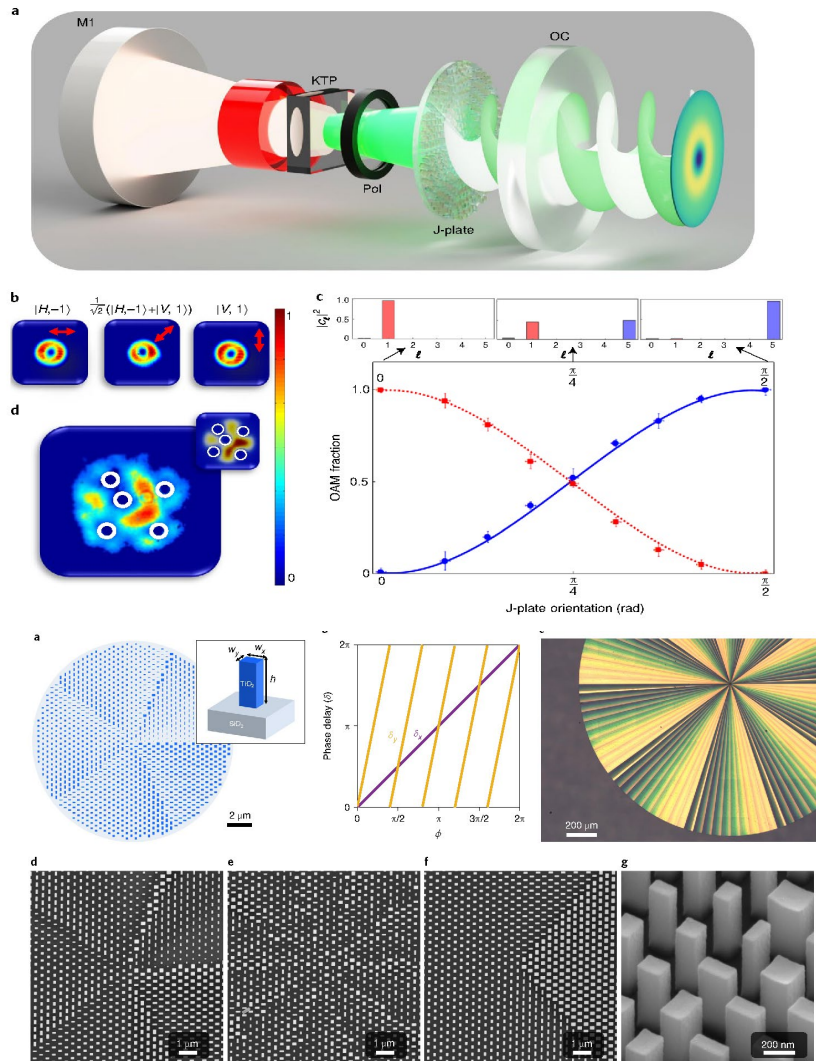
A metasurface laser generates orbital angular momentum states with quantum numbers reaching $l = 100$. Simultaneous output vortex beams, with Δl as great as 90, are demonstrated in the visible regime.

Demonstrated are new high-purity OAM states with quantum numbers reaching $l = 100$ and non-symmetric vector vortex beams that lase simultaneously on independent OAM states as much as $\Delta l = 90$ apart, an extreme violation of previous symmetric spin-orbit lasing devices. This laser conveniently outputs in the visible, producing new OAM states of light as well as all previously reported OAM modes from lasers, offering a compact and power-scalable source that harnesses intracavity structured matter for the configuration of arbitrary chiral states of structured light.

H. Sroor, Y.-W. Huang, B. Septho, D. Naido, A. Vallés, V. Ginis, C.-W. Qiu, A. Ambrosio, F. Capasso, & A. Forbes, Harvard. This work was performed at Harvard Center for Nanoscale Systems.

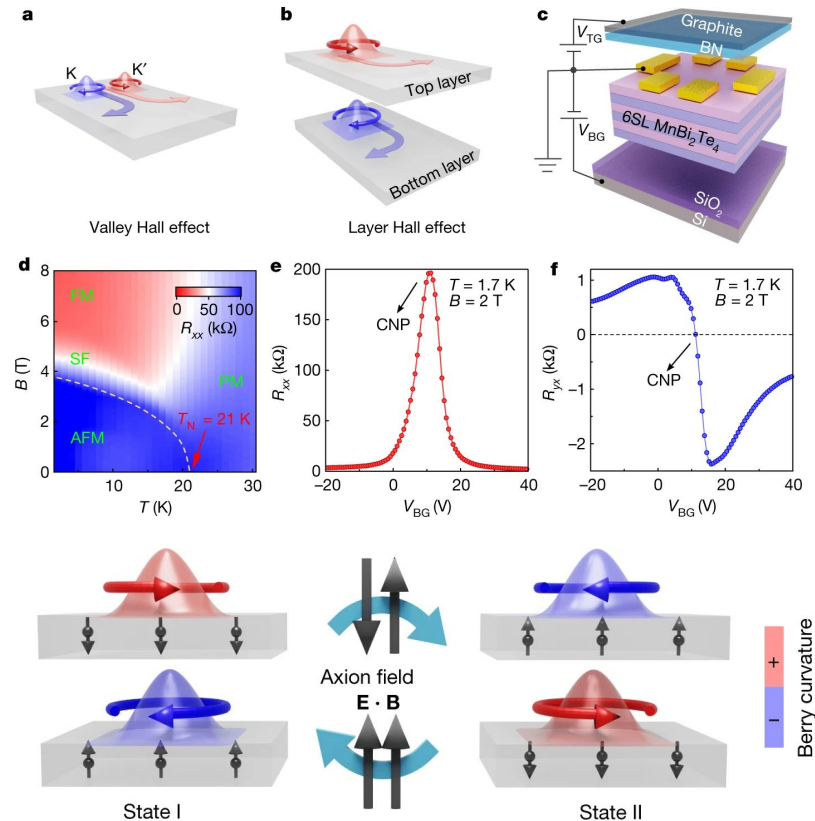
Supported by Air Force Office of Scientific Research (MURI: FA9550-14-1-0389, FA9550-16-1-0156). *Nature Photonics* 14, 498–503 (2020).

National Research Priority: NSF–Quantum Leap



Layer Hall effect in a 2D topological axion antiferromagnet

Ferromagnets have been known and used for millennia, antiferromagnets were only discovered in the 1930s. At large scale, because of the absence of global magnetization, antiferromagnets may seem to behave like any non-magnetic material. At the microscopic level, however, the opposite alignment of spins forms a rich internal structure. In topological antiferromagnets, this internal structure leads to the possibility that the property known as the Berry phase can acquire distinct spatial textures. Here we study this possibility in an antiferromagnetic axion insulator—even-layered, two-dimensional MnBi_2Te_4 in which spatial degrees of freedom correspond to different layers. Observed is a type of Hall effect—the layer Hall effect—in which electrons from the top and bottom layers spontaneously deflect in opposite directions. This layer Hall effect uncovers an unusual layer-locked Berry curvature, which serves to characterize the axion insulator state. Moreover, we find that the layer-locked Berry curvature can be manipulated by the axion field formed from the dot product of the electric and magnetic field vectors. These results offer new pathways to detect and manipulate the internal spatial structure of fully compensated topological antiferromagnets.



Gao, Liu, Hu, Qiu, Tzschaschel, Ghosh, Ho, Berube, Chen, Sun, Zhang, Zhang, Wang, Wang, Huang, Felser, Agarwal, Ding, Tien, Akey, Gardener, Singh, Watanabe, Taniguchi, Burch, Bell, Zhou, Gao, Lu, Bansil, Lin, Chang, Fu, Ma, Ni, Xu, Harvard Univ. This work was performed at Harvard Center for Nanoscale Systems.

Supported by Center for Integrated Quantum Materials, NSF (ECCS-2025158). *Nature* 595, 521–525 (2021).

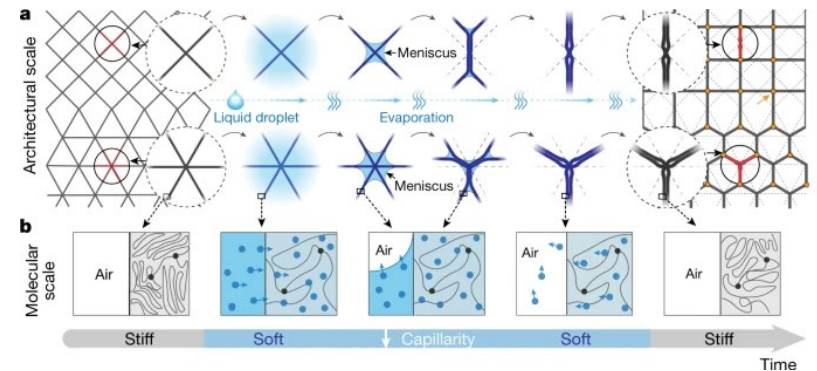
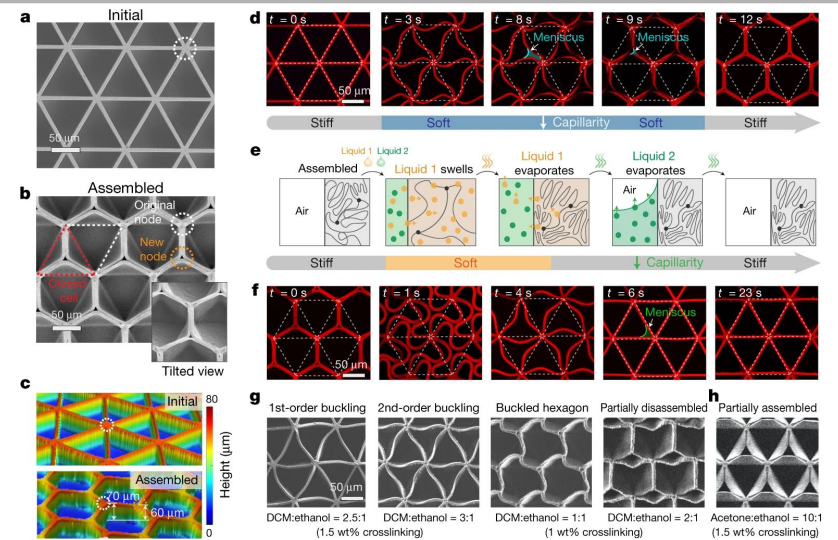
National Research Priority: NSF–Quantum Leap

Liquid-induced topological transformations of cellular microstructures

The fundamental topology of cellular structures—the location, number and connectivity of nodes and compartments—can profoundly affect their acoustic, electrical, chemical, mechanical and optical properties, as well as heat, fluid and particle transport. Achieving topological transformation presents a distinct challenge for existing strategies: it requires complex reorganization, repacking, and coordinated bending, stretching and folding, particularly around each node, where elastic resistance is highest owing to connectivity. Here we introduce a two-tiered dynamic strategy that achieves systematic reversible transformations of the fundamental topology of cellular microstructures, which can be applied to a wide range of materials and geometries.

Li, Deng, Grinthal, Schneider-Yamamura, Kang, Martens, Zhang, Li, Yu, Bertoldi, Aizenberg, Harvard University. This work was performed at Harvard Center for Nanoscale Systems.

This work was supported by NSF Designing Materials to Revolutionize and Engineer our Future (DMR-1922321) and the Harvard University MRSEC (DMR-2011754). *Nature* 592, 386–391 (2021).

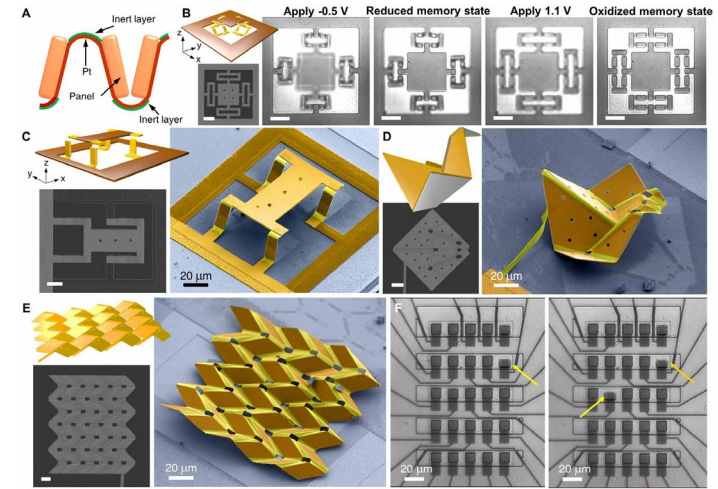


National Research Priority: NAE Grand Challenge—Engineer the Tools of Scientific Discovery

Cornell Nanoscale Science and Engineering Facility (CNF)

Micrometer-sized Electrically Programmable Shape-memory Actuators For Low-power Microrobotics

In *Science Robotics*, Cohen (Cornell), Miskin (UPenn) and collaborators (Cornell) used the CNF to fabricate origami-inspired shape-memory actuators that allow machines ranging from robots to medical implants to hold their form without continuous power. Here, they report a new class of fast, high-curvature, low-voltage, reconfigurable, micrometer-scale shape-memory actuators. They function by the electrochemical oxidation/reduction of a platinum surface, creating a strain in the oxidized layer that causes bending. They bend to the smallest radius of curvature of any electrically controlled microactuator (~500 nanometers), are fast (<100-millisecond operation), and operate inside the electrochemical window of water, avoiding bubble generation associated with oxygen evolution. These shape-memory actuators can be used to create basic electrically reconfigurable microscale robot elements including actuating surfaces, origami-based three-dimensional shapes, morphing metamaterials, and mechanical memory elements.

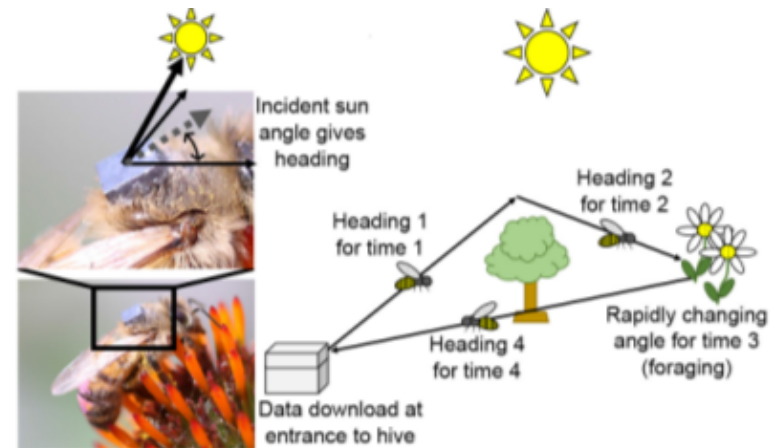


Qingkun Liu, Wei Wang, Michael F. Reynolds, Michael C. Cao, Marc Z. Miskin, Tomas A. Arias, David A. Muller, Paul L. McEuen, Itai Cohen. This work was performed in part at Cornell Nanoscale Science and Technology Facility.

This work was supported by ARO (W911NF-18-1-0032), NSF (EFMA-1935252), Cornell Center for Materials Research (DMR-171987 5), AFOSR (MURI: FA9550-16-1-0031), and Kavli Institute at Cornell for Nanoscale Science. *Sci. Robot.* **6**, eabe6663 (2021)

An Autonomous, Optically-Powered, Direct-to-Digital Sun-Angle Recorder for Honey Bee Flight Tracking

In *IEEE Transactions*, Palmer and Molnar (Cornell) used the CNF to fabricate an autonomous sensor for insect flight tracking that captures and stores solar angle-of-incidence without the use of a conventional ADC. The chip uses pairs of Angle-Sensitive Pixels as differential 1-bit ADCs; an array of these sensors provides a many-bit encoding of angle-of-incidence. Digitization occurs immediately within the pixel by use of a novel in-pixel comparator, thus enabling ultra-low-power, direct-to-digital capture of angle-of-incidence. These measurements are stored in an on-chip memory throughout the flight and uploaded to a base station at the end of the flight. The system is powered by on-chip photovoltaics. The chip is envisioned as a flight recorder to be mounted on honeybees to track their trajectories. Bee flights were emulated by carrying the chip along a 226 m outdoor trajectory, which emulates a small sample of tagged bees visiting known feeding sites and returning to their hive, the average reconstructed final position is 9.6 m away from the the true final position, an error less than 5% of the total trajectory length.

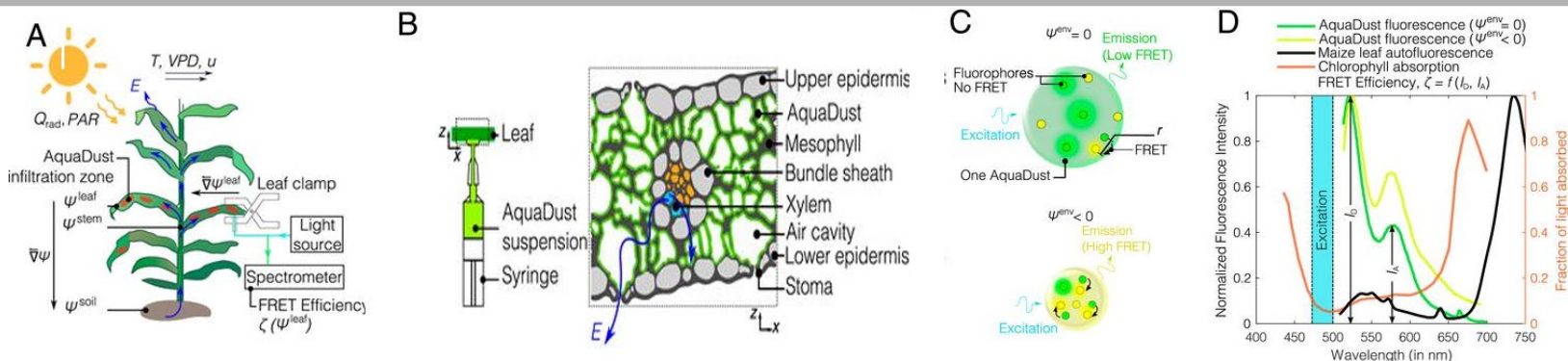


Daniel M. Palmer and Alyosha C. Molnar. This work was performed, in part, at Cornell NanoScale Facility.

IEEE TRANSACTIONS ON CIRCUITS AND SYSTEMS—II: EXPRESS BRIEFS, VOL. 68, NO. 5, MAY 2021

National Research Priority: Food Security

A Minimally Disruptive Method For Measuring Water Potential In Plants Using Hydrogel Nano-reporters



In PNAS, Gore (Florapulse), Stroock (Cornell) and colleagues used the Cornell Nanoscale Facility to produce nanoscale water potential sensors. Leaf water potential is a critical indicator of plant water status, integrating soil moisture status, plant physiology, and environmental conditions. There are few tools for measuring water potential *in situ*, presenting a critical barrier for developing appropriate phenotyping (measurement) methods for crop development and modeling efforts aimed at understanding water transport in plants. Here, they present the development of an *in situ*, minimally disruptive hydrogel nanoreporter (AquaDust) for measuring leaf water potential. The gel matrix responds to changes in water potential in its local environment by swelling; the distance between covalently linked dyes changes with the reconfiguration of the polymer, leading to changes in the emission spectrum via Förster Resonance Energy Transfer (FRET). Upon infiltration into leaves, the nanoparticles localize within the apoplastic space in the mesophyll; they do not enter the cytoplasm or the xylem. They conclude that AquaDust offers potential opportunities for high-throughput field measurements and spatially resolved studies of water relations within plant tissues

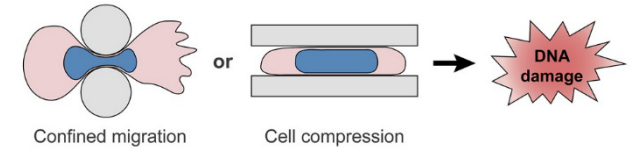
P. Jaina, W. Liub, S. Zhu, C. Yao-Yun Chang, J. Melkonian, F. E. Rockwell, D. Pauli, Y. Sun, W. R. Zipfel, N. Michele Holbrook, S. Jean Rihag, M. A. Gore and A. D. Stroock. Work performed, in part, at Cornell NanoScale Facility.

This work was supported by USDA National Institute of Food and Agriculture 2017-67007-25950; and AFOSR FA9550-18-1-0345. PNAS 2021 118(23) 1-9, e2008276118

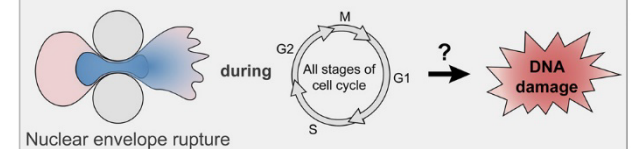
Nuclear Deformation Causes DNA Damage by Increasing Replication Stress

Lammerding (Cornell) and colleagues used to use CNF to fabricate microscale structures for the study of cancer progression. Cancer metastasis, i.e., the spreading from the primary tumor to distant organs, is responsible for the vast majority of cancer deaths. In the process, cancer cells migrate through narrow interstitial spaces substantially smaller in cross-section than the cell. During such confined migration, cancer cells experience extensive nuclear deformation, nuclear envelope rupture, and DNA damage. The molecular mechanisms responsible for the confined migration-induced DNA damage remain incompletely understood. Nuclear deformation, resulting from either confined migration or external cell compression, increases replication stress, possibly by increasing replication fork stalling, providing a molecular mechanism for the deformation-induced DNA damage. Thus, they have uncovered a new mechanism for mechanically induced DNA damage, linking mechanical deformation of the nucleus to DNA replication stress. This mechanically induced DNA damage could not only increase genomic instability in metastasizing cancer cells but could also cause DNA damage in non-migrating cells and tissues that experience mechanical compression during development, thereby contributing to tumorigenesis and DNA damage response activation.

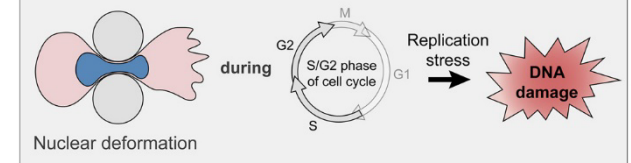
Mechanical stress on the nucleus causes DNA damage



Nuclear envelope rupture-associated DNA damage



Nuclear deformation-associated DNA damage



Pragya Shah, Chad M. Hobson, Svea Cheng, Marshall Colville, Matthew Paszek, Richard Superfine, Jan Lammerding, This work was performed, in part, at Cornell NanoScale Facility.

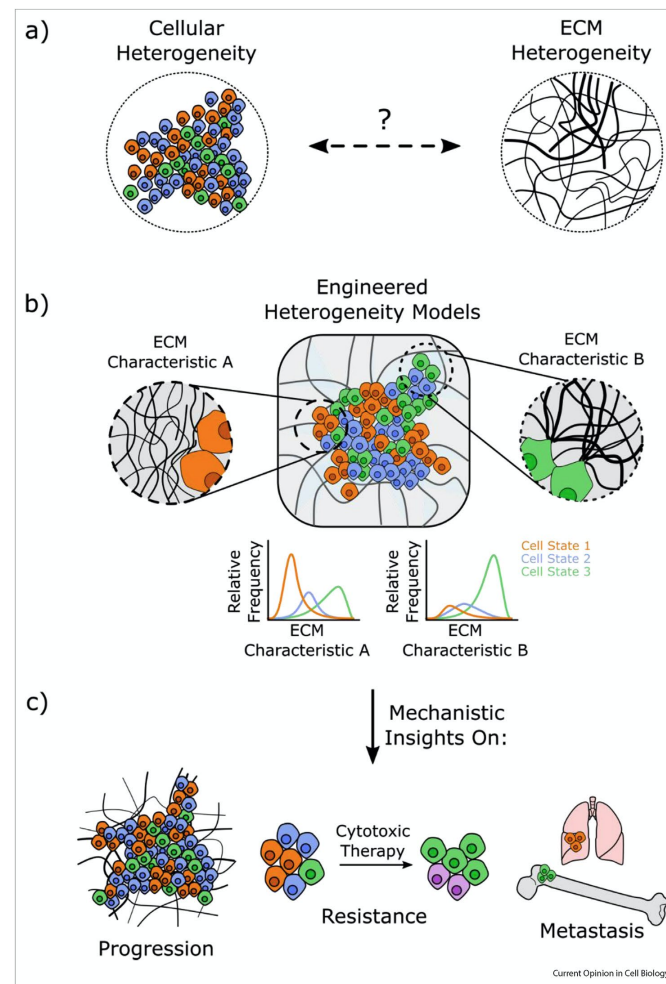
This work was supported by NIH R01 HL082792, R01 GM137605, U54 CA210184, and U54 CA193461. *Current Biology*, 31(4), 2021, 753-765.e6.

Engineered ECM Models: Opportunities to Advance Understanding of Tumor Heterogeneity

Shimpi and Fischbach (Cornell) used the Cornell NanoScale Facility to study the extracellular matrix (ECM). Intratumoral heterogeneity is a negative prognostic factor for cancer and commonly attributed to microenvironment-driven genetic mutations and/or the emergence of cancer stem-like cells. How aberrant ECM remodeling regulates the phenotypic diversity of tumor cells, however, remains poorly understood due in part to a lack of model systems that allow isolating the physicochemical heterogeneity of malignancy-associated ECM for mechanistic studies. Here, they review the compositional, microarchitectural, and mechanical hallmarks of cancer-associated ECM and highlight biomaterials and engineering approaches to recapitulate these properties for *in vitro* and *in vivo* studies. Subsequently, they describe how such engineered platforms may be explored to define the spatiotemporal dynamics through which cancer-associated ECM remodeling regulates intratumoral heterogeneity and the cancer stem-like cell phenotype. Finally, they highlight future opportunities and technological advances to further elucidate the relationship between tumor-associated ECM dynamics and intratumoral heterogeneity.

A.A. Shimpi and C. Fischbach, This work was performed, in part, at Cornell NanoScale Facility.

Supported by the NCI Center on the Physics of Cancer Metabolism (1U54CA210184-01) and NSF Graduate Research Fellowship (DGE-1650441). *Current Opinion in Cell Biology* 2021, 72:1–9



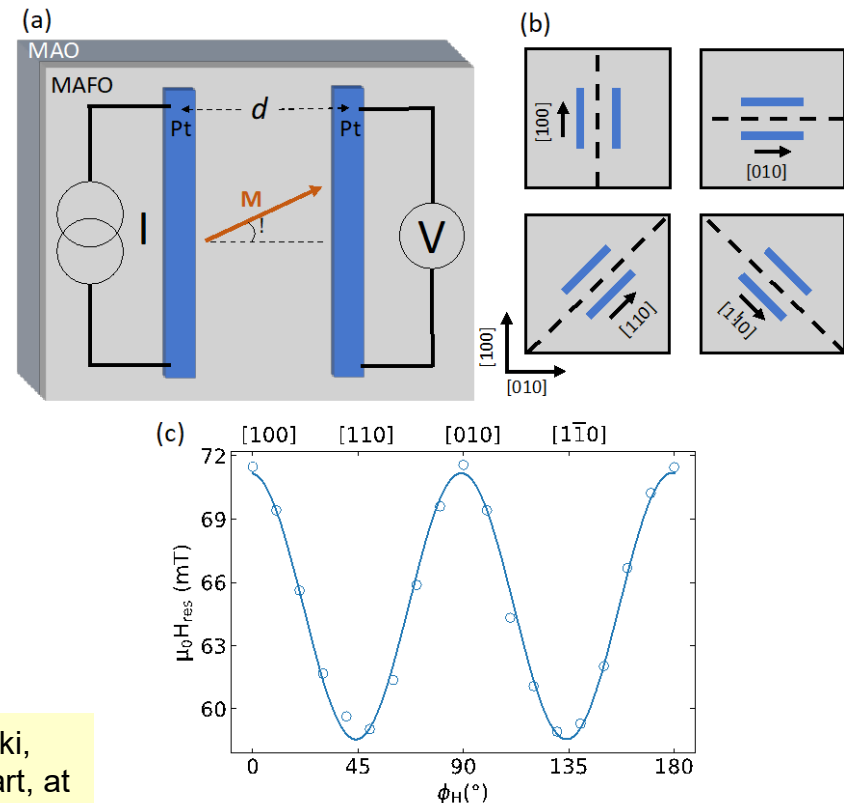
National Research Priority: NSF–Understanding the Rules of Life

Anisotropic Magnon Spin Transport In Ultra-thin Spinel Ferrite Thin Films – Evidence For Anisotropy In Exchange Stiffness

Ralph (Cornell) and colleagues at Stanford and Tsinghua used the Cornell NanoScale Facility to produce devices to enable study of spin transport. Here they report measurements of magnon spin transport in a spinel ferrite, magnesium aluminum ferrite $\text{MgAl}_{0.5}\text{Fe}_{1.5}\text{O}_4$ (MAFO), which has a substantial in-plane four-fold magnetic anisotropy. They observe spin diffusion lengths $> 0.8 \mu\text{m}$ at room temperature in 6 nm films, with spin diffusion length 30% longer along the easy axes compared to the hard axes. The sign of this difference is opposite to the effects just of anisotropy in the magnetic energy for a uniform magnetic state. They suggest instead that accounting for anisotropy in exchange stiffness is necessary to explain these results.

Ruofan Li, Peng Li, Di Yi, Lauren Riddiford, Yahong Chai, Yuri Suzuki, Daniel C. Ralph and Tianxiang Nan. This work was performed, in part, at Cornell NanoScale Facility.

Research at Cornell was supported by the Cornell Center for Materials Research NSF MRSEC program (DMR-1719875). *arXiv:2105.13943v1*



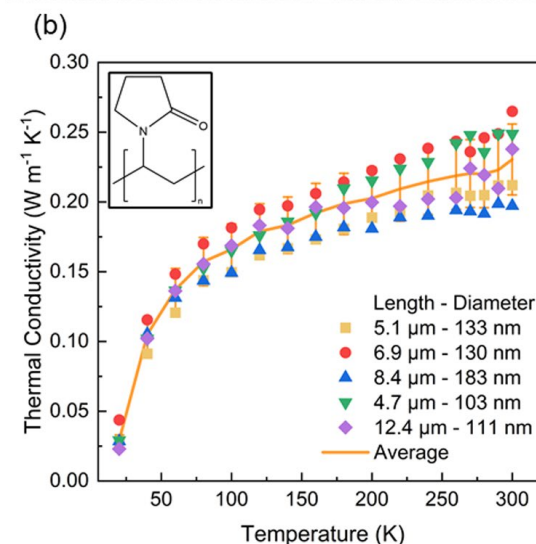
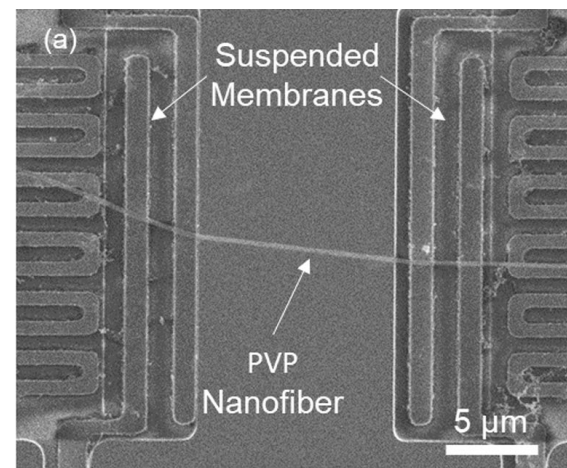
National Research Priority: NSF–Quantum Leap

Contact Thermal Resistance between Silver Nanowires with Poly(vinylpyrrolidone) Interlayers

Li and colleagues (Vanderbilt, NASA) used the Cornell NanoScale Facility to fabricate nanofiber test structures for measuring thermal transport. Various nanofillers have been adopted to enhance the thermal conductivity of polymer nanocomposites. While it is widely believed that the contact thermal resistance between adjacent nanofillers can play an important role in limiting thermal conductivity enhancement of composite materials, lack of direct experimental data poses a significant challenge to perceiving the effects of these contacts. This study reports on direct measurements of thermal transport through contacts between silver nanowires (AgNWs) with a poly(vinylpyrrolidone) (PVP) interlayer. The results indicate that a PVP layer as thin as 4 nm can increase the total thermal resistance of the contact by up to an order of magnitude, when compared to bare AgNWs, even with a larger contact area. On the other hand, the thermal boundary resistance for PVP/silver interfaces could be significantly lower than that between polymer-carbon nanotubes (CNTs). Analyses based on these understandings further show why AgNWs could be more effective nanofillers than CNTs

Matthew L. Fitzgerald, Yang Zhao, Zhiliang Pan, Lin Yang, Shihong Lin, Godfrey Sauti, and Deyu Li. This work was performed, in part, at Cornell NanoScale Facility.

Work supported by NSF (1903645 and 1532107) and NASA Fellowship (NSTRF18_80NSSC18K1165). *Nano Lett.* 2021, 21, 4388–4393



National Research Priority: NAE Grand Challenge—Engineer the Tools of Scientific Discovery

National Nanotechnology
Coordinated Infrastructure

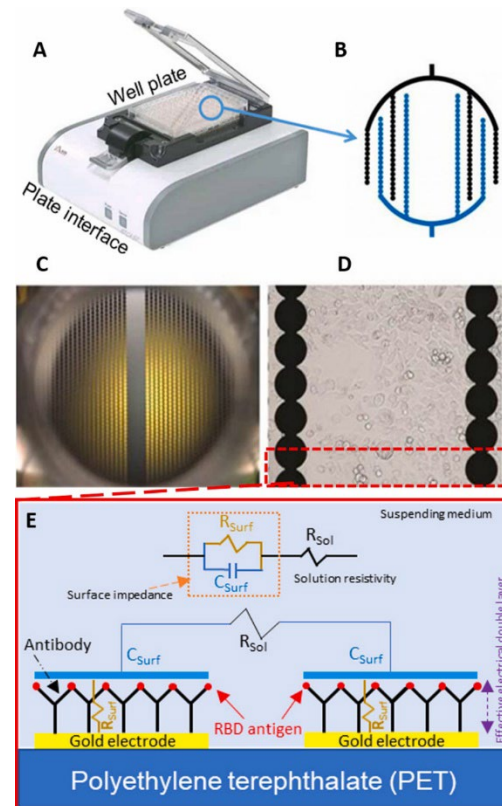


Kentucky Multi-Scale Manufacturing and Nano Integration Node (KY Multiscale)

Rapid Detection of SARS-CoV-2 Antibodies Via Impedance Spectroscopy

Coronavirus disease (COVID-19) caused by severe acute respiratory syndrome coronavirus 2 (SARS-CoV-2) is a worldwide pandemic that has caused over 5 million deaths worldwide and significant hardships. Accurate and scalable point-of-care devices would increase screening, diagnosis, and monitoring of COVID-19 patients. Here, we demonstrate rapid label-free electrochemical detection of SARS-CoV-2 antibodies using a commercially available impedance sensing platform. A 16-well plate containing sensing electrodes was pre-coated with receptor binding domain of SARS-CoV-2 spike protein. The platform was able to differentiate spikes in impedance measurements from a negative control for all anti-SARS-CoV-2 monoclonal antibody CR3022 samples. Measured impedance values were consistent when compared to standard ELISA test results. This platform provides a simplified and familiar testing interface that can be readily adaptable for use in clinical settings.

(A) Image of ACEA Bioscience's 96-well platform with a (B) schematic of the electrode layout. (C) Actual image of the electrodes themselves within the well and a (D) magnified image of the electrodes. Images A–D are modified from ACEA Bioscience. (E) Schematic of electrical impedance equivalent circuit model of the protein/antibody in solution



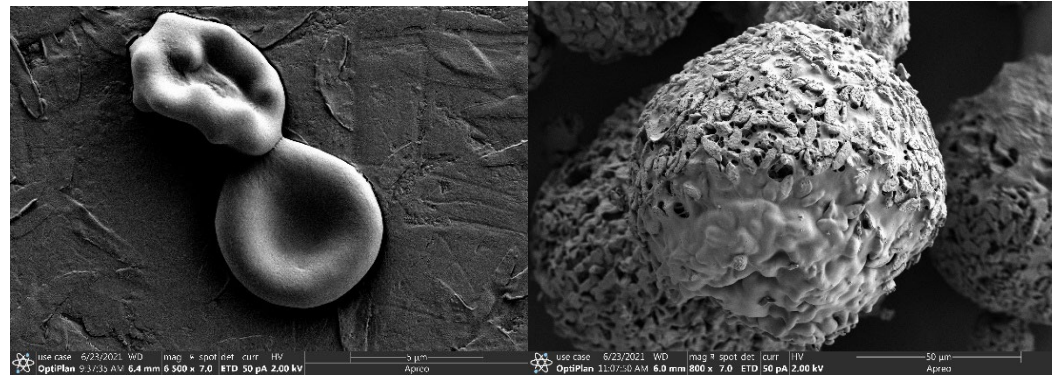
Stuart J. Williams (Department of Mechanical Engineering) and Jonathan Kopechek (Bioengineering Department), University of Louisville. Work was performed at the University of Louisville MicroNanoTechnology Center (MNTC).

Biosensors and Bioelectronics, **171**, 112709 (2021)

National Research Priority: NSF–Understanding the Rules of Life

Dry Preservation of Red Blood Cells for Long-Term Storage at Ambient Temperature

There is currently no method that is safe and cost-effective enough for routine long-term preservation of red blood cells (RBCs). This work focuses on using a preservative sugar (trehalose) to protect RBCs during freeze-drying and enable storage as a dried powder at ambient temperatures for long periods of time. We conducted SEM imaging of freeze-dried RBCs and confirmed the presence of protective trehalose on RBCs. This approach could help solve the blood supply challenges that frequently occur and may also enable transfusions in remote locations.



SEM images of red blood cells (RBCs). Left image: RBCs prior to freeze-drying. Right image: Freeze-dried RBCs coated with protective sugar (trehalose).

Brett Janis, Charles Elder, Michael Menze, and Jonathan Kopechek, University of Louisville. Work performed at the University of Louisville Huson Imaging & Characterization Laboratory.

DoD CDMRP #190149. *Cryobiology*, 98:73-79 (2021).

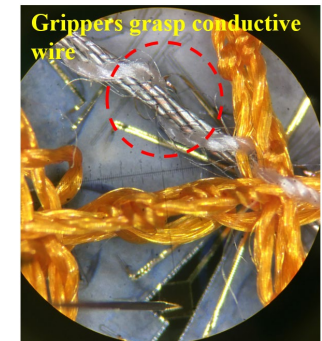
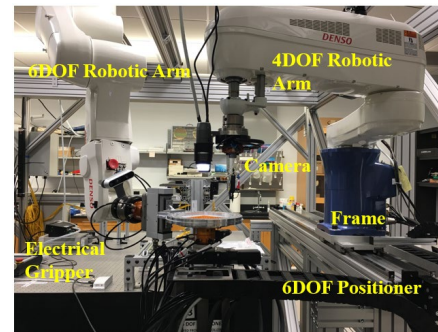
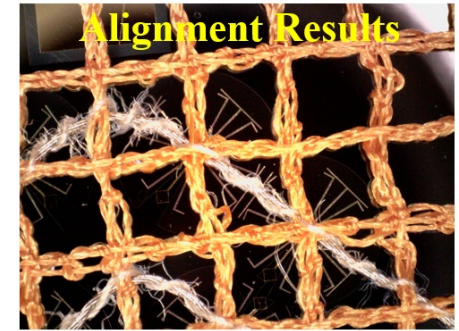
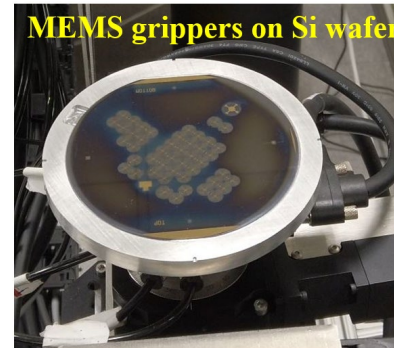
National Research Priority: NSF–Understanding the Rules of Life

E-Textile Manufacturing with MEMS

Fabrication and Multi-Robot Collaboration

This work investigates manufacturing processes for electronic textiles (E-textiles) with MEMS grippers fabricated in the cleanroom and multi-robot collaboration within the NeXus for alignment with of grippers and fabric. The NeXus is a custom additive manufacturing system developed at UofL.

MEMS grippers are designed and positioned by using an image process algorithm according to the intersections' position of fabric structures, then fabricated and released in the cleanroom. Two industrial robotic arms and one custom positioner along with different tools, such as electrical gripper, adhesive dispenser, and microscope camera, are employed to accomplish the alignment and attachment process of gripper and fabric. process of the MEMS grippers and fabric structures in NeXus.



E-textiles manufacturing process

Danming Wei, Sushmita Challa, Shafquatul Islam, Cindy Harnett, and Dan Popa. Work performed at University of Louisville Micro/Nano Technology Center (MNTC) and Louisville Automation and Robotics Research Institute (LARRI).

Supported by NSF MRI#1828355, EPSCOR#1849213 and # ECCS-2025075.

National Research Priority: NSF–Future of Work at the Human–Technology Frontier

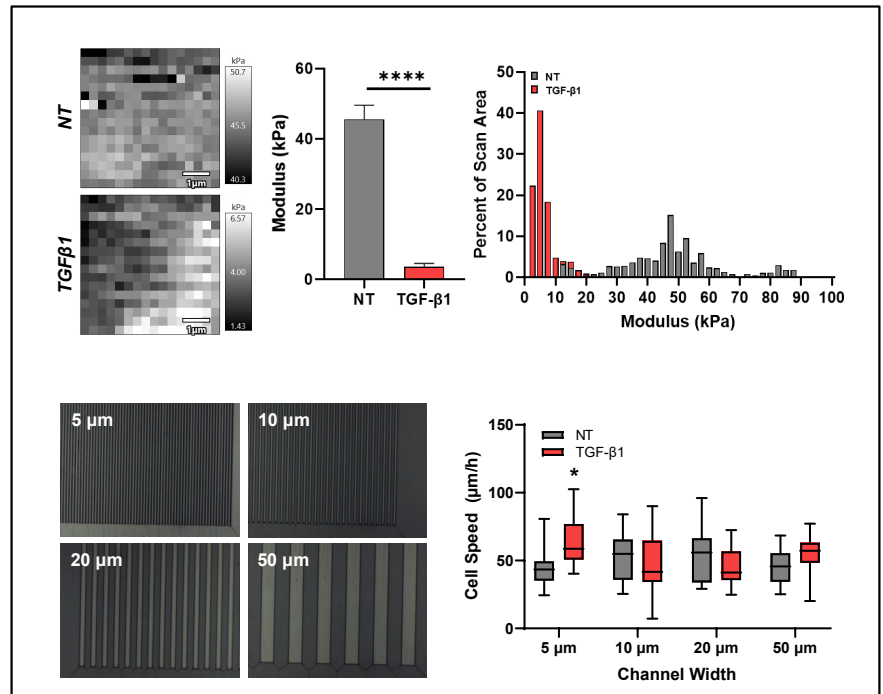
Examination of Cancer Cell MechanoType via Biophysical Tools and Microfabrication

Rapid cancer cell invasion is a hallmark of aggressive cancer and correlates with poor prognosis. Efficient cancer spread requires cells to navigate tight confined microenvironments that force them to squeeze through sub-micron pores and deform along vascular tracts. These phenomenon point to changes to cell mechanical properties; however, these aspects of cell invasion are poorly understood. We employed biophysical tools and biomaterial platforms to examine the cell mechanical phenotype or “mechanotype”. Using AFM force mapping, we determined that aggressive cohorts were mechanically softer. Further, using microchannel platforms of varying widths, we showed that softer cells are functionally more invasive under tight constriction. These findings offer new perspectives towards the rules of cancer invasion and may provide new routes of mechanics focused therapies for limiting cancer spread.

Joseph Chen, Department of Bioengineering, University of Louisville. Work was performed at University of Louisville MicroNano Technology Center (MNTC).

BMES 2021, Orlando, FL

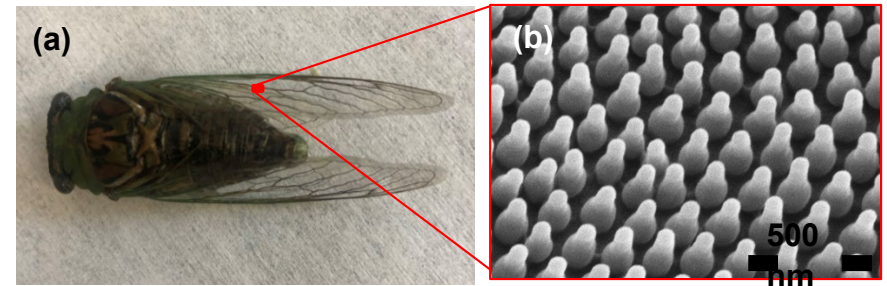
National Research Priority: NSF–Understanding the Rules of Life



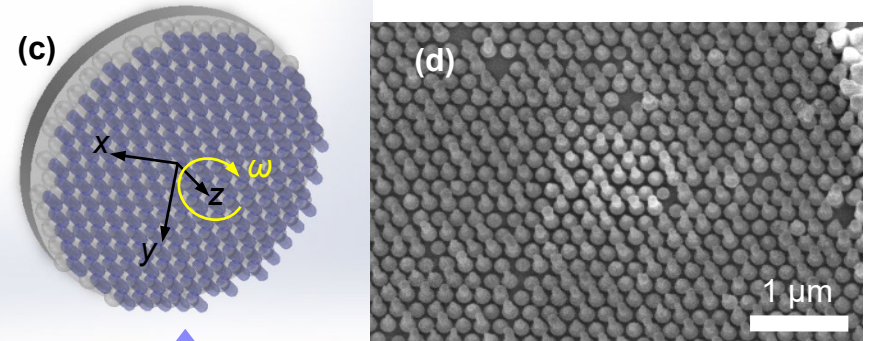
Cancer cell aggressiveness correlates with mechanoType. AFM force mapping reveals that more aggressive cancer (TGF-β1) is associated with reduced cellular stiffness (A,B,C), which enables rapid migration under tight constriction (5 μm) as revealed through microfabrication platforms (D,E).

Bio-Inspired Antibacterial Metasurfaces Fabricated by Glancing Angle Deposition (GLAD)

The goal of this research is to propose an easy and cost-effective fabrication approach of Glancing Angle Deposition (GLAD) for creating antibacterial surfaces, which are inspired by cicada wings. Antibacterial surfaces are known to be applied in a variety of specific interfaces, such as medical implants and food packaging. Nanopillar cones semi-hexagonally distributed on the cicada wings with ~ 170 nm between the neighboring pillars (Fig. b). The nanopillar cones puncture into bio cells falling on top and keep the surface bacteria free. Given the nano-level three-dimensional features, it is extremely difficult to replicate these naturally occurred nanostructure using conventional top-down nanofabrication processes. GLAD is versatile bottom-up process which uses physical vapor deposition while maneuvering with incident angle and rotation of the substrate, and the cicada wing replica surfaces are created by GLAD (Fig. d). Gram negative bacteria (E Coli) are applied on top of the surface for antibacterial testing. The preliminary results show the effectiveness of the antibacterial property of our synthetic nanostructured film.



(a) Annual cicada (also known as dog-day cicada) (b) SEM image of the nanostructures on the wings of annual cicadas



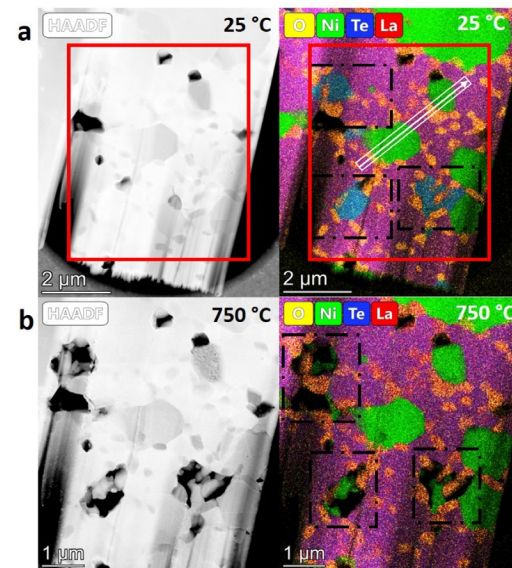
(c) GLAD scheme for nanopillar cone structures on cicada wings (d) SEM image of the nanopillar cones created by GLAD

Qu, C., Rozsa J., Jung, H J., Running, M., McNamara, S., and Walsh, K. Research was performed at the University of Louisville MicroNanoTechnology Center (MNTC).

This work was supported by NSF NNCI Award 2025075.

Structure and Stability of Thermoelectric $\text{La}_{3-x}\text{Te}_4\text{-Ni}$ Composites

Thermoelectric materials convert thermal to electrical energy. Lanthanum telluride is a high performance thermoelectric material that is well suited for use in radioisotope thermoelectric generators (RTG) powering long duration space missions. Introduction of nickel nanoparticles into lanthanum telluride systems can increase their figure of merit by 30%, but the characteristics and stability of the $\text{La}_{3-x}\text{Te}_4\text{-Ni}$ interfaces are not well understood. This research effort used *in situ* transmission electron microscopy techniques to mimic the working environment of an RTG in deep space while studying of the smallest structural details of the $\text{La}_{3-x}\text{Te}_4\text{-Ni}$ interfaces. The results of this study provide design guidance for next-generation thermoelectric materials with the potential for longer life span in RTG applications.



***In situ* TEM study of a partially oxidized $\text{La}_{3-x}\text{Te}_4\text{-Ni}$ sample.** (a, b) Micrographs and elemental maps collected at 25 and 750 °C, respectively. The interfaces in oxidized areas (dashed squares) have degraded while nonoxidized areas (green) remained intact.

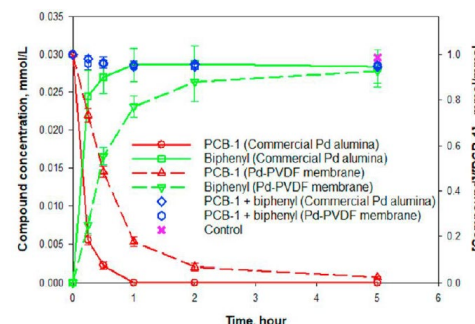
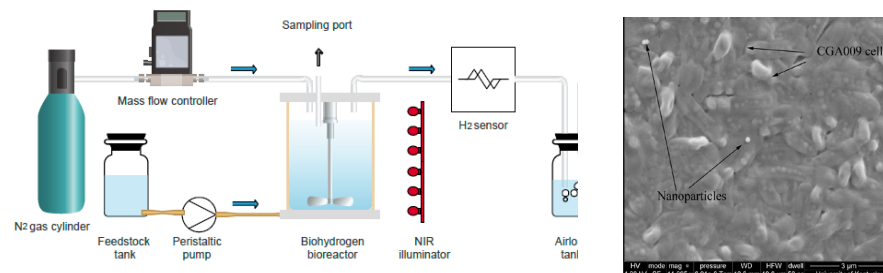
A collaboration between the Univ. of Kentucky and JPL/Caltech led by Prof. Beth Guiton (UK Chemistry). Work was performed at KY Multiscale EMC.

Work was supported by DMR 1455154Y, OIA 1355438, NN15AK28A. Scialog Award 26329. *J. Phys. Chem. C* 125, 21131 (2021).

National Research Priority: NSF–Growing Convergence Research and Windows on the Universe

Nanoparticle Enhanced Biohydrogen Production and Pollutant Hydrogenation

A photoinduced fermentation process using *Rhodopseudomonas palustris* provides an alternative to traditional hydrogen production. In this study, biohydrogen production was investigated in the near IR region using near-field enhancement by silica-core gold-shell nanoparticles (NPs). Maximum increases in H₂ and CO₂ productions from NPs were 115% and 113% without affecting the bacterial growth rates. Model simulations showed that the energy conversion efficiency increased with NPs concentration but decreased with light intensity. In addition, the application of this biohydrogen generation process to environmental remediation was investigated by treating toxic 2-chlorobiphenyl (PCB-1) by hydrogenation using Pd catalysts.



(a) Near-infrared illuminated biohydrogen reactor containing *Rhodopseudomonas palustris* and silica-core gold-shell nanoparticles. (b) Electron micrograph of nanoparticles and cells. (c) Graph showing the remediation of toxic 2-chlorobiphenyl.

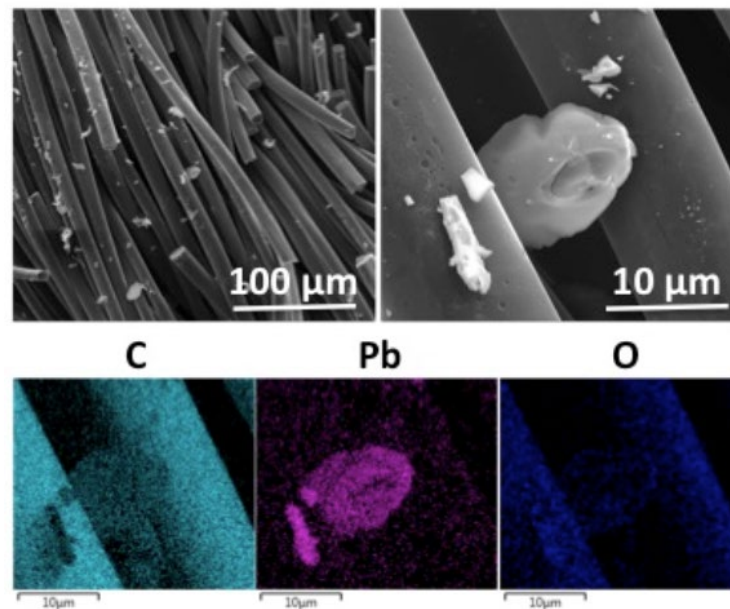
A collaboration between U. of Kentucky and Southern Company led by D. Bhattacharyya (UK Chem. Engr.). Work was performed at KY Multiscale EMC.

Work was supported by CBET-1700091, NIH-NIEHS SRP (P42ES007380), and Southern Company. *International Journal of Hydrogen Energy*, 2021.

National Research Priority: NSF–Growing Convergence Research

Lead and Copper Removal from Water Using Carbon Electrodes in an Electrochemical Filter

Lead concentrations in drinking water are nationwide concerns in the U.S. Likewise metals removal from industrial waste water is a critical for many industries. PowerTech Water's recent research demonstrated that carbon electrodes in an electrochemical filter can target certain metals for removal or recovery. The device uses activated carbon electrodes and a small applied voltage to precipitate metals from solution and trap them in the porous electrode matrix. This system achieved >90% lead removal, while leaving other species (eg. Na^+ and Ca^{2+}) in solution. Targeted Cu removal was also demonstrated. The results of these studies show the promise of electrochemical treatment for both public water supplies and industrial waste streams.



Electron micrographs (upper panels) and energy dispersive X-ray spectroscopy maps (lower panels) of lead immobilized on a carbon electrode.

L. Boehme, J. Landon, A. Rassoolkhani, J. Rentschler, and C. Lippert. PowerTech Water, Inc. Work performed at KY Multiscale EMC.

Work was supported by DOE DE-SC0021567, NIH R44ES028171. *ECS Meetings Abstracts* MA2021-02, 1771 (2021).

National Research Priority: NSF–Growing Convergence Research

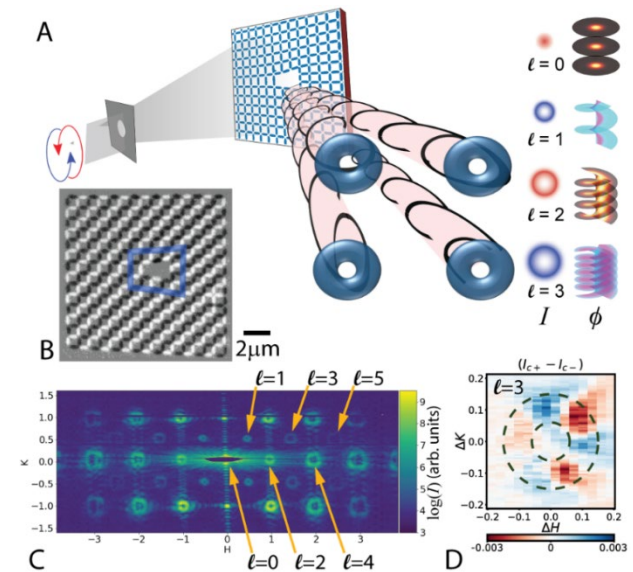
Switchable X-ray Orbital Angular Momentum from an Artificial Spin Ice

The orbital angular momentum (OAM) of visible photons has found application in fields as diverse as quantum cryptography, optical tweezers, and telecommunications. There is rapidly growing interest in X-ray OAM for imaging and probing materials at the nanoscale. This research showed that X-ray diffraction from an artificial spin ice (ASI) yields X-rays carrying OAM. ASIs are patterned arrays of nanomagnets that share some characteristics with water ice. The researchers confirmed that a particular ASI structure orders antiferromagnetically near room temperature and that X-ray photons have even- and odd- OAM quantum numbers depending on whether they scatter from the structure itself or from its magnetic texture. The researchers also showed that magnetically scattered OAM beams could be turned on and off by modest variations of temperature and applied magnetic field. These results imply reconfigurable X-ray optics could be designed using ASIs, and these structures may enable selective probing of electronic and magnetic states in materials.

A collaboration between the Univ. of Kentucky, Lawrence Berkeley NL, Argonne NL, and Brookhaven NL. Work was performed at KY Multiscale CeNSE, EMC, and CAM.

Supported by DE-SC0016519. *Phys. Rev. Lett.* 126, 117201 (2021).

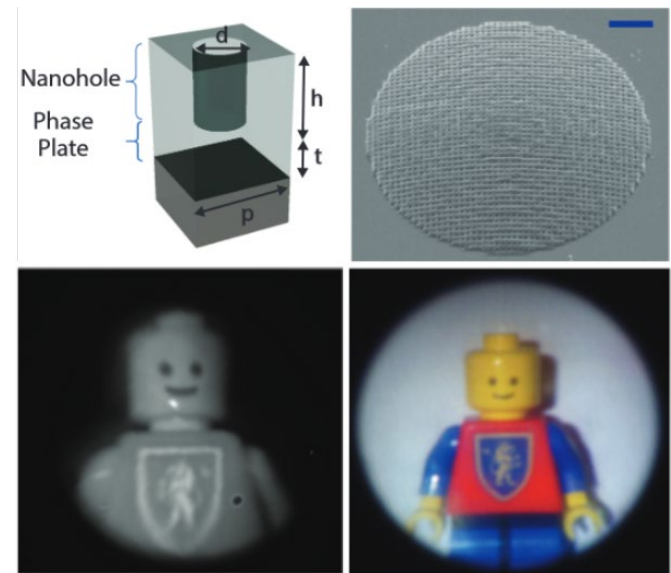
National Research Priority: NSF–Quantum Leap



(A) X-ray photons scattered from an artificial spin ice (ASI) acquire orbital angular momentum. (B) The ASI's antiferromagnetic ground state. (C) Odd- and even- order OAM is generated at the magnetic and structural Bragg conditions. (D) Difference between left- and right- circular polarizations confirms OAM quantum numbers.

An Ultrabroadband 3D Achromatic Metalens

Metalenses are nearly flat optics that employ nanostructured surfaces to manipulate light. The compact size, light weight, and mass manufacturability of metalenses make them ideal for mobile, airborne, and *in-vivo* imaging. This effort built and characterized lenses 50 times thinner than a human hair. The lenses show diffraction limited performance with light ranging from blue (450 nm) to the short-wave infrared (1700 nm). The broadband capabilities of this lens are particularly well suited to emerging visible-to-short wave infrared camera technology. A hybrid 3D architecture, which combines nanoholes with a phase plate, allows realization in low refractive index materials. As a result, two-photon lithography can be used for prototyping while molding can be used for mass production. These results show that 3D metalens architectures yield excellent performance even using low-refractive index materials, and that two-photon lithography can produce metalenses operating at visible wavelengths.



(a) The unit structure of the metalens merges a nanohole and a phase plate. (b) Scanning electron micrograph of 20 μm diameter metalens. Scale bar is 3 μm . (c) Image taken with at 200 μm diameter metalens and broadband illumination (450–1700 nm). (d) Image taken by a color camera sensitive to the visible spectrum.

F. Balli, M. Sultan, A. Ozdemir, and J. T. Hastings, U. of Kentucky (ECE and Physics) and U. of Arizona (Optical Sciences). Work was performed at KY Multiscale CeNSE and EMC.

Supported by Intel Corp. *Nanophotonics* 10(4):1259–1264 (2021).

National Research Priority: NSF–Growing Convergence Research

Mid-Atlantic Nanotechnology Hub (MANTH)

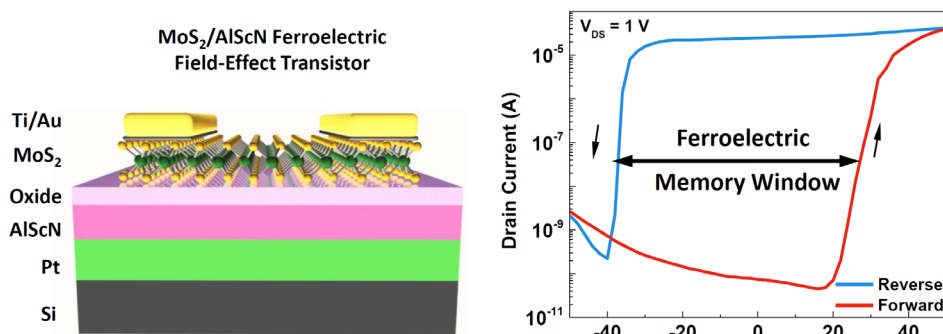
Memory for the Future

Processing large amounts of data such as images and videos requires intense shuffling of information between memory and the processor which demands realization of dense memory, operating at low-power in close proximity to the processor.

Ferroelectric materials have long been sought to realize such dense, low-power, high performance and non-volatile memory devices. However, most known ferroelectric materials are not well suited for the job since they don't possess the desired electrical polarization or cannot be integrated well with Si chips at high densities.

Similarly, two-dimensional semiconductors have now been investigated over a decade and while they are far from replacing Silicon in processors, they bring in a unique advantage when combined with a ferroelectrics to make memory devices.

These ideas led Penn researchers to marry the 2D semiconductor MoS₂ with the ferroelectric material scandium doped aluminium nitride (AlScN) in order to create a ferroelectric field-effect transistor (FE-FET) memory. A key advantage is that the devices can be made directly on top of a Silicon processor without destroying or disrupting its performance during the fabrication process.



Xiwen Liu, Kwan-Ho Kim, Jeffrey Zheng, Paria Musavigharavi, Dixiong Wang, Jinshui Miao and Keshava Katti, with Profs. Jariwala, Olsson, and Stach, Univ. Penn. Work was performed at MANTH.

The work was supported by DARPA via the TUFEN program with facilities support from NSF and DOE and partial support from AFOSR. *Nano Letters* DOI: 10.1021/acs.nanolett.0c05051

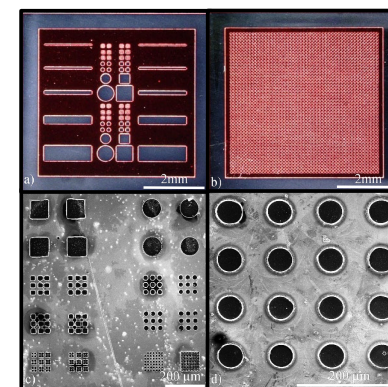
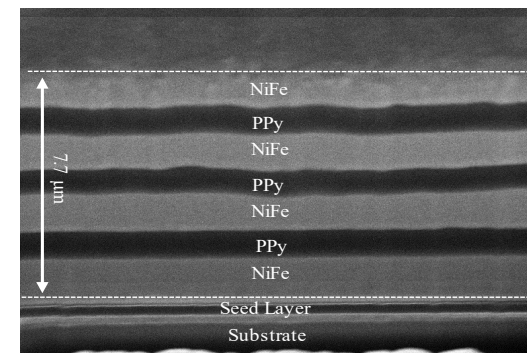
National Research Priority: NSF–Harnessing the Data Revolution

Laminated Multilayer Structures

Laminated multilayer structures comprising alternating layers of metals and insulators are useful in many applications such as capacitors, induction coils, magnetic cores, and sensors. Structures consisting of these sequentially alternating layers can display interesting highly anisotropic material characteristics. In particular, micron-scale laminated cores that consist of electrical insulators and soft magnetic metallic alloys are regarded as a potential enabler of on-chip miniaturized magnetic devices such as transformers that will operate at high frequencies, handling watt-level power within small device volumes.

However, there haven't been scalable and economical fabrication methods to make such anisotropic multilayer structures. Sequential, "top-down" physical vapor deposition of magnetic and insulating material can create laminated structures with controlled, nanoscale individual layer thicknesses. However, due to high built-in stress, it has poor scalability and vacuum-based deposition processes are costly. Typical electrodeposition-based lamination technologies are completed by subtractive processes. After completing the multilayer electrodeposition, the sacrificial layers are selectively removed from the structure which is a complex process primarily due to the need for lithographically defined anchors to support suspended structure.

A scalable and continuous fabrication (thus economical) process for building an anisotropic multilayer structure using the unique properties of the polypyrrole conductive polymer is proposed. A laminated structure created using the developed process shows great promise for use in microfabricated inductor cores that operate at high frequencies, thus contributing to inductor volume reduction needed in MEMS power sources and sensing or actuation systems.



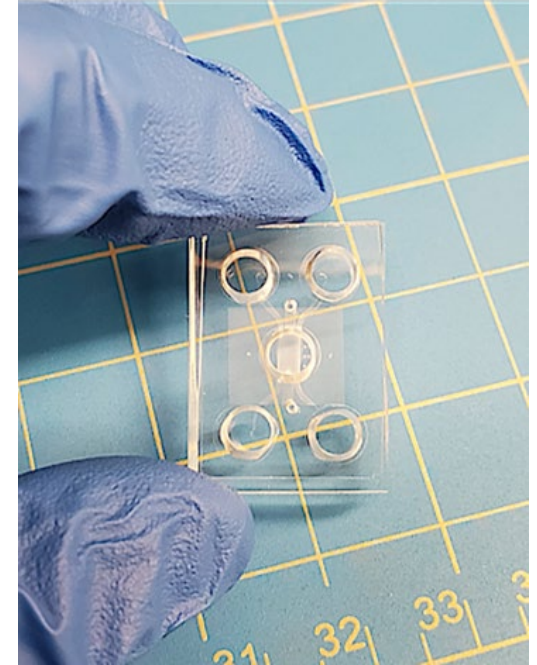
Michael Synodis (MicroSensors MicroActuators group) and Mark Allen (Electrical and Systems Engineering), University of Pennsylvania, and in part by Enachip, Inc (Disclaimer: PI and MANTH Director Allen holds an equity position in Enachip).

National Research Priority: NSF–Harnessing the Data Revolution

Lung-on-a-Chip

Chlorine is one of the most commonly manufactured chemicals in the US, which is mostly used in industry and house cleaning products. Gaseous chlorine is poisonous and it has intermediate water solubility with the capability of causing acute damage to the upper and lower respiratory tract.

This project describes a major interdisciplinary research and development effort motivated by the significant and evolving threat posed by chlorine (Cl_2). The overarching goal of the project is to establish an entirely new approach to the development of biomarkers and effective medical countermeasures for Cl_2 -induced respiratory complications by transforming the conventional methods of modeling and predicting the toxicity of inhaled Cl_2 gas in human lungs. To this end, the project uses the power of lung-on-a-chip technology to create bioengineered *in vitro* platforms that can reproduce the living tissues of the human respiratory tract and their native microenvironment, simulate realistic and physiologically relevant exposure conditions, and visualize and measure an array of biological responses to inhaled Cl_2 gas for quantitative microfluorimetric and multi-omics analysis. It represents a major undertaking that seeks to address the pressing unmet need for predictive and alternative technologies for inhalation toxicology of Cl_2 by exploiting recent innovations made in the field of organs-on-a-chip.



Sezin Aday Aydin, Pouria Fattahi, Dan Huh, Scott Worthen, Univ. Penn. Department of Bioengineering and Children's Hospital of Philadelphia. Work was performed at MANTH.

Work supported by the Biomedical Advanced Research and Development Authority (BARDA).

National Research Priority: NSF–Understanding the Rules of Life

Unexpected Mechanism Behind Friction For 2D Materials

In this study, published in the journal ACS Nano, a team from Penn and UC Merced found that the presence of larger atoms within the lattice of a 2D material unexpectedly decreased the friction encountered by the tip of an atomic force microscope probe as it slid along the surface.

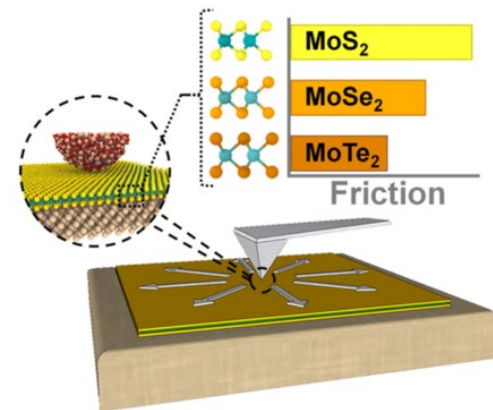
In their study, the researchers compared three 2D materials from the same family, transition-metal dichalcogenides (TMD). These materials consist of a metal atom, molybdenum (Mo), bonded to two atoms of one of the chalcogens, the group of elements that include sulfur (S), selenium (Se) and tellurium (Te). Because these elements are all in the same column of the periodic table, they bond equally well with molybdenum and can make 2D lattices with the same overall pattern under carefully controlled conditions.

In its common form as a thick coating, a powder or a suspension, MoS₂ is a ubiquitous industrial lubricant, so the possibility of increasing its performance has spurred research into advanced synthesis and manufacturing techniques for it and other TMDs. The Authors' research has been motivated by a desire to better understand the dynamics that govern friction when such materials are in their 2D form, and when their composition is altered.

Based on prior computational results, the researchers expected that selenium and tellurium atoms, being larger than sulfur atoms, would present larger energy barriers for the tip to overcome and thus increase the overall amount of friction. In other words, larger atoms means a “bumpier” road, and thus more friction encountered to move across it

That expectation was proven to be incorrect. “Other researchers predicted that friction would go up as the size of the chalcogen increased,” says Martini. “But our results show that it goes in the opposite direction, because the larger chalcogen makes the lattice spacing larger.”

Understanding the interplay between the sizes of individual atoms and the spacing of the lattice they produce will be critical in tailoring the properties of new 2D materials. This study not only revealed an unexpected friction mechanism but showed the potential for entirely novel 2D materials — beyond MoS₂ and graphene — for low friction applications.



This work was done conducted by a team of engineers and physicists from the University of Pennsylvania and the University of California, Merced, including Penn PI Robert Carpick. Work performed at MANTH.

ACS Nano, 14(11), pp.16013-16021, 2020.

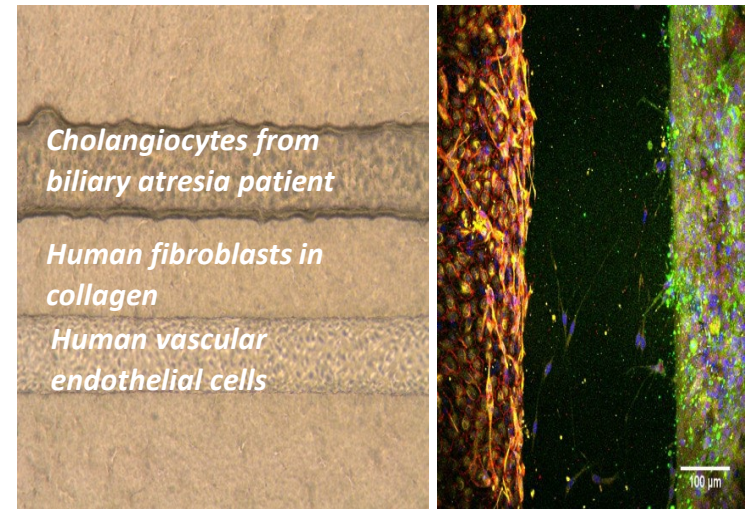
National Research Priority: NAE Grand Challenge—Engineer the Tools of Scientific Discovery

Bile-Duct-on-a-Chip

The extrahepatic bile duct transports highly toxic bile from the liver to the intestine. The duct is lined with epithelial cells called cholangiocytes that form a tight and impermeable monolayer and have specialized, bile-resistant apical domains, protecting the duct submucosa and surrounding tissues from bile leakage and associated damage. The bile ducts are targets in multiple diseases in patients of all ages, but their function is not well understood.

The microfabrication resources at MANTH have been used to develop a bile duct-on-a-chip and vascularized bile duct-on-a-chip. Both devices contain a perfusable biliary channel lined by polarized cholangiocytes (human or mouse); these channels are remarkably impermeable, with tightness of the monolayer similar to that recorded in vivo. The vascularized bile duct-on-a-chip also includes a channel lined by vascular endothelial cells.

The devices are being used to study the impact of biliary toxins on cholangiocyte permeability and function, details of the immune and inflammatory responses to bile duct damage, and the relationship between fibroblasts and cholangiocyte monolayers.



Yu Du and Rebecca Wells, Dept. of Medicine, Perelman School of Medicine. Work was performed at MANTH.

Funding support from NIDDK and the Fred and Suzanne Biesecker Center for Pediatric Liver Disease. *Hepatology*, 71(4), pp. 1350-1363, 2020.

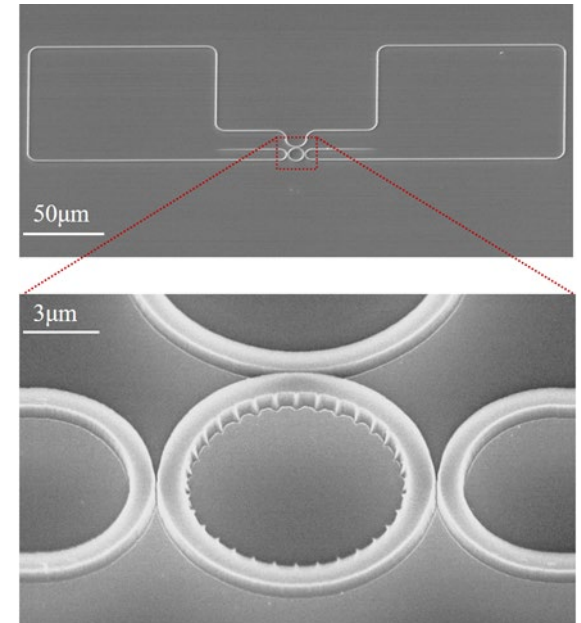
National Research Priority: NSF–Understanding the Rules of Life

Tunable Vortex Microlaser

For the first time, a tunable orbital angular momentum (OAM) microlaser capable of emitting vortex beams of 5 different topological charges at room temperature on an III-V semiconductor platform has been demonstrated. The non-Hermitian manipulation of chiral spin-orbit interaction offers fundamentally new functionality of controllable vortex light emission in a scalable way.

The toolbox of generating various vortex light at a single wavelength holds the promise for future development of multi-dimensional OAM-spin-wavelength division multiplexing for high-density data transmission in classical and quantum regimes.

Furthermore, based on the same platform, ultrafast, dynamic control of the fractional OAM of microlaser emission from -2 to 2 within 100 picoseconds was realized.



Collaboration of the Liang Feng group and Ritesh Agarawal group at the University of Pennsylvania; with Natalia Litchnitsner, Duke University; Josep Jornet, Northeastern University; Stefano Longhi, IFISC, CSIC-UIB. Work performed at MANTH.

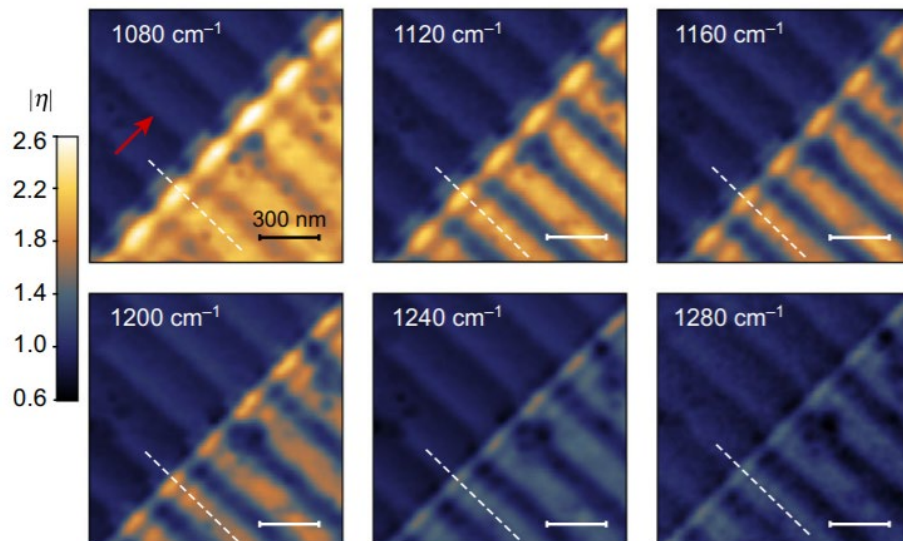
Science, pp. 760-763, 2020.

National Research Priority: NSF–Quantum Leap and Harnessing the Data Revolution

Midwest Nanotechnology Infrastructure Corridor (MiNIC)

Real-Space Imaging of Acoustic Plasmons in CVD-Grown Graphene

This work seeks to demonstrate a direct optical probing of the plasmonic fields reflected by the edges of graphene *via* near-field scattering. The results show a relatively small propagation loss of the mid-infrared acoustic plasmons in that allows for their real-space mapping at ambient conditions even with unprotected, large-area graphene grown by chemical vapor deposition. An acoustic plasmon mode is observed that is twice as confined compared to the graphene surface plasmon under similar conditions. The results highlight the promise of acoustic plasmons for graphene-based optoelectronics, and in particular, molecular sensing applications.



Near-field index contrast obtained at different frequencies over the same sample area showing acoustic graphene plasmons. The red arrow indicates the tip illumination direction

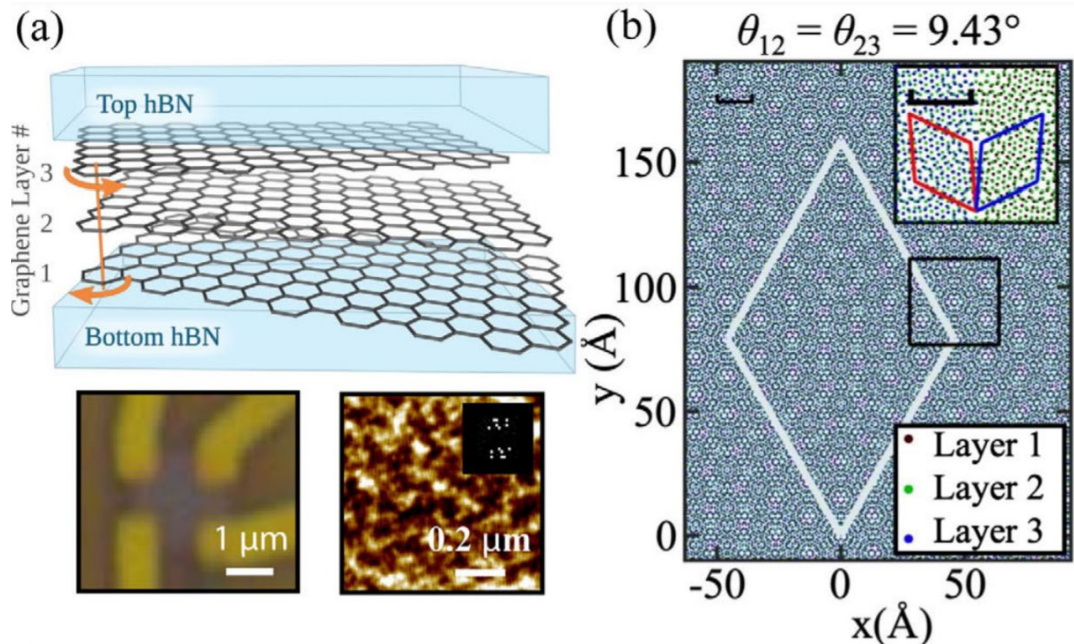
Work performed by members of the Low and Oh groups at the Midwest Nano Infrastructure Corridor (MiNIC) in collaboration with the Jang group at KAIST, South Korea.

Supported by the Samsung Global Research Outreach program and NSF (ECCS-2025124). *Nat. Commun.* **12**, 938 (2021).

National Research Priority: NSF–Understanding the Rules of Life

Correlated Insulating States in Twisted Graphene Multilayers

Two-dimensional (2D) materials stacked with a small twist angle give rise to beating periodic patterns on a scale much larger than the original lattice, referred to as a moire superlattice. In this work, transport in twisted trilayer graphene with two consecutive small twist angles is studied. Correlated insulating states are observed at an extremely low carrier density ($\sim 10^{10} \text{ cm}^{-2}$), near which a zero-resistance transport behavior is observed, indicative of a possible superconducting state.



Twisted graphene multi-layer structure and resulting moire pattern at a twist angle of 9.43° .

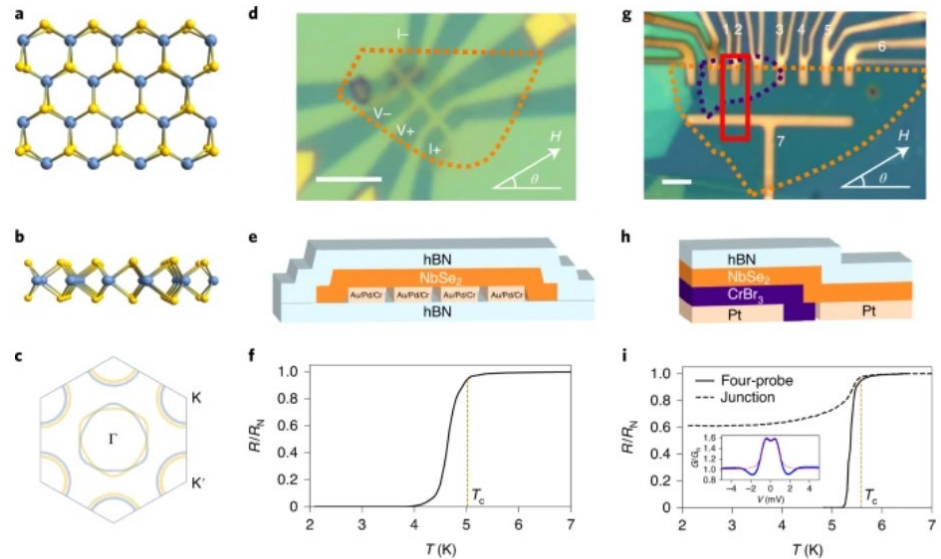
Work performed by members of Ke Wang and Luskin groups at the Midwest Nano Infrastructure Corridor (MiNIC).

Supported by ARO MURI (W911NF-14-1-0247) and NSF (ECCS-2025124). *Phys. Rev. Lett.* **127**, 166802 (2021)

National Research Priority: NSF–Quantum Leap

Unusual Superconductivity in 2D NbSe₂

NbSe₂ is an Ising superconductor, an effect that stabilizes the superconducting state against magnetic fields up to ~35 T, and could lead to topological superconductivity. In this work, it was found that NbSe₂ has a two-fold rotational symmetry of the superconducting state under in-plane magnetic fields, in contrast to the three-fold symmetry of the lattice. The anisotropy vanishes in the normal state, demonstrating that it is an intrinsic property of the superconducting phase. This is an important discovery for understanding topological superconductivity which has applications in fault tolerant quantum computing.



(a)-(c) Crystal structure of NbSe₂, (d)-(e) Optical image and structure device 1 used for magnetoresistance measurements. (f) Superconducting transition for device 1. (g) SEM image of device 2 used for junction studies. R vs. T plot of device 2.

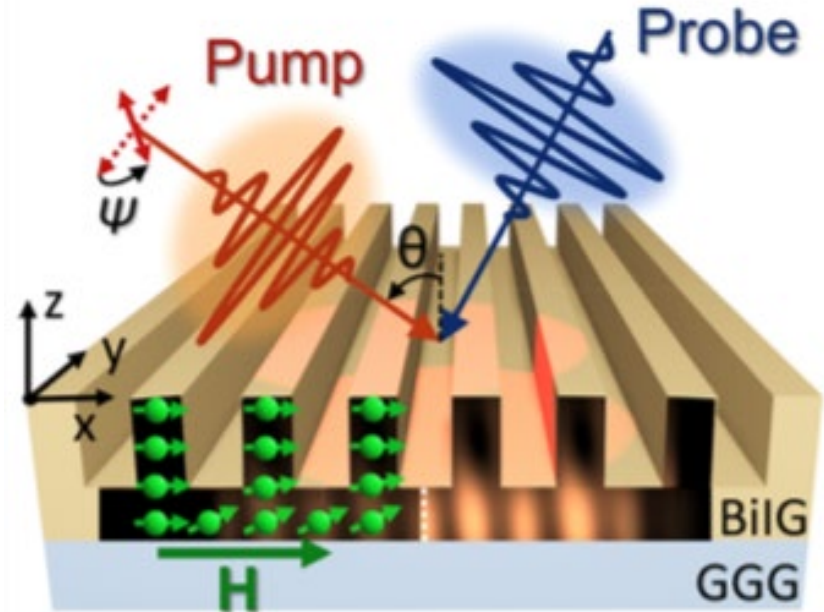
Work performed by members of the Pribyag and Ke Wang groups at the Midwest Nano Infrastructure Corridor (MiNIC) in collaboration with partners at the Cornell NanoScale Facilities (CNF) and others.

Supported by NSF (DMR-2011401, DMR-1644779 and ECCS-2025124) and ONR (N00014-18-1-2368). *Nature Physics* 17, 949–954 (2021).

National Research Priority: NSF–Quantum Leap

Controlling Spin Dynamics in Magnetic Dielectric Structures

Launching and controlling magnons with laser pulses can open up new routes for applications including opto-magnetic switching and all-optical spin wave emission. In this work, localization of light in spots with sizes of tens of nanometers can be achieved by nanopatterning of 1D grating of trenches which allows launching standing spin waves of different orders. Nanostructuring of the magnetic media provides a unique possibility for the selective spin manipulation, a key issue for further progress of magnonics, spintronics, and quantum technologies.



Sample design and pump-probe scheme for all-optical excitation of magnetization dynamics.

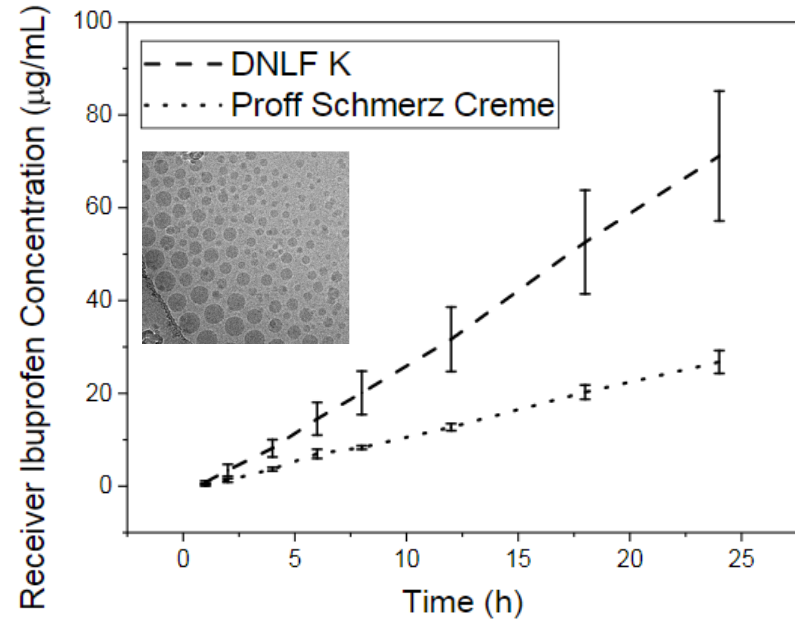
Chernov, M. Kozhaev, D. Ognatyeva, E. Beginin, A. Sadovnikov, A. Voronov, D. Karki, M. Levy, and V. Belotelov. Electron-beam lithography performed at the Midwest Nano Infrastructure Corridor (MiNIC).

Supported by NSF (ECCS-2025124). *Nano Lett.* **20** 5259-5266 (2020).

National Research Priority: NSF-Quantum Leap

Development of Nanoparticle Drug Delivery System

Dynation has used nanoparticle analyzers to develop micellular nanoparticles for improved transdermal delivery of therapeutics such as ibuprofen and paclitaxel. This work reports that nanoparticle dispersions are stable, bind ibuprofen tightly and yet provide high transdermal drug permeation. Ibuprofen dense nanolipid fluid (DNLF) dispersions provide up to five times greater flux of the pharmacologically active S-ibuprofen isomer through human skin than a commercially available racemic ibuprofen emulsion product. This work is a key step towards development of a commercially viable, FDA approvable topical ibuprofen medicine.



Human cadaver skin permeation of S-ibuprofen from DNLF dispersion compared to permeation of both ibuprofen racemates from Proff Schmerz Crème. Inset: cryogenic TEM image of ibuprofen nanoparticles

Work performed by Dynation LLC at the Midwest Nano Infrastructure Corridor (MiNIC).

Supported by NSF SBIR Grant No. 164792 and by (ECCS-2025124). *International Journal of Pharmaceutics* **598**, 120289 (2021).

National Research Priority: NSF–Understanding the Rules of Life

Voltage Assisted Writing of Ferrimagnetic Spin Devices

Voltage control of magnetic order is desirable for spintronic device applications, but 180° magnetization switching is not straightforward because electric fields do not break time-reversal symmetry. In this study, solid-state hydrogen gating is used to control the ferrimagnetic order in rare earth–transition metal thin films dynamically. Reversible, gate voltage-induced net magnetization switching and full 180° Néel vector reversal in the absence of external magnetic fields is observed. This work has broad implications for the use of magnetic and spintronic materials for logic switching and computing-in-memory applications.

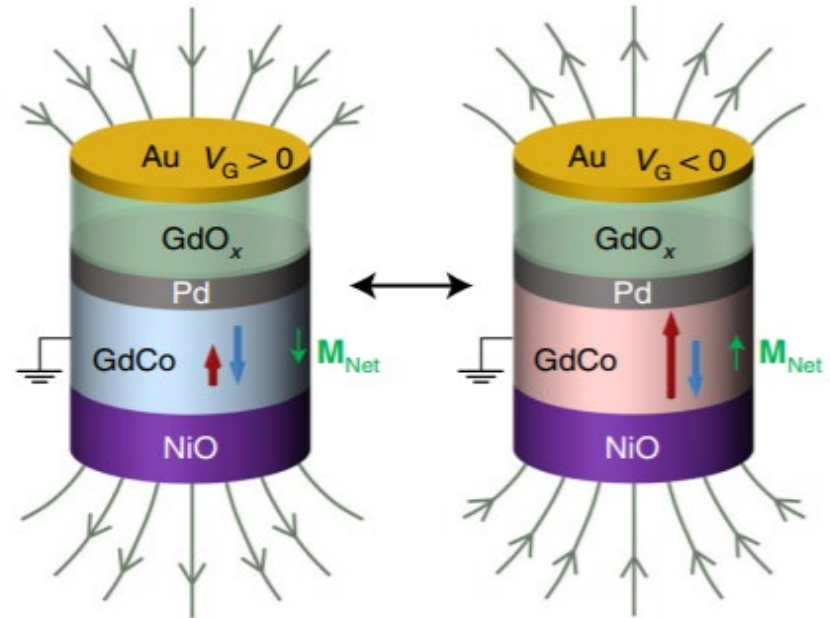


Diagram showing mechanism of voltage-controlled switching using in ferrimagnetic GdCo films.

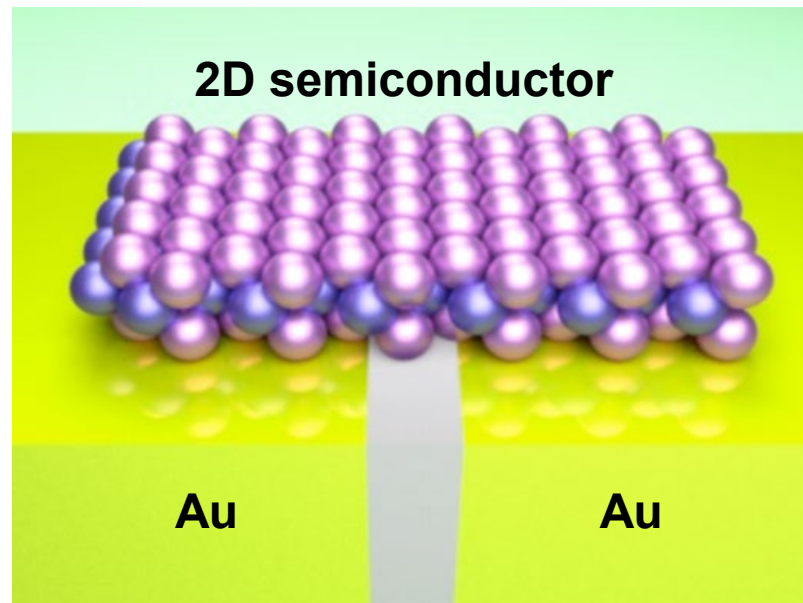
Work performed by members of the JP Wang group at the Midwest Nano Infrastructure Corridor (MiNIC) in collaboration with the Beach group at MIT.

Supported by SMART, one of seven centers of nCORE, a Semiconductor Research Corporation program supported by several industrial partners and NIST and by NSF (ECCS-2025124). *Nature Nanotech.* **16**, 981-988 (2021).

National Research Priority: Microelectronics and High Performance Computing

Ultraflat Sub-10 Nanometer Gap Electrodes for Two-Dimensional Optoelectronic Devices

Two-dimensional (2D) materials are promising candidates for building ultrashort-channel devices because their thickness can be reduced down to a single atomic layer. In this work, an ultra-flat nanogap platform based on atomic layer deposition (ALD) was used to create 2D-material transistors with source-drain spacing as small as 10 nm. The same platform was also used to demonstrate photodetectors with a nanoscale photosensitive channel, exhibiting higher photosensitivity compared to microscale gap channels. The platform has tremendous potential for realization of a wide variety of nano-scale electronic and photonic devices.



Schematic diagram ultra-short-channel 2D MOSFET patterned on ultra-flat nanogap electrodes, where the nanogap spacing is determined using atomic layer deposition.

Work performed by members of the Koester and Oh groups at the Midwest Nano Infrastructure Corridor (MiNIC).

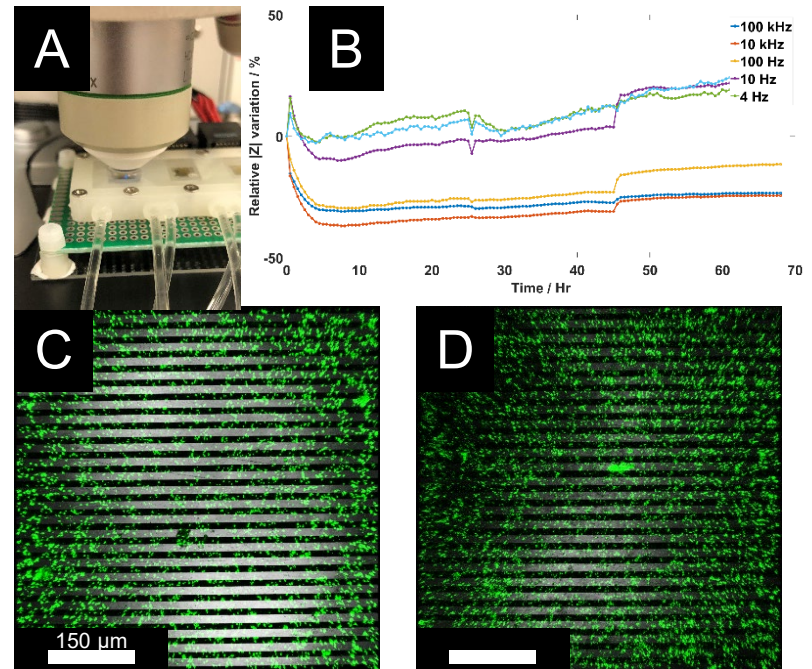
Supported by AFOSR (FA9550-14-1-0277) and NSF (ECCS-2025124). *ACS Nano* **15**, 5276-5283 (2021).

National Research Priority: Microelectronics and High Performance Computing

Montana Nanotechnology Facility (MONT)

Impedance Spectroscopy Sensor Platform to Detect Biofilm in Industrial Settings

In this work, microfabricated electrochemical impedance spectroscopy (EIS) sensors were used to monitor biofilm development in an industrial machining process fluid. 7% metalworking fluid (MWF) was inoculated with GFP labeled *Pseudomonas aeruginosa* and continuously circulated through a custom-made microscopy flow-cell device with integrated EIS sensors for 72 hours (Panel A). EIS was measured at different frequencies over time. An increase in relative impedance variation was observed over time, suggesting changes to the sensor surface (panel B). Confocal imaging was used to visualize the sensor surface and biofilm accumulation. Microscopy confirmed microbial attachment on the EIS sensors with a denser biofilm monolayer over time (panels C and D).



Matthew McGlennen, Markus Dieser, Heidi Smith, Christine Foreman, Stephan Warnat, Montana State University. Work performed at MONT Montana Microfabrication Facility and the Center for Biofilm Engineering.

This work was supported by NSF (#1760616) and NNCI MONT Project Initiation Grants.

Custom-made microscopy flow-cell with integrated EIS sensors used to monitor biofilm growth over time (A). EIS measured at different frequencies over time associated with biofilm growth (B). Confocal images of biofilm accumulating on the EIS sensors at 24 hours (C) and 48 hours (D).

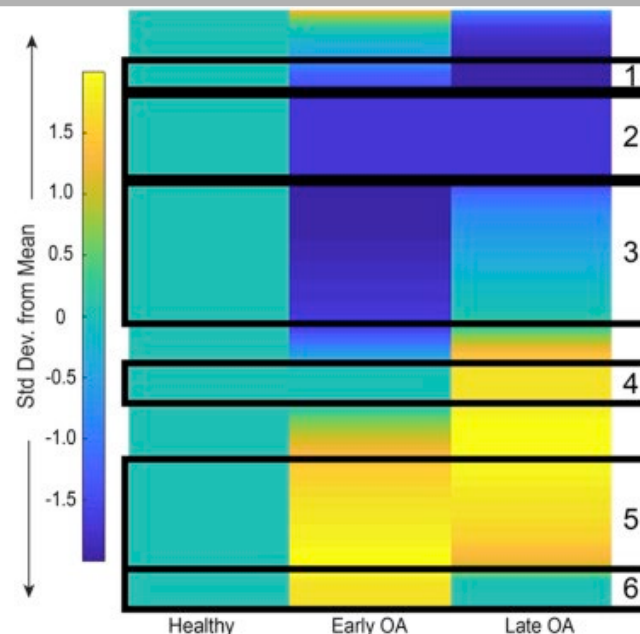
National Research Priority: NSF–Growing Convergence Research

Metabolic Profiling of Synovial Fluid for Early Detection of Osteoarthritis

Osteoarthritis (OA) affects more than 50 million people in the US, eventually leading to chronic pain and disability. Currently, no FDA-approved biomarkers for OA exist, limiting a clinician's ability to detect early stage disease. Early detection of OA is a rate-limiting step toward improved clinical care because recent studies show that early intervention can limit or reverse OA symptoms. However, early detection of OA is not currently possible.

Metabolomic profiling is an emerging approach to characterize biological systems like synovial joints. While OA is classically described by degeneration of the articular cartilage, the pathophysiology of the disease involves cell stress, inflammatory activity, and abnormal tissue metabolism. Since the synovial fluid contains many of the molecules produced by the articular joint's multiple cell types (eg chondrocytes, synoviocytes, and osteoblasts), metabolic profiling of the synovial fluid could provide a unique window into active disease processes in the OA-affected joint, and metabolomic profiles from synovial fluid could facilitate early detection of OA.

While synovial fluid is "the scene of the crime" for OA, serum is easier to obtain clinically. Because metabolites are smaller than 1000 Daltons, there is a good chance that serum metabolite profiles may also reflect OA pathophysiology. As such, the goal of this project is to advance global metabolite profiles as clinical biomarkers of OA grade. Our vision is to develop a panel of biomarkers capable of detecting OA before the onset of symptoms.



Heatmap of metabolite expression from healthy patients, or those with early or late OA. The different patterns of expression provide insight into pathophysiology and may yield biomarkers for early detection of OA.

AK Carlson, RA Rawle, CW Wallace, EG Brooks, E Adams, MC Greenwood, M Olmer, MK Lotz, B Bothner, and RK June, Montana State University. Work performed at Montana State University, Mass Spectrometry Core Facility.

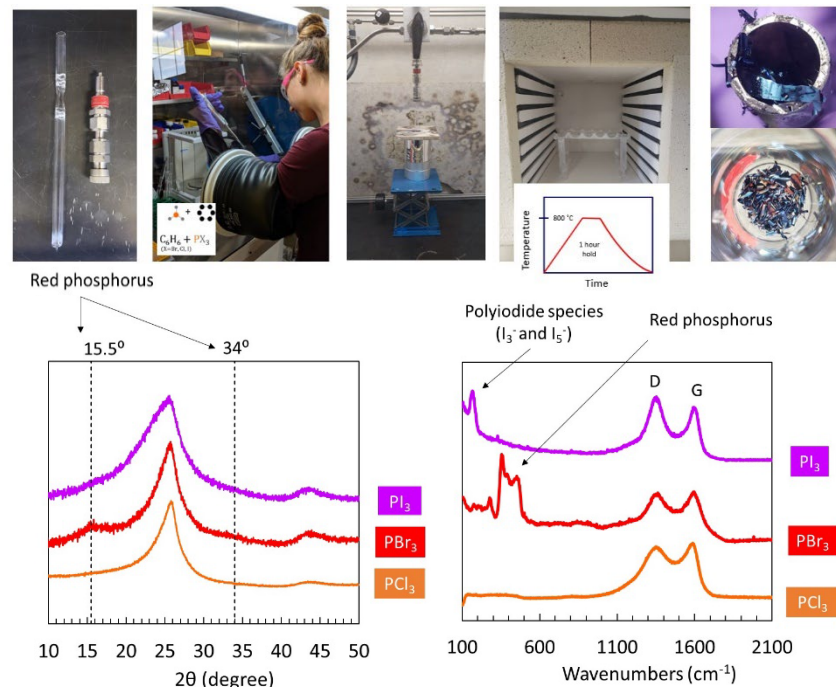
Supported by NIH R01AR073964 and NSF CMMI 1554708. *Osteoarthritis & Cartilage*. 2020 Aug;27(8):1174-1184.

National Research Priority: NSF–Understanding the Rules of Life

Novel P-C Materials for Energy Storage

The direct synthesis of substitutional P-doped graphitic carbon at high P content is known to be accompanied by the formation of one or several common allotropes of elemental phosphorus (e.g., white, red, and black). Such materials are synthesized in a closed quartz ampule from a liquid mixture of benzene and a phosphorus containing halide at elevated temperatures (800-1050 °C).[\[ref\]](#)

In this work we aim to control the presence of white, red, and/or black phosphorus by variation of the phosphorus halide precursor: PCl_3 , PBr_3 , or PI_3 . An early result of the latest work is that for materials produced from PBr_3 , red phosphorus is favored over white. Such materials may be interesting for lithium or sodium ion storage as electrodes in electrochemical energy storage devices.



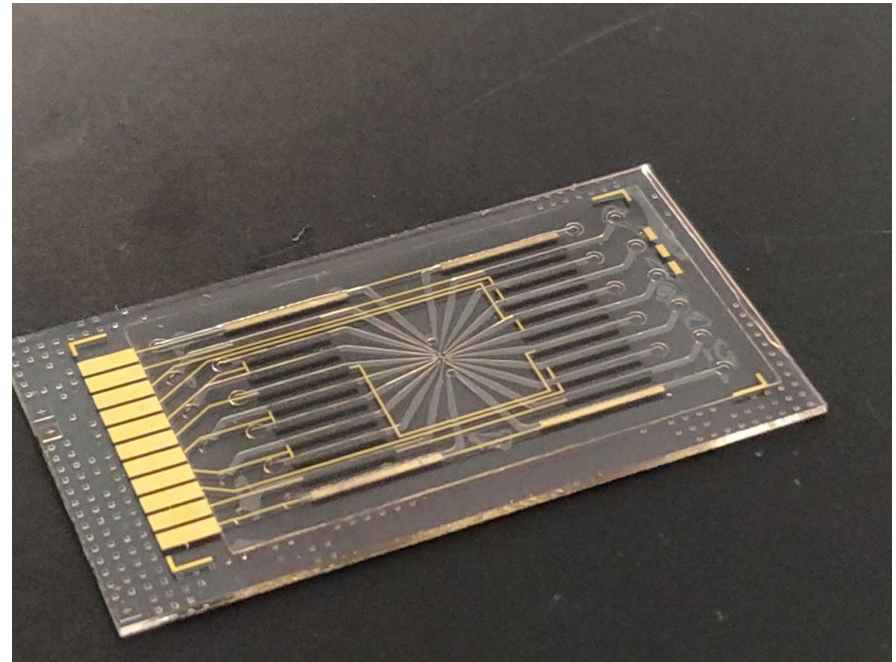
Top: Direct synthesis protocol to produce graphitic PC_x composite materials from liquid mixtures. Bottom: XRD patterns and Raman spectra of a series of directly-synthesized PC_x materials.

Isabelle Gordon, Sophia Randak, and Nicholas P. Stadie, Montana State University. Work performed at Montana State's Imaging and Chemical Analysis Laboratory (ICAL).

National Research Priority: NAE Grand Challenge—Making Solar Energy Economical

BETR- Bioelectronics for Tissue Regeneration

The goal of the project is to develop bioelectronic devices that can reduce time taken to heal wounds by stimulating and monitoring the wound. The idea is to deliver ions to control the electrochemical environment of the wound, as well as small molecules and growth factors to promote healing using the bioelectronic device while monitoring the physiological processes in the wound using optical sensors at the same time.



Bioelectronic device that can deliver ions, small molecules and growth factors.

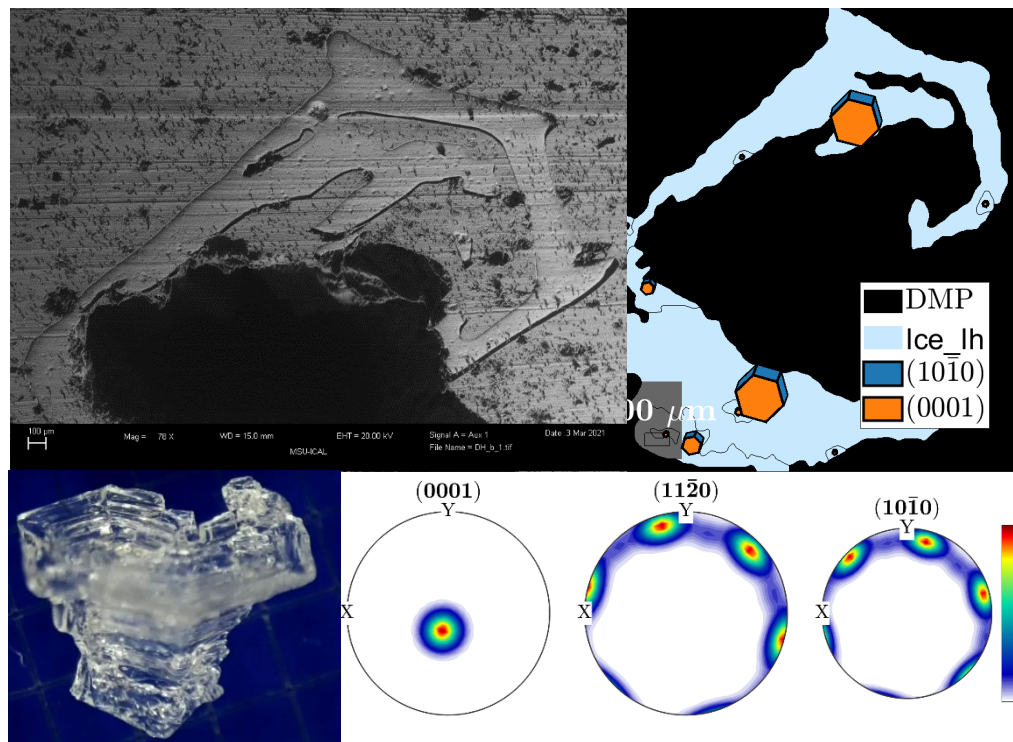
Marco Rolandi, University of California Santa Cruz. Work performed at Montana State University, Montana Microfabrication Facility.

Supported by DARPA (D20AC00003)

National Research Priority: NSF–Growing Convergence Research

Characterizing Depth Hoar Snow Grain Preferred Growth Orientation with EBSD

A great deal of information about snow microstructures pertinent to better understanding both seasonal and perennial snow cover processes, can be derived from advanced and classical materials characterization techniques, including X-ray computed microtomography (micro-CT) and cross-polarized light imaging. However, there currently exists no standardized technique for ascertaining the full microstructural detail of snow, including both c-axis and a-axis crystallographic orientations of individual snow grains. This missing piece of information is relevant to better understanding a variety of physical snow processes including its mechanical behavior, wet and dry snow metamorphism, sintering, and its dielectric response to incident electromagnetic radiation.



Electron Backscatter Diffraction (EBSD) map of a hexagonal depth hoar snow grain collected from the field and casted in dimethyl phthalate.

Evan Schehrer and Kevin Hammonds. Work performed at Montana State University, MONT facility ICAL.

This research was supported by the NASA New Investigator Program Award 80NSSC18K0822

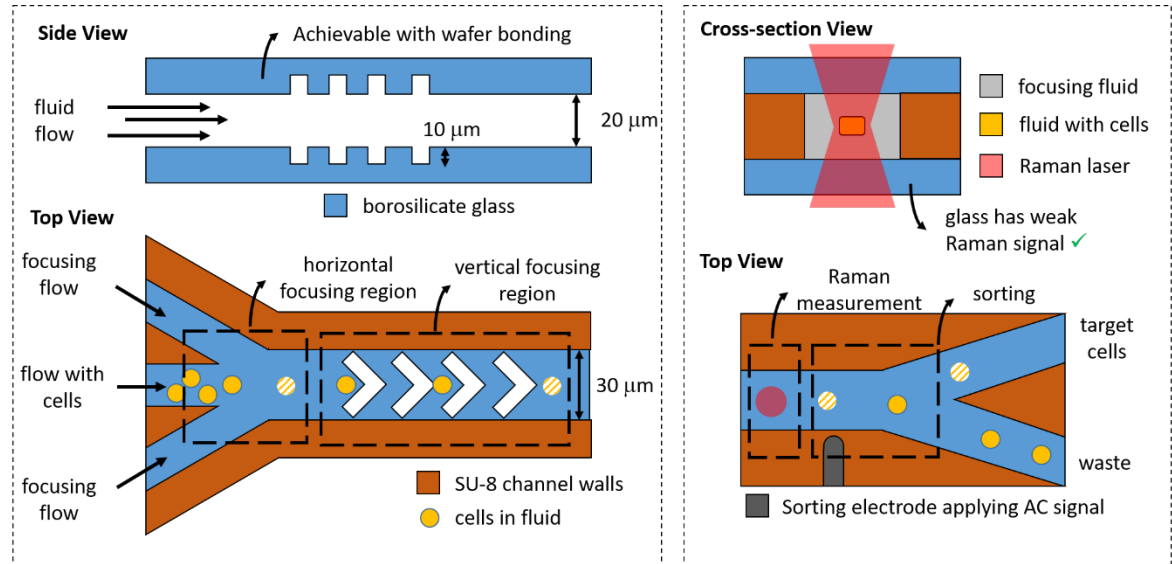
National Research Priority: NSF–Navigating the New Arctic

Glass-Glass Microfluidic Device Fabrication for Raman Activated Cell Sorting

High signal-to-noise ratio measurements are required for high-throughput Raman activated cell sorting (1000 cells/s).

Glass is an optimal material for this purpose because of its high light-transmission and weak Raman-signal.

Polymers such as PDMS are more common materials in microfluidics but are more Raman active and therefore increase measurement time and decrease the device efficiency



Michael Neubauer and Stephan Warnat, Montana State University.

Supported by MONT NNCI Project Initiation Grant

National Research Priority: NSF–Growing Convergence Research

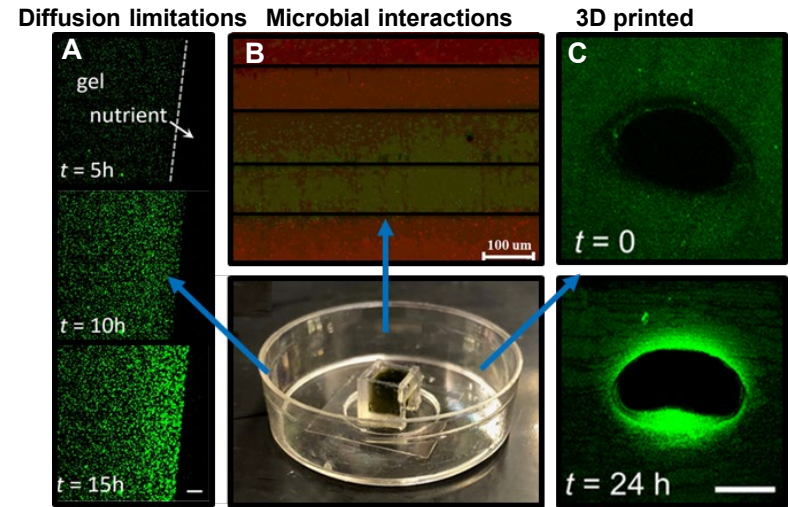
3D Bioprinting of Microbial Biofilms

3D bioprinting is a rapid fabrication technique that provides exquisite control over the structure and composition of living materials.

3D bioprinting of microorganisms can be used to structure microbial bioreactors and biofilters and study complex cell-cell interactions in biofilms.

We are developing methods to structure microbial communities and technologies improve material transport in 3D-printed biofilms.

Fluorescent confocal microscopy is an ideal tool to visualize microorganisms embedded in 3D printed hydrogels.



Fluorescence confocal microscopy of microorganisms in a 3D printed PEG-DA hydrogel. (A) Time-lapse images of *P. aeruginosa* growth over time. (B) 3D printed *E. coli* strains with red and green fluorescent proteins. (C) Cross-sectional images of gel containing *P. aeruginosa* showing growth near a nutrient filled channel. Scale bars in (A), (B) and (C) are 50 μm , 100 μm , and 500 μm , respectively.

Reha Abbasi, Isaak Thornton, Tom LeFevre, and James Wilking. Work performed at MONT.

This work is supported by the NSF (DMR-1455247 and OIA-1736255) and the Army Research Office (W911NF-19-1-0288). *Lab Chip* (2021).

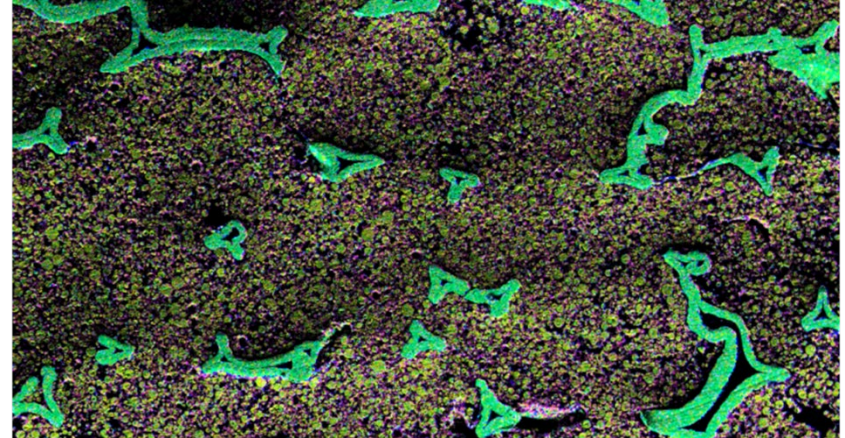
National Research Priority: NSF–Understanding the Rules of Life

Characterization of Zn-based Batteries

Æsir Technologies specializes in the development and commercialization of next-generation Nickel-Zinc (Ni-Zn) and zinc-based battery technologies that utilize sustainable materials that can be safely and easily recycled.

Our technological advancements require combining inhouse electrochemical performance testing with compositional and structural analysis of our synthesized materials and electrodes.

The use of analysis equipment at Montana State University will help lead to further optimization of our current Ni-Zn electrodes and accelerate R&D on experimental zinc-based chemistries.



Energy dispersive X-ray spectroscopy (EDX) elemental mapping of a Ni-Zn cathode.



Melissa McIntyre and Adam Weisenstein at Æsir Technologies. Work performed at Montana State University, MONT facility ICAL.

National Research Priority: NAE Grand Challenge—Making Solar Energy Economical

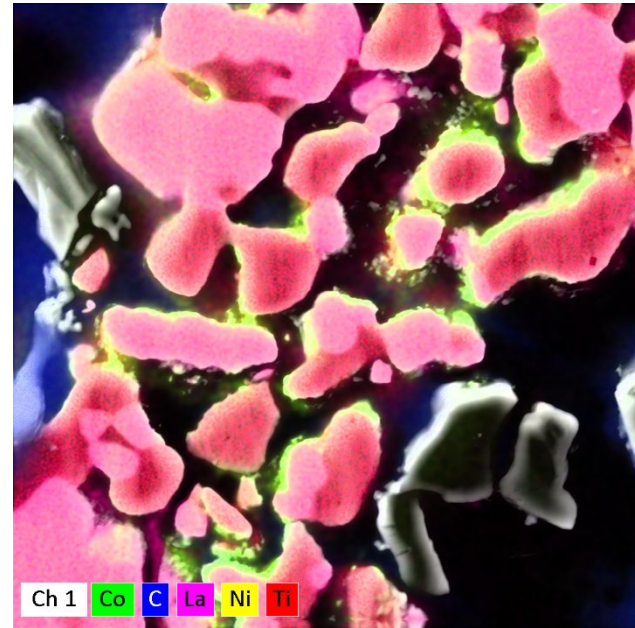
Advanced Processing for Solid-State Li-Ion Conduction

The Stephen Sofie group at Montana State University is working to apply advanced microstructural processing techniques to solid state battery designs. The group simultaneously is performing fundamental characterization of the solid Li-conductors which comprise these batteries.

X-Ray Diffraction to study phase formation, Li-loss and structural evolution of LLZO/LLTO during processing.

Nano-auger for surface sensitive, highly-resolved interfacial mapping.

Scanning electron microscopy for analysis of processing protocols.



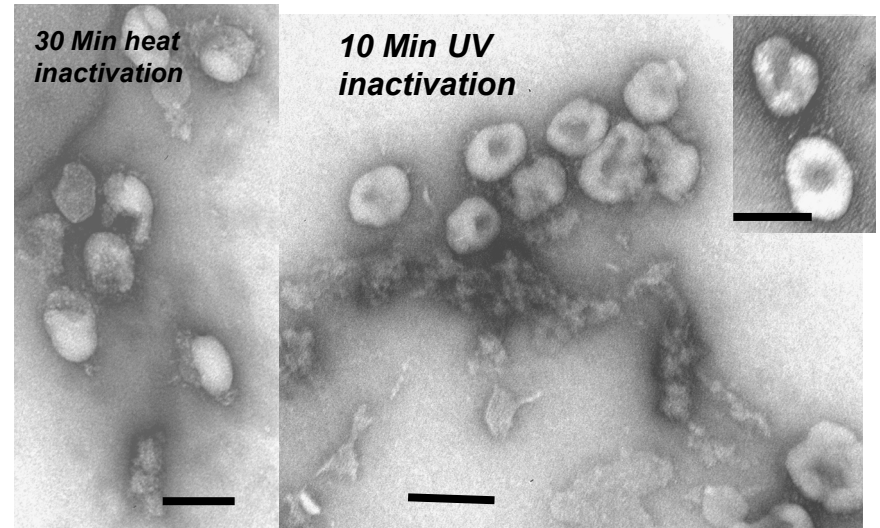
Elemental mapping with Auger Nano-Probe of Lithium Cobalt Oxide (LCO) chemical buffer layer on Lithium Lanthanum Zirconate (LLZO) scaffold in prototype cathode for solid state battery.

Dr. Stephen Sofie, Dr. David Driscoll, Stephen Heywood. Work performed at Montana State University, MONT facility ICAL

National Research Priority: NAE Grand Challenge—Making Solar Energy Economical

Using TEM to Visualize inactivated SARS-CoV-2 WA01

This work highlights the current need for research and testing of the SARS-CoV-2 coronavirus. The WA01 strain, used here and grown in E6-Vero cells, was inactivated and purified to provide controls for qPCR testing, the assessment of virus concentration in sewage, indoor air and common surfaces areas, and for research activities such as antibody production. Viral supernatant was subjected to either UV-C irradiation or 65°C incubation to inactivate viral infectivity. Total infectivity is lost within 15 seconds upon subjecting the virus to UV irradiation and 15 minutes after heating at 65°C. The virus was purified and concentrated on a two-step sucrose cushion. The LEO 912 transmission electron microscope was used to visualize any viral damage the inactivation procedure may have caused. Heat inactivation was more damaging to the particles than was UV.



TEM micrographs of 30 minute heat inactivated and 10 minute UV inactivated SARS-CoV-2. Scale bars are 100 nm.

Matthew Tayler, Mark Young Susan Brumfield, Depts. of Microbiology and Immunology and Plant Science and Plant Pathology, Montana State University . TEM work performed at Montana State University, TEM MONT facility.

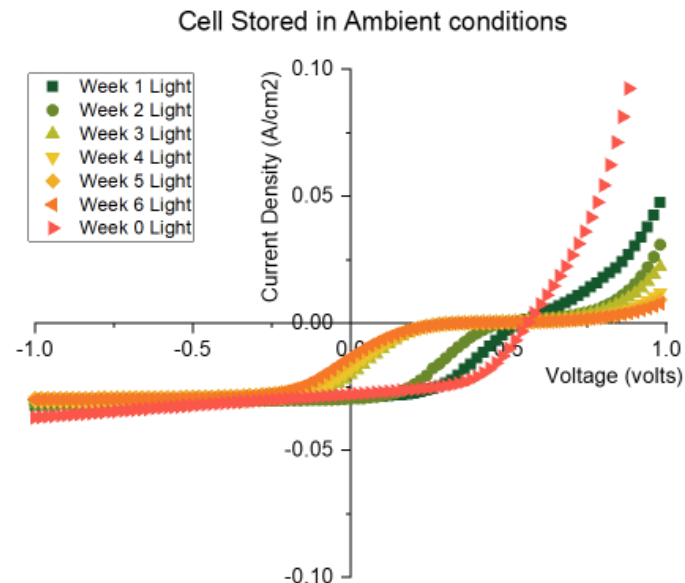
Viruses **2021**, 13, 562.

National Research Priority: NSF–Understanding the Rules of Life

Nanotechnology Collaborative Infrastructure Southwest (NCI-SW)

Understanding S-shape Curves in PEDOT:PSS Based Silicon Heterojunction Solar Cells

To study the impact of air, water, and light on PEDOT:PSS based solar cells, completed cells were subjected to three different environments. JV measurements revealed that the cells started to develop non-ideal behavior often characterized as “S-shape” characteristics in the light. Studies have shown that the “S” shape JV curve can arise due to valence band offset changes resulting in formation of a barrier for hole transport, and the presence of an opposing diode in the front of the cell. The S-shape degrades the fill factor and open circuit voltage of the solar cells as clearly seen in the figure. An increased water-uptake by PEDOT:PSS due is a very plausible explanation resulting in drastic changes to the properties of the emitter.



Light JV of cells exposed to ambient conditions over time

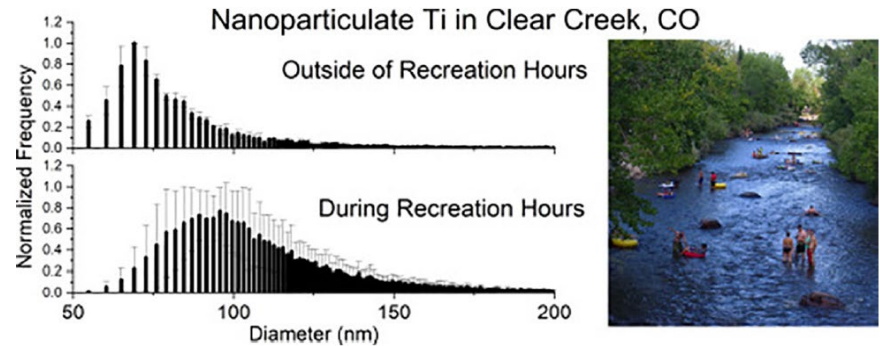
Robert Opila, Department of Material Science and Engineering, University of Delaware. Work performed at NCI-SW.

2020 47th IEEE Photovoltaic Specialists Conference (PVSC), 2020, pp. 2786-2789.

National Research Priority: NAE Grand Challenge—Make Solar Energy Economical

Measuring Nanoparticles from Sunscreen in Recreational Rivers

Detection of metal nanoparticles (NPs) in the environment is of interest due to increasing use of nanomaterials in consumer and industrial products. Detecting NPs associated with human activities is affected by both the magnitude and variation in background concentrations of natural NPs. In this work, we investigated the potential release of titanium dioxide NPs from sunscreen in three recreational rivers, with a time-intensive sampling regime on one river, to determine the range and variability of background titanium. Statistically significant increases in Ti concentrations were observed in Clear Creek, CO during one recreation period, but the significance of other instances of recreation-associated Ti increases was unclear.



Distribution in the size of Ti nanoparticles in the Clear Creek river during and outside recreation hours

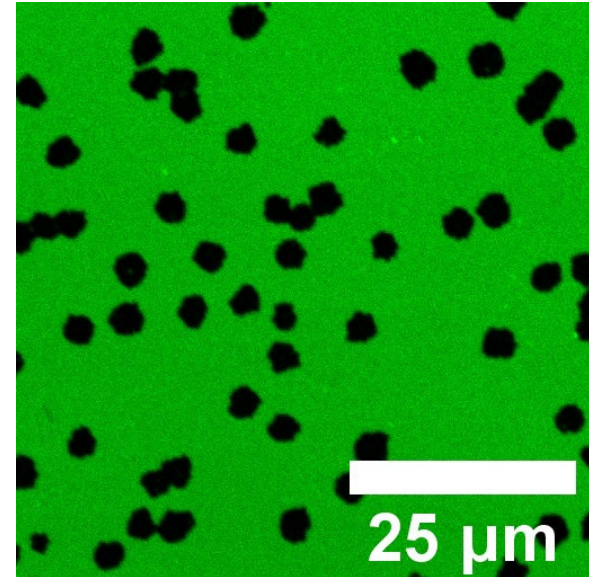
James Ranville, Colorado School of Mines, David Hanigan, University of Nevada, Reno, Paul Westerhoff, ASU. Work performed at NCI-SW.

Science of the Total Environment, vol. 743, article 140845, 2020.

National Research Priority: NAE Grand Challenge—Provide Access to Clean Water

LPS-Membrane Interactions as a Function of Lipid Composition and Environmental Factors

Lipopolysaccharide (LPS) is a unique lipoglycan, with two major physiological roles: 1), as a major structural component of the outer membrane of Gram-negative bacteria and 2), as a highly potent mammalian toxin when released from cells into solution (endotoxin). Much of our understanding of LPS and its interactions with the cell membrane is based upon cellular level responses. In this project, LPS-membrane interactions and subsequent membrane disruption as a function of membrane composition is explored with potential implications in LPS biochemistry and membrane material modification. AFM capabilities and expertise within NCI-SW ¡MIRA! along with optical microscopy and spectroscopy expertise at LANL allow for correlation of LPS interactions with model lipid membranes composed of varying lipid and membrane cofactor composition.



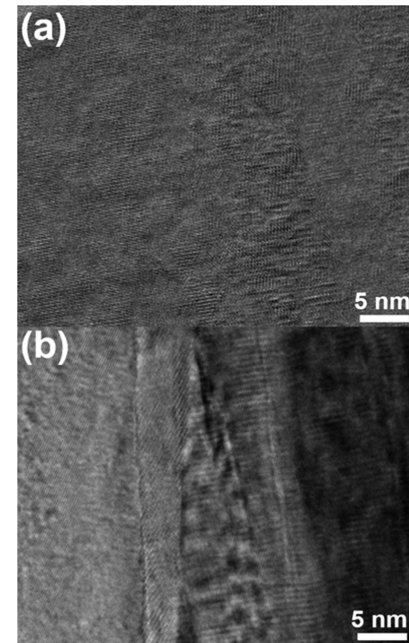
Fluorescence microscopy image of model membrane after incubation with LPS resulting in fixed membrane holes.

Loreen Stromberg, Harshini Mukundan, Los Alamos National Laboratory, Gabriel A. Montañó, ¡MIRA! Center, Northern Arizona University. Work performed at NCI-SW.

National Research Priority: NSF–Understanding the Rules of Life

Changes in band alignment during annealing at 600 °C of ALD Al₂O₃ on (In_xGa_{1-x})₂O₃

As Ga₂O₃-based technologies develop, there is growing interest in alloying Ga₂O₃ with In₂O₃ to tune the wavelength response of photodetectors and increase the mobility in heterostructure transistors. An important aspect for any application of (In_xGa_{1-x})₂O₃ is the band alignment with dielectrics commonly used for surface passivation or metal–oxide–semiconductor (MOS) gates on transistors. The effects of post-deposition annealing on the band alignment of Al₂O₃/(In_xGa_{1-x})₂O₃ heterostructures were measured over a range of In concentrations ($x = 0.25$ – 0.74). Prior to annealing, the band alignment is type I across this composition range. The valence band offset was reduced after annealing at 600°C, with the change being larger for higher In concentrations. The band alignment remains type I for $x = 0.25$, 0.42 , and 0.60 but becomes type II for the (In_{0.74}Ga_{0.26})₂O₃ sample after annealing.



TEM images taken from (a) the Ga-rich portion of the (InGa)₂O₃ wafer and (b) the In-rich portion of the (InGa)₂O₃ wafer.

S. J. Pearton, Dept. of Materials Science and Engineering, University of Florida. Work performed at NCI-SW.

Journal of Applied Physics, vol. 127, article 105701, 2020.

Monte Carlo Solution of High Field Hole Transport in Avalanche Amorphous Selenium

Amorphous selenium lacks the structural long-range order present in crystalline solids. An in-house bulk Monte Carlo algorithm is employed to solve the semiclassical Boltzmann transport equation, providing microscopic insight to carrier trajectories and relaxation dynamics of non-equilibrium “hot” holes in extended states. The extended-state hole–phonon interaction and the lack of long-range order in the amorphous phase is modeled as individual scattering processes. We have used a non-parabolic approximation to the density functional theory calculated valence band density of states. To validate our transport model, we calculate and compare our time-of-flight mobility, impact ionization gain, ensemble energy and velocity, and high field hole energy distributions with experimental findings. We reached the conclusion that hot holes drift around in the direction perpendicular to the applied electric field and are subject to frequent acceleration and deceleration caused by the presence of high phonon, disorder, and impurity scattering.

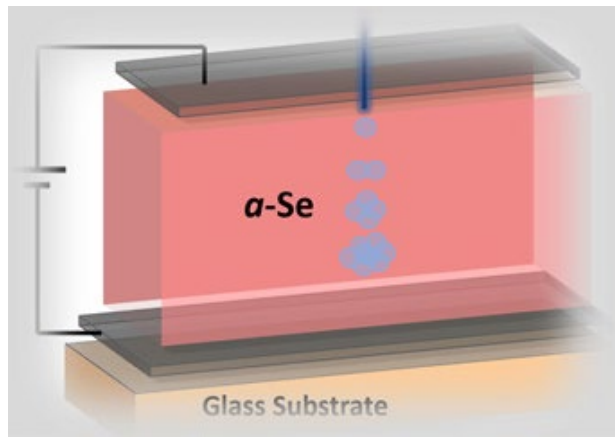


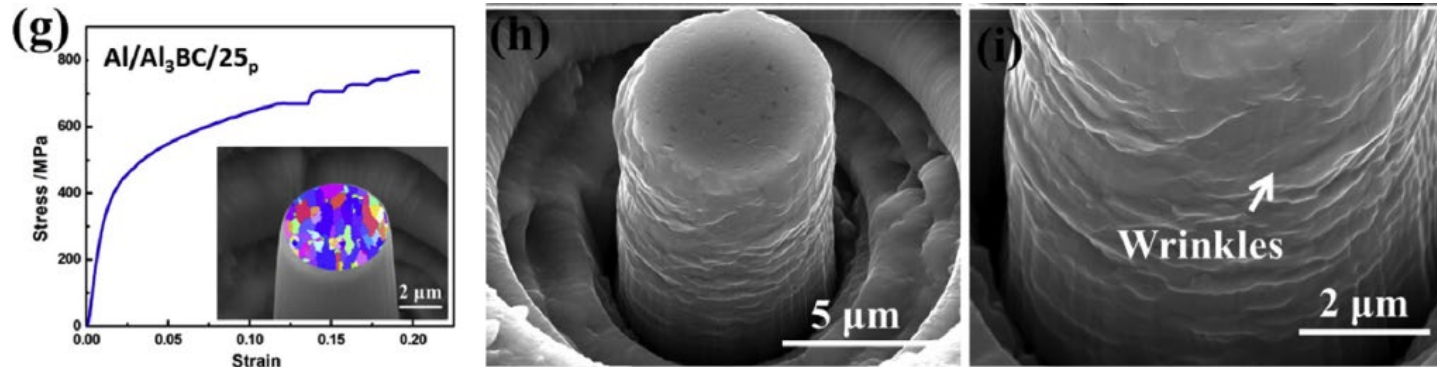
Illustration of the avalanche process in an amorphous selenium photoconductor for large area medical imaging applications

Amir H. Goldan, Atreyo Mukherjee, and John Akis, Stony Brook University. Dragica Vasileska, ASU. Work performed at NCI-SW

ACS Omega, vol. 6, pp. 4574–4581, 2021.

Measuring the deformation of Al_3BC/Al composites via in-situ micropillar compression

Al_3BC is a promising candidate as the reinforcement for Al alloys. However, the deformation behavior and strengthening mechanisms remain unclear hitherto. In this work, the deformation behavior and strengthening mechanisms of Al_3BC/Al composites were investigated via in-situ micropillar compression. Wrinkled slip bands and slip homogenization were observed in the composites instead of large parallel slip bands in pure Al. The interaction between Al_3BC and dislocations was investigated in this work. Microstructural characterization reveals that the high-density dislocations and Al_3BC -induced ultrafine sub-grains determine its excellent strengthening effects on the Al matrix.



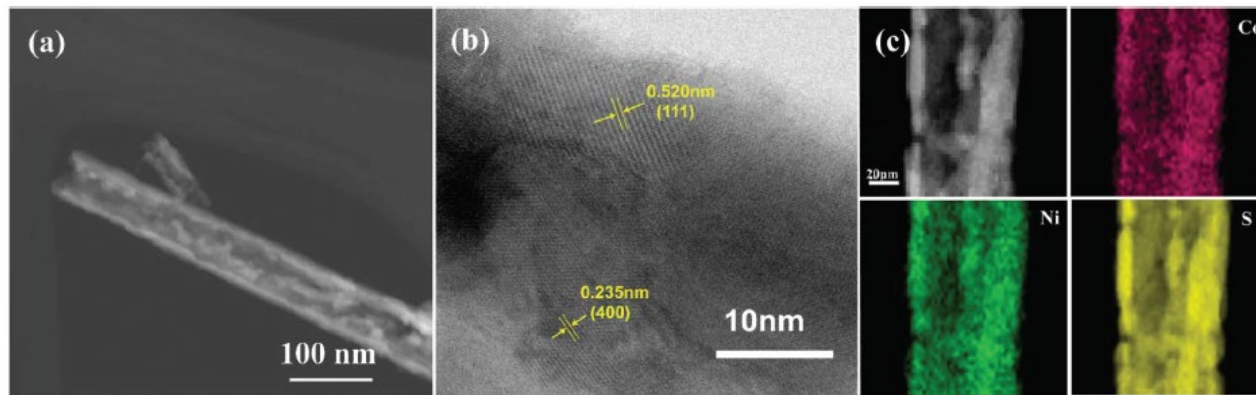
Stress-strain curve and post-compressed pillar of Al/Al_3BC composites with 25% mass fraction of Al_3BC .

Y. Zhao, X. Ma and X. Liu, Shandong University, China, and N. Chawla, ASU. Work performed at NCI-SW.

Journal of Alloys and Compounds, vol. 823, article153842, 2020.

Hollow NiCo_2S_4 nanotubes for flexible solid-state supercapacitors

Flexible, lightweight, and high-energy-density asymmetric supercapacitors (ASCs) are highly attractive for portable and wearable electronics. However, the implementation of such flexible ASCs is hampered by the low specific capacitance and sluggish reaction kinetics of the electrode materials. Herein, a hierarchical core-shell structure of hybrid glucose intercalated NiMn-LDH (NiMn-G-LDH)@ NiCo_2S_4 hollow nanotubes is deliberately constructed on flexible carbon fiber cloth. The highly conductive hollow NiCo_2S_4 nanotube arrays provide high-speed pathways for ion and electrolyte transfer. The as-assembled flexible all-solid-state supercapacitor device can work at various bending angles and exhibits an impressive energy density of 60.3 W h kg^{-1} at a power density of 375 W kg^{-1} .



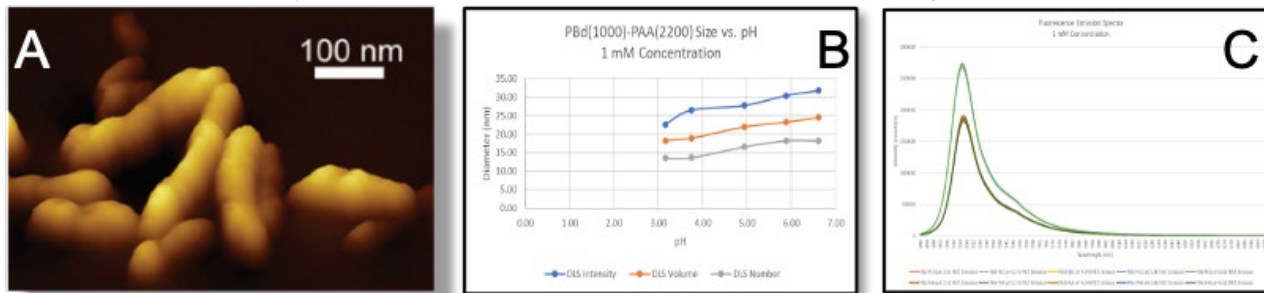
TEM and HRTEM images of (a, b) NiCo_2S_4 and (c) the corresponding EELS mappings.

S. Chen, Q. Deng and Z. Zeng, Nanchang University, China, and S. Deng, ASU. Work performed at NCI-SW.

Nanoscale, vol. 12, pp. 1852-1863, 2020.

Dynamic Supramolecular Polymer Nanocomposites for Advanced Photonics

Previous work has demonstrated the unique organizational control of amphiphilic block copolymers (ABCs) as scaffolds for other molecules and nanoparticles. Certain ABCs can form biomimetic membranes whose properties resemble lipid bilayers but with greatly enhanced stabilities, and these membranes can also enable precise organization of nanoscale materials such as chromophores and quantum dots, resulting in “nanocomposites” with controlled functional response and potential emergent phenomena. In this work, dynamic, poly-acrylic acid-b-polybutadiene (pAA-b-pBD) ABC polymers were explored in terms of structural stability and photonic response as a function of pH and ionic strengths. The results have demonstrated that pAA-pBD micelles are feasible for the generation of dynamic polymer chlorosome nanocomposites (PCN) with potential unique photonic properties. Continuing work will explore rational design of photonic activity through an iterative theory-experiment approach toward inducing quantum photonic behavior.



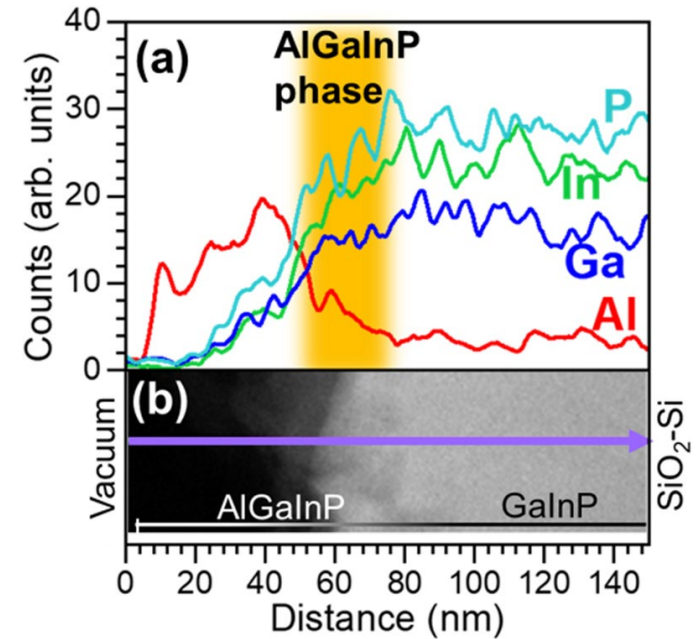
(A) AFM of PCN indicating chlorosome-like morphology. (B) Dynamic Light Scattering of pAA-b-pBD micelles indicating increase in size as a function of pH. (C) Fluorescence emission of chromophores inside pAA-b-pBD micelles as a function of pH indicating photonic stability across pH

Jonathan Chin, Gabriel A. Montañó, and Ines Montañó, ¡MIRA! Center, Northern Arizona University. Work performed at NCI-SW.

Polycrystalline $Ga_xIn_{1-x}P$ for use as a solar cell absorber with a tunable bandgap

There is ongoing interest in developing a stable, low-cost, 1.6–1.8 eV top-cell material that can be used for two-junction (tandem) solar cells, particularly in combination with a silicon bottom cell. In this work, polycrystalline GaInP is grown and characterized to explore its properties and use for this purpose. The film composition and deposition temperature are varied to determine their effects on grain size, morphology, and photoluminescence (PL) over a range of bandgaps from 1.35 to 1.7 eV. An Al-assisted post-deposition treatment for 1.7-eV polycrystalline GaInP results in a 90-fold increase in peak photoluminescence (PL) intensity, a 220-fold increase in integrated PL intensity, and increased time-resolved PL lifetime from <2 ns to 44 ns. The increase in PL intensity and lifetime is attributed to a reduction of nonradiative minority-carrier recombination at the top surface, and at grain boundaries near the surface, due to the formation of a higher-bandgap AlGaInP alloy. These materials provide a viable path toward increased minority-carrier concentration under illumination and improved recombination properties needed for high-efficiency tandem solar cells

Richard King, School of ECEE, ASU. Work performed at NCI-SW.

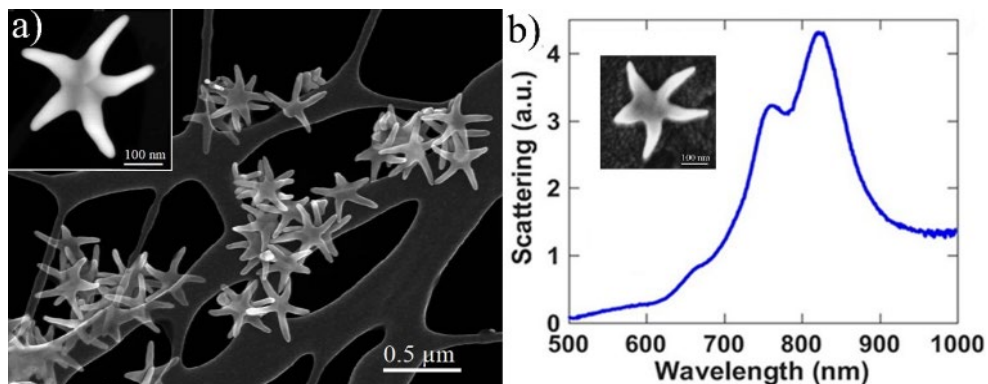


EDS line scan from top surface toward the bottom Si substrate plotting the variation of Al, Ga, In, and P concentrations near the top surface of one GaInP grain. (b) TEM image of GaInP highlighting the region along which EDS line scan was measured.

National Research Priority: NAE Grand Challenge—Make Solar Energy Economical

Detection of the COVID-19 virus using Surface Enhanced Raman Spectroscopy

The COVID-19 pandemic has demonstrated the critical need for accurate and rapid testing for virus detection. Most of the testing techniques use biochemistry and require chemicals that are often expensive and might become scarce in a crisis. An alternative approach uses novel nanomaterials for surface enhanced Raman spectroscopy (SERS) that provides a very distinct spectroscopic signature of the COVID-19 virus. The spectrum is mainly composed of signals from the spike and nucleocapsid proteins on the surface of the virus and can be used to develop a fast, inexpensive, and reliable COVID-19 test.



SEM image of the Au-Cu nanostars used as the SERS substrate (a). Optical absorption spectra of the nanostars revealed a strong peak in the near IR (b).

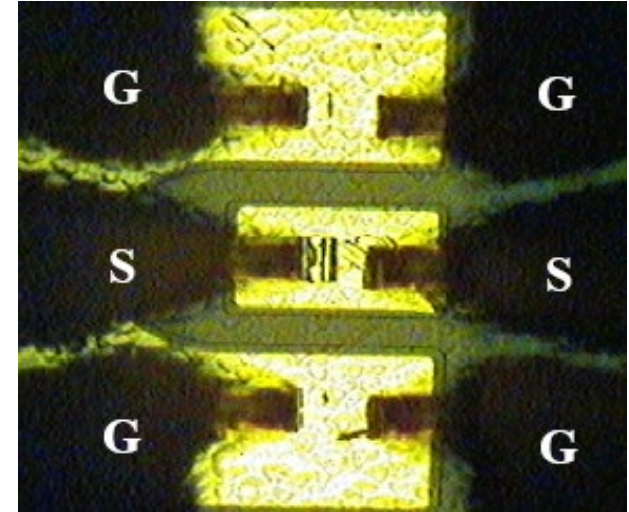
Miguel José Yacamán, ¡MIRA! Center, Northern Arizona University. Work performed at NCI-SW.

RSC *Advances*, vol. 11, pp. 25788-25794, 2021.

National Research Priority: NAE Grand Challenge—Engineer the Tools of Scientific Discovery

Diamond Schottky PIN Diodes for Receiver Protector Applications

Diamond Schottky p-i-n diodes have been grown by PECVD and incorporated as a shunt element within co-planar striplines for RF characterization. The PIN diodes have a thin, lightly doped n-type layer that is fully depleted by the top metal contact and they operate as high-speed Schottky rectifiers. In the off state, the diode insertion loss is less than 0.3 dB at 1 GHz and increases to 14 dB when forward biased to 7.6V. Compared to conventional silicon or compound semiconductor-based power limiters the superior thermal conductivity of the diamond Schottky PIN diodes make them ideally suited for RF receiver protectors that require high power handing capability for national security applications.



Ground-Signal-Ground probe arrangement on the diamond p-i-n diode co-planar stripline.

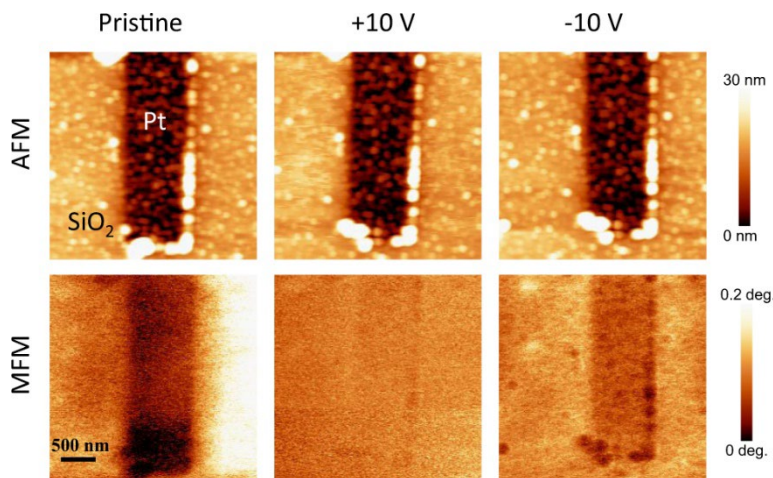
Trevor Thornton, School of ECEE, ASU. Work performed at NCI-Sw.

Solid-State Electronics, vol. 186, article 108154, 2021.

Nebraska Nanoscale Facility (NNF)

Voltage controlled Néel vector rotation in zero magnetic field

Binek and coworkers utilized the NNF Facilities and fabricated a Boron doped chromia based energy efficient memory which operates up to 400K in zero magnetic field. Their work showed that B-doping of chromia creates a single-phase material, which enables voltage-controlled nonvolatile rotation of the Néel vector in zero H-field and CMOS compatible operation temperatures. They found that B:Cr₂O₃ simultaneously acquires new tunable functionalities in addition to the linear magnetoelectricity known from Cr₂O₃. Those include T_N and resistivity enhancement, reduced and voltage controllable anisotropy, spin-canting and transient electric polarizability not observed in pure chromia. Emerging functionality associated with B-doping include purely electric-controlled 90° nonvolatile rotation of the Néel vector up to T = 400 K. Indirect coupling between polar and AFM order explains the experimental findings and allows to estimate switching speeds on the order of 100 ps. Theoretical modeling estimates switching speeds of about 100 ps making B:Cr₂O₃ a promising multifunctional single-phase material for energy efficient nonvolatile CMOS compatible memory applications.



Top row: topographic images of a segment of the Pt Hall cross before and after application of the poling pulses (2 s; ± 10 V). Bottom row: MFM images of the same segment after application of the poling pulses.

Mahmood, W. Echtenkamp, M. Street, J.-L. Wang, S. Cao, T. Komesu, P. A. Dowben, P. Buragohain, H. Lu, A. Gruverman, A. Parthasarathy, S. Rakheja & C. Binek, Dept. of Elect. Eng. New York University, & Holonyak Micro and Nanotechnology Laboratory, University of Illinois at Urbana–Champaign, Nebraska Center for Materials and Nanoscience (NCMN), Dept. of Physics and Astronomy, University of Nebraska-Lincoln. Work performed at Nebraska Nanoscale Facility.

Nature Comm. 12, 1674 (2021).

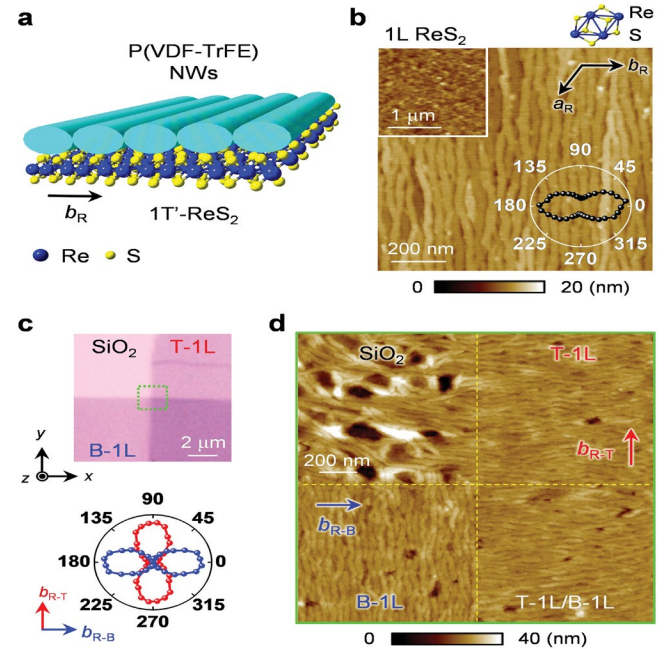
National Research Priority: NSF–Quantum Leap

Assembly of Close-Packed Ferroelectric Polymer Nanowires via Interface-Epitaxy with ReS_2

The flexible, transparent, and low-weight nature of ferroelectric polymers makes them promising for wearable electronic and optical applications. Xia Hong and coworkers utilized NNF facilities and developed P(VDF-TrFE) thin films composed of close-packed crystalline nanowires via interface-epitaxy with 1T'- ReS_2 . Upon controlled thermal treatment, uniform P(VDF-TrFE) films restructure into about 10 and 35 nm-wide (010)-oriented nanowires that are crystallographically aligned with the underlying ReS_2 , as revealed by high-resolution TEM. Piezoresponse force microscopy studies confirm the out-of-plane polar axis of the nanowire films and reveal coercive voltages as low as 0.1 V. Reversing the polarization can induce a conductance switching ratio of $>10^8$ in bilayer ReS_2 , over six orders of magnitude higher than that achieved by an untreated polymer gate. This study points to a cost-effective route to large-scale processing of high-performance ferroelectric polymer thin films for flexible energy-efficient nanoelectronics.

D. Li, S. Sun, K. Wang, Z. Ahmadi, J. E. Shield, S. Ducharme, X. Hong, Nebraska Center for Materials and Nanoscience (NCMN), *Dept. of Mech. and Mater. Eng.*, Dept. of Physics and Astronomy, University of Nebraska – Lincoln. Work performed at Nebraska Nanoscale Facility.

This work was supported by DOE (DE-SC0016153). *Advanced Materials* 2021, 33, 2100214.

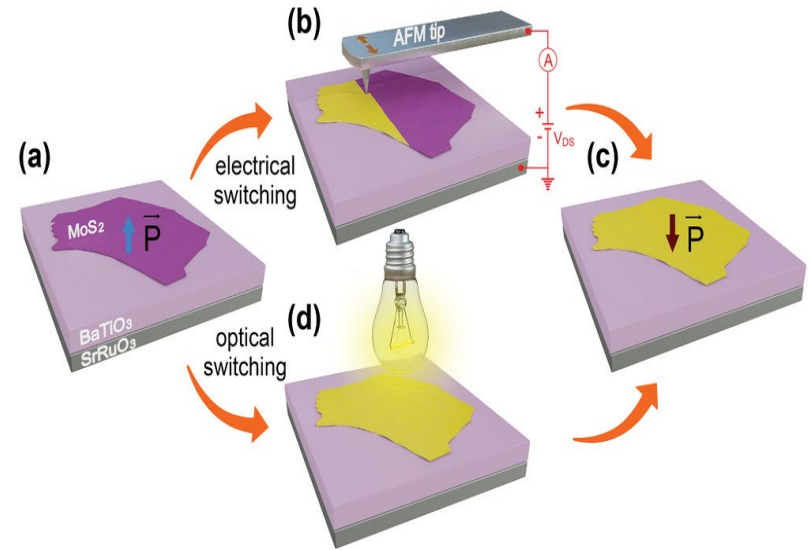


P-NW film on ReS_2 . a) Sample schematic. b) AFM topography image of a P-NW film formed on 1L ReS_2 . Upper inset: AFM image of the initial 9 ML LB film. Lower inset: polarization-resolved Raman signal of mode V of the 1L ReS_2 . c) Optical image of two perpendicularly stacked 1L ReS_2 flakes (top), and the polar plots of parallel polarization-resolved Raman signal of mode V for the T-1L (red) and B-1L (blue) ReS_2 (bottom). d) AFM image of the boxed area in (c). The crystalline orientations of ReS_2 are labeled.

National Research Priority – Growing Convergence Research

Using Light for Better Programming of Ferroelectric Devices

The recent discoveries of light–matter interactions in heterostructures based on 2D semiconductors and FE materials open new opportunities for using light as an additional tool for device programming. Sinitskii and coworkers utilized NNF Facilities and demonstrated that the combined use of an electrical field and visible light improves the nonvolatile ON/OFF ratios in MoS₂-PZT memories by several orders of magnitude compared to their purely electrical operation. The memories are read at zero gate voltage (V_G) in darkness, but their ON and OFF currents, which routinely varied for different devices by over 10^5 , are achieved by programming at the same $V_G = -6$ V with (ON state) and without (OFF state) light illumination, demonstrating its crucial importance. The light can likely serve as an important tool for better programming of a large variety of other semiconductor-FE devices.



Scheme of electrical and optical switching of FE polarization of BTO under a MoS₂ flake in a MoS₂-FE heterostructure; see text for details. The purple and yellow colors and the vertical arrows represent the polarization of BTO under the MoS₂ flake.

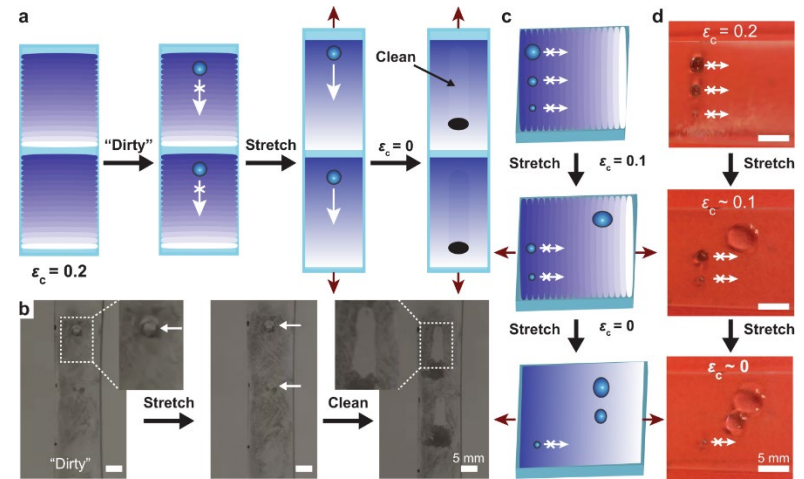
Alexi Lipatove, Natalia S. Vorobeva, Tao Li, Alexei Gruverman, Alexander Sinitskii, Dept. of Chemistry, Nebraska Center for Materials and Nanoscience (NCMN) and Dept. of Physics and Astronomy, University of Nebraska – Lincoln. Work performed at Nebraska Nanoscale Facility.

This work was supported by NSF (DMR-1420645). *Adv. Elect. Mater.* 2021, 7, 2001223

National Research Priority: NSF–Growing Convergence Research

Dynamic manipulation of droplets using mechanically tunable microtextured chemical gradients

Stephen Morin and coworkers used NNF facilities and reported the fabrication of mechano-tunable, microtextured chemical gradients on elastomer films and their use in controlled microdroplet transport. Specifically, discrete mechanical deformations of these films enabled dynamic tuning of the microtextures and thus transport along surface-chemical gradients. The interplay between the driving force of the chemical gradient and the microtopography was characterized, facilitating accurate prediction of the conditions (droplet radius and roughness) which supported transport. In this work, the use of microtextured surface chemical gradients in mechano-adaptive materials with microdroplet manipulation functionality was highlighted. We believe that extensions of the demonstrated concepts will lead to more sophisticated surface-fluidic capabilities useful to, for example, biomedical and analytical devices, mechano-switchable water sorting devices, surface lab-on-chip devices, and adaptive materials for emergent robotic applications.



a Schematic illustration of the use of mechanical deformations to activate droplet transport and thus self-cleaning functionality. **b** Optical micrographs of the mechanically activated self-cleaning process (insets are higher magnification of the highlighted regions, and compressive strain, ϵ_c is given). **c** Schematic illustration of the operation of a mechanically controlled droplet sorting device. **d** Optical micrographs of a droplet sorting device in operation. Transport of a $5\ \mu\text{L}$ droplet occurs following activation of the gradient using a compressive strain of $\epsilon_c = 0.1$. Transport of a $2.5\ \mu\text{L}$ droplet occurs following maximal activation of the gradient by reducing compressive strain to $\epsilon_c = 0.0$. The $1\ \mu\text{L}$ droplet is below the critical radius of transport for this device and does not move.

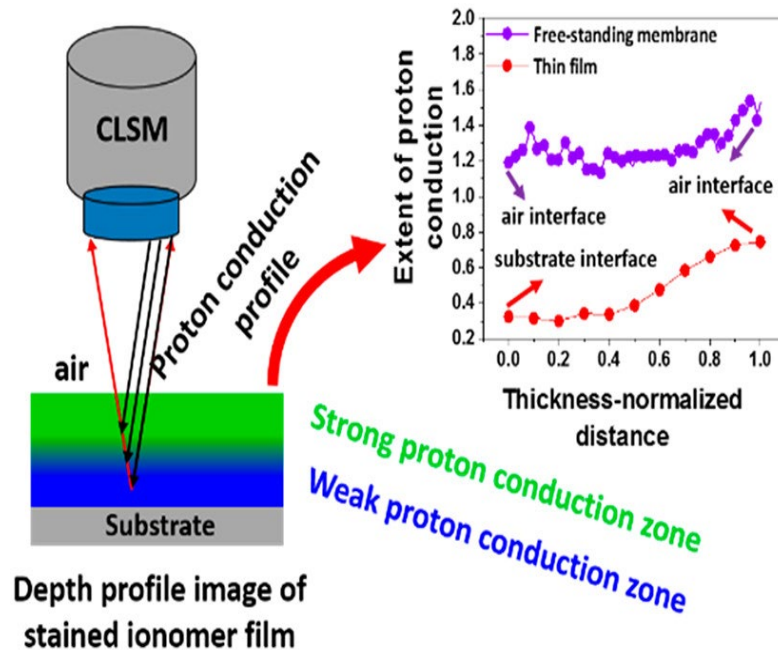
Ali J Mazaltarim, John J Bowen, Jay M Taylor, Stephen A Morin, Dept. of Chemistry, Nebraska Center for Materials and Nanoscience (NCMN) & NCIBC, University of Nebraska – Lincoln. Work performed at Nebraska Nanoscale Facility.

This work was supported by NSF Award # 1555356. *Nature Comm.* 2021, 12, 3114

National Research Priority: NSF–Understanding the Rules of Life

Unraveling Depth-Specific Ionic Conduction and Stiffness Behavior across Ionomer Thin Films and Bulk Membranes

Interfacial behavior of submicron thick polymer films critically controls the performance of electrochemical devices. Shudipto Dishari and coworkers developed a robust, everyday-accessible, fluorescence confocal laser scanning microscopy (CLSM)-based strategy that can probe the distribution of mobility, ion conduction, and other properties across ionomer samples. When fluorescent photoacid probe 8-hydroxypyrene-1,3,6-trisulfonic acid trisodium salt (HPTS) was incorporated into $<1\ \mu\text{m}$ thick Nafion films on substrates, the depth-profile images showed thickness- and interface-dependent proton conduction behavior. In these films, proton conduction was weak over a region next to substrate interface, then gradually increased until air interface at 88% RH. The CLSM-based strategy now allows us to reveal how the ionic conductivity is at different depths and how far the interfacial effects propagate inside very thin films. Such information will guide us to design catalyst layers for electrochemical devices.



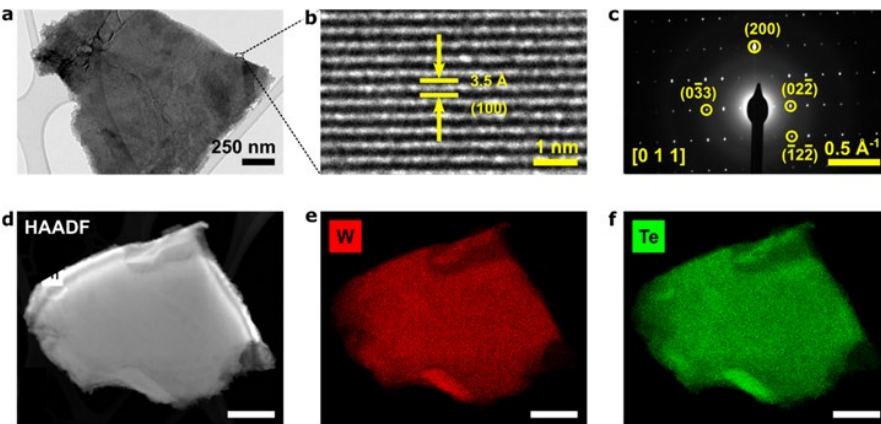
Seefat Farzin, Ehsan Zamani, and Shudipto K. Dishari, Dept. of Chem. and Biomolecular Eng., University of Nebraska-Lincoln. Part of the work performed at Nebraska Nanoscale Facility.

This work was supported by NSF Award # 1750040. *ACS Macro Letters*, 2021, 10, 791

National Research Priority: NSF–Growing Convergence Research

Weyl semimetal orthorhombic Td-WTe₂ as an electrode material for sodium- and potassium-ion batteries

Gurpreet Singh and coworkers at the Kansas State University used NNF facilities to study orthorhombic tungsten ditelluride or Td-WTe₂ as an electrode material for sodium- (SIB) and potassium-ion batteries (KIB) in propylene carbonate (PC) based electrolyte. Results show that despite larger Shannon's radius of potassium-ions and their sluggish diffusion in Td-WTe₂ due to higher overpotential, at 100 mA.g⁻¹ KIB-half cells showed higher cycling stability and low capacity decay of 4% versus 16% compared to SIB-half cells. Likewise, in a rate capability test at 61st cycle (at 50 mA.g⁻¹), the KIB-half cells yielded charge capacity of 172 mAh.g⁻¹ versus 137 mAh.g⁻¹ of SIB-half cells. The superior electrochemical performance of Td-WTe₂ electrode material in KIB-half cells is explained based on the concept of Stokes' radius—smaller desolvation activation energy resulted in higher mobility of potassium-ions in PC-based electrolyte.



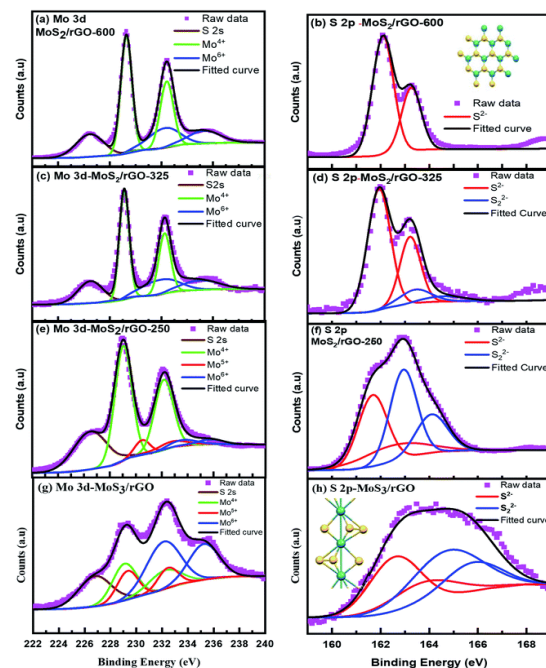
Morphology characterization of Td-WTe₂: TEM images of (a) Td-WTe₂ nanosheets, and (b) Td-WTe₂ lattice fringes assigned to plane (100). (c) SAED image of pristine Td-WTe₂ (ICSD collection code 259467). (d) High-angle annular dark-field imaging (HAADF). Scanning transmission electron microscope (STEM) showing (e) W, and (f) Te. Scale bars in (d)–(f), 300 nm..

Davi Marcelo Soares, Gurpreet Singh, Department of Mechanical and Nuclear Engineering, Kansas State University, Kansas. Part of the work performed at Nebraska Nanoscale Facility..

This work was supported by NSF (#1454151). *Nanotechnology* 2021, 32, 505402

Tuning the defects in MoS₂/reduced graphene oxide 2D hybrid materials for optimizing battery performance

Jun Li and coworkers from Kansas State University utilized NNF Facilities to demonstrate that defect engineering is critical for improving Zn-ion storage. The study reports the preparation of a set of hybrid materials consisting of molybdenum disulfide (MoS₂) nanopatches on reduced graphene oxide (rGO) nanosheets by microwave specific heating of graphene oxide and molecular molybdenum precursors followed by thermal annealing in 3% H₂ and 97% Ar. The unique defect-engineered hybrid material of MoS₂ on reduced graphene oxide opens a new road to enhance monovalent and divalent ion storage. The few-layered MoS₂ nanopatches stacked on the rGO nanosheets significantly improve the intercalation of Li⁺ ions while the high-density Mo-deficient defects enhance the Zn-ion storage at the defective S-edges. The highly defective MoS₂/rGO hybrid prepared by annealing at 250 ° C shows the highest initial Zn-ion storage capacity (~300 mA h g_{MoS_x}⁻¹) and close to 100% coulombic efficiency.



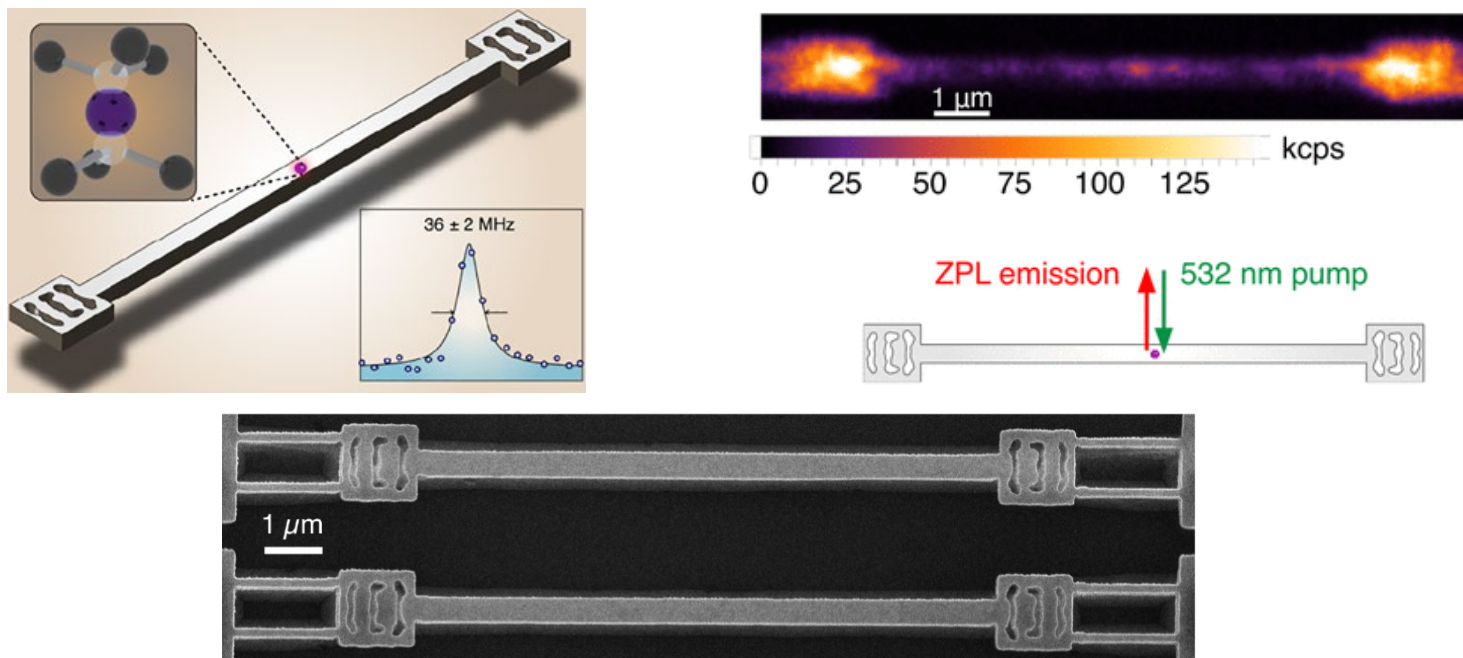
The Mo 3d and S 2p XPS spectra of (a, b) MoS₂/rGO-600, (c, d) MoS₂/rGO-325, (e, f) MoS₂/rGO-250 and (g, h) the MoS₃/rGO-intermediate product. The inset of panel (b) shows the schematic structure of the hexagonal MoS₂ nanopatches. The inset of panel (h) shows the schematic structure of the MoS₃ chain.

Kamalambika Muthukumar, Levon Leban, II Archana Sekar, Ayyappan Elangovan, Nandini Sarkar & Jun Li, Dept. of Chemistry, Kansas State University. Part of the work performed at Nebraska Nanoscale Facility.

Sustainable Energy Fuels, 2021, 5, 4002.

NNCI Site @ Stanford (nano@stanford)

Tin-Vacancy Centers in a Diamond Waveguide



Narrow-Linewidth Tin-Vacancy centers coupled to a 400nm diamond waveguide, fabricated by shallow ion implantation, are promising candidates for quantum emitters in quantum photonic processors. Right: PL map of a waveguide containing SnV-centers. Bottom: SEM image of a waveguide device.

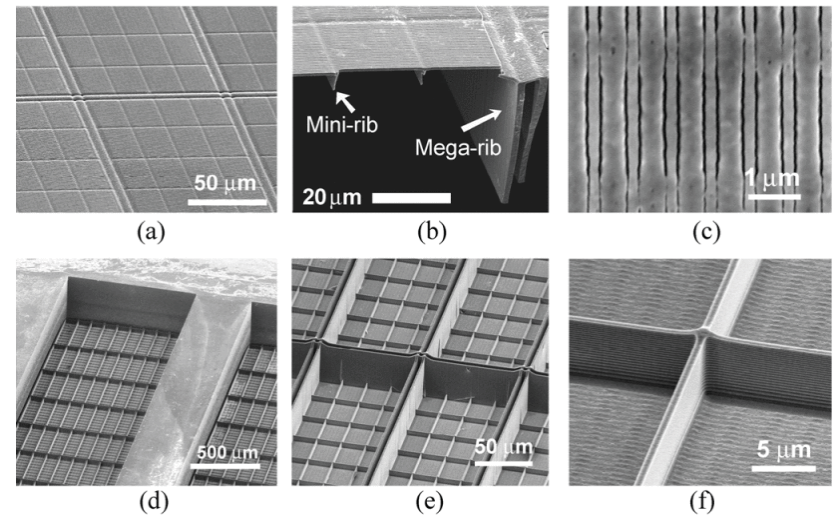
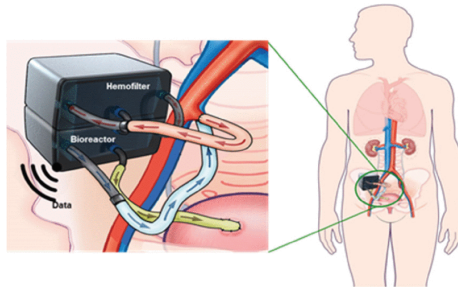
Profs. Zhi-Xun Shen, Nicholas Melosh, and Jelena Vučković (Stanford University). Work performed using E-Beam system at Stanford Nano Shared Facilities, nano@stanford site.

This work was supported by NSF Award # ECCS-2026822. *ACS Photonics* (2020) doi:10.1021/acsphotonics.0c00833

National Research Priority: NSF–Quantum Leap

Nanoporous Membranes for the Implantable Bio-Artificial Kidney

Silicon nanoporous membranes provide the fundamental underlying technology for the development of an implantable bio-artificial kidney. These membranes, which are comprised of micromachined slit-pores that are nominally 10 nm wide, allow for high-efficiency blood filtration as well as immunoprotection for encapsulated cells. Relying on a two-step Deep Reactive Ion Etch (DRIE) process, and the availability of the ASML stepper system with a unique 3-D align capability, both at nano@stanford, the group has fabricated and tested freestanding membrane spans that are up to 14 times wider than before, with approximately double the measured permeability per unit area. The new architecture can also improve cross-membrane mass-transfer rates and reduce chip-fabrication costs.



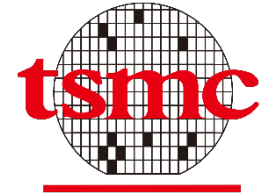
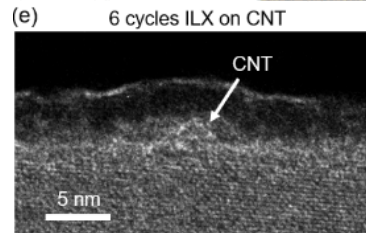
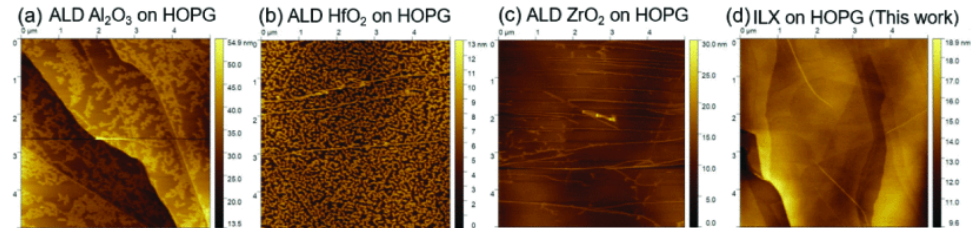
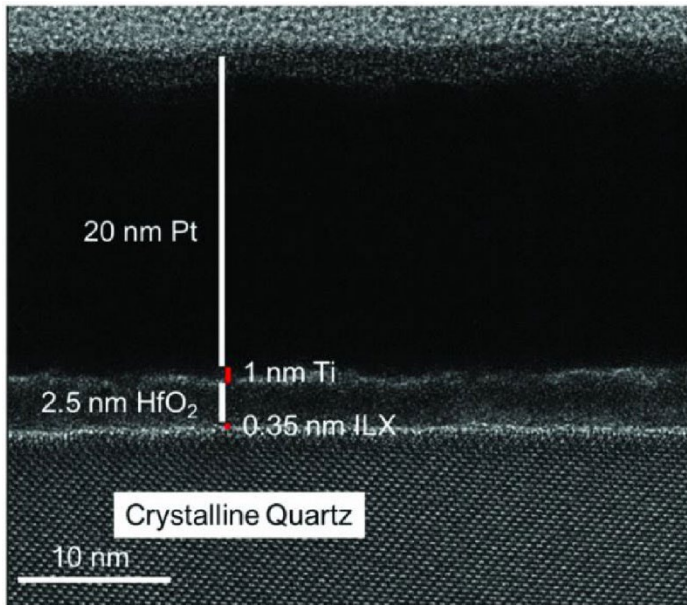
Above: Scanning electron micrographs (SEMs) of (a) Top view of mega-rib membrane; (b) Cross-section showing mini-ribs and mega-rib; (c) Close-up top view of nanopores; (d) Backside image of mega-rib membrane showing silicon-wafer “frame” and mega-ribs; (e) Further close-up showing mega-ribs and mini-ribs; (f) Even further close-up showing mini-ribs and nanopores.

Benjamin W. Chui, Shuvo Roy, et al., (University of California at San Francisco). Work performed on ASML at Stanford Nanofabrication Facility and SEM at Stanford Nano Shared Facilities, nano@stanford site.

This work was supported by NSF Award # 2026822. *JMEMS* (2020) doi:10.1109/JMEMS.2020.3013606

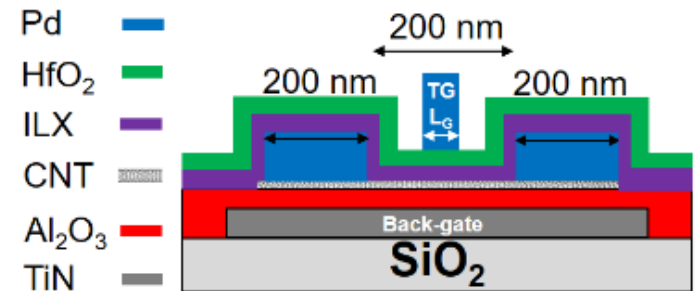
National Research Priority: NSF–Growing Convergence Research

Sub-0.5 nm Interfacial Dielectric Enables Superior Electrostatics



0.35nm Interfacial layer dielectric (ILX), composed of Al₂O₃ deposited by low temperature “nanofog” method, followed by 2.5nm high-k ALD HfO₂ dielectric, provides energy and performance gains of carbon nanotube field-effect transistors (CNFETs).

Fabricated and characterized at nano@stanford.



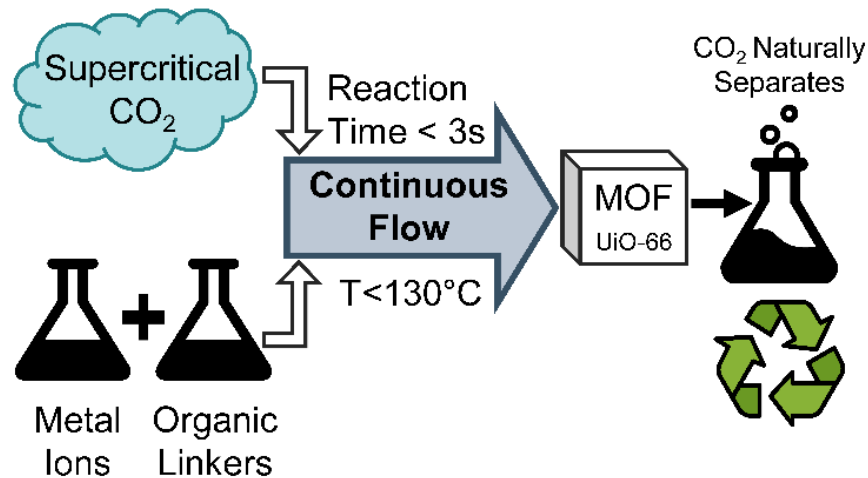
Greg Pitner (TSMC), Subhasish Mitra, H.-S. Philip Wong (Stanford University), Andrew Kummel, Prabhakar Bandaru (UCSD), et al. Fabrication done at Stanford Nanofabrication Facility and TEM at Stanford Nano Shared Facilities, nano@stanford site.

This work was supported by NSF Award # 2026822. *IEEE IEDM* (2020) doi:10.1109/IEDM13553.2020.9371899

Northwest Nanotechnology Infrastructure (NNI)

Continuous Flow Synthesis of Metal-Organic Frameworks in Supercritical CO₂

The high surface areas and tunable porous structures of Metal-Organic Framework (MOF) materials offer desirable capabilities in a wide range of applications, including gas separation, catalysis, batteries, fuel cells, supercapacitors, drug delivery and imaging. One challenge to the widespread use of MOFs is a lack of large-scale manufacturing synthesis processes. We demonstrated a novel method of continuous synthesis of MOF using supercritical carbon dioxide (scCO₂), introduced through a custom counter-current mixer, to provide enhanced heat and mass transfer to MOF precursor materials. The method was used to synthesize several MOFs at a production rate several orders magnitude faster than batch methods. Additionally, testing showed that this method could be used to activate as well as continuously synthesize MOF materials. Our method results in rapid reaction time (<3s), can be easily scaled, and it allows for recovery of effluent and unreacted material, which is challenging in hydrothermal and supercritical water-based systems. The UW has a pending PCT application; our current efforts are aimed at extending the method for synthesis of Graphene – MOF composites for gas separation and biomedical applications.



The reactor incorporates two reagent feeds: a metal precursor and an organic precursor injected into scCO₂, which provides rapid heating and mixing. The mixture enters the heated reactor section with controlled temperature and pressure. Following the reactor section, the effluent is cooled to room temperature and passed through a back pressure regulator. The MOFs are collected in the liquid phase.

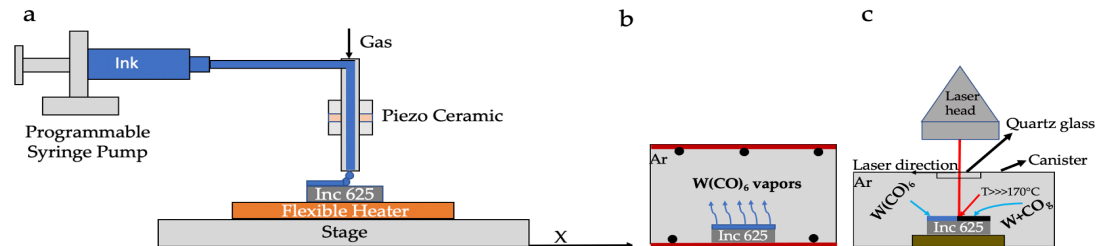
Igor Novosselov. Work performed at NanoES, MAF, CEI .

Funding support from DoD (HDTRA1-17-1-0001). doi.org/10.1021/acssuschemeng.0c01429.

National Research Priority: NSF–Growing Convergence Research

A Scalable Solution Route to Porous Networks of Nanostructured Black Tungsten

The work focusses on solution based printing of W from volatile CVD precursor for hybrid additive manufacturing. This hybrid additive manufacture is capable of producing functional alloys by integrating commercial LPBF machine with inkjet printhead (or could be a aerosol jet printhead) without using ball milling of different materials. Laser was used to convert the precursor to manufacture porous networks of nanostructured tungsten for solar-thermal applications. The solar absorptivity of Inconel 625 is enhanced using these coatings.



Schematics of experimental setup a) precursor deposition setup; b) precursor deposited substrate placed in a conventional furnace; C) laser canister setup used in this work.

V. Vinay K. Doddapaneni, Kijoon Lee, Tyler T. Colbert, Saereh Mirzababaei, Brian K. Paul, Somayeh Pasebani, and Chih-Hung Chang, School of Chemical, Biological, and Environmental Engineering, School of Mechanical, Industrial, and Manufacturing Engineering, Advanced Technology and Manufacturing Institute, Oregon State University. Work performed at Advanced Technology and Manufacturing Institute and Oregon Process Innovation Center.

This work was supported by DOE (DE-EE0007888-10-4), Advanced Manufacturing Office, the Rapid Advancement in Process Intensification Deployment Institute, Murdock Charitable Trust (contract #2016231), NSF (MRI 1040588), NSF Advanced Manufacturing Program (856412). *Nanomaterials* **2021**, 11, 2304.

National Research Priority: NAE Grand Challenge—Making Solar Energy Economical

Sub-surface Contributions to Electrocatalysis in LaSrMnO_3

Electrocatalytic processes are acutely sensitive to the chemistry and structure of catalyst–electrolyte interfaces, and active sites are often assumed to be governed by the properties of their terminating surface layers. However, thickness-dependent activity in numerous metal-oxide systems suggests that crucial interactions exist between surface and subsurface layers.

Here, dramatic variations appeared in electric resistivity and electrocatalytic activity for thin LaSrMnO_3 films as a function of thickness in model conductive oxide heterostructures (LaSrMnO_3 - SrRuO_3 - NbSrTiO_3). X-ray photoelectron spectroscopy revealed distinct thickness-dependent film composition, suggesting Sr segregation yielding an ultra-thin insulating layer at the film-substrate interface. Electrochemical activity in these systems was modulated by interaction with subsurface layers across an electrochemically active depth, t_{ec} , of ten unit cells, demonstrating sub-surface contributions to the activity.

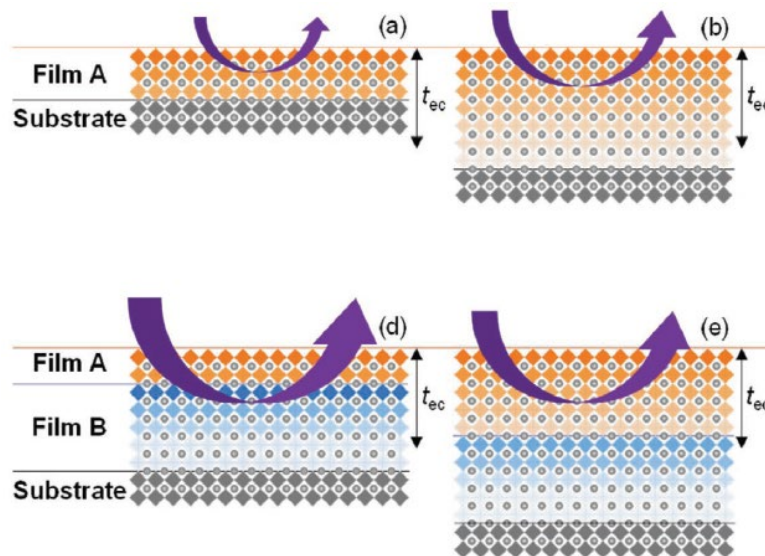


Illustration of the electrochemically active depth, t_{ec} , in different oxide heterostructures. Within t_{ec} , variations in the oxide heterostructure composition play a key role in electrochemical activity.

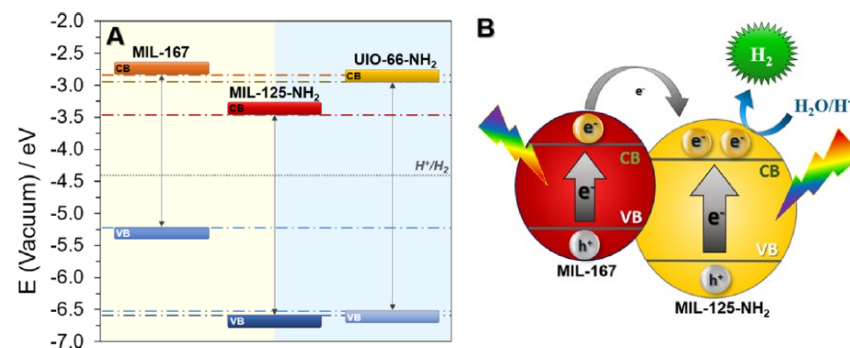
J. Lee, P. Adiga, S. A. Lee, S. H. Nam, H.-A. Ju, M.-H. Jung, H. Y. Jeong, Y.-M. Kim, C. Wong, R. Elzein, R. Addou, K. A. Stoerzinger, W. S. Choi, Dept. of Physics, Dept. of Energy Science, Sungkyunkwan University; CBEE, Oregon State University; Dept. of Physics, Pukyong National University; GSSMDE, Ulsan National Institute of Sci. & Tech., Physical Sciences Division, PNNL. Work performed at OSU Ambient Pressure Surface Characterization Laboratory.

This work was supported by NSF–MRI DMR-1429765. *Small*, **2021**, 2103632.

MOF-MOF Heterojunctions for Enhanced Visible-Light-Driven H_2 Production

Metal–organic frameworks (MOFs) have attracted significant attention in fields from water remediation, to catalysis, and energy storage/transfer. Recently, MOFs have been applied in MOF-MOF heterojunctions for enhanced electrocatalytic and photocatalytic activity. A major challenge in MOF photocatalysis is the development of systems with narrow band gap and excellent charge separation efficiency.

Here, MOF-MOF heterojunctions with proper band alignment, visible light absorption, and charge separation were constructed, yielding enhanced photocatalytic H_2 production compared with either of the individual MOF heterojunction constituents. Valence band measurements confirm the energy level alignment predicted by density functional theory calculations, providing a picture of the electronic properties leading to enhanced photocatalytic activity.



(A) Computed electronic band alignment relative to the vacuum level of MOF photocatalysts investigated here. XPS revealed that the energy levels of the MOF VBs follow the same trend as the computed VB positions.

(B) Schematic representation of a type II heterojunction with MOFs MIL-167 and MIL-125-NH₂.

S. Kampouri, F. M. Ebrahim, M. Fumanal, M. Nord, P. A. Schouwink, R. Elzein, R. Addou, G. S. Herman, B. Smit, C. P. Ireland, K. C. Stylianou. Inst. of Chemical Sciences and Engineering, École Polytechnique Fédérale de Lausanne; CBEE, Oregon State University. Work performed at OSU Ambient Pressure Surface Characterization Laboratory.

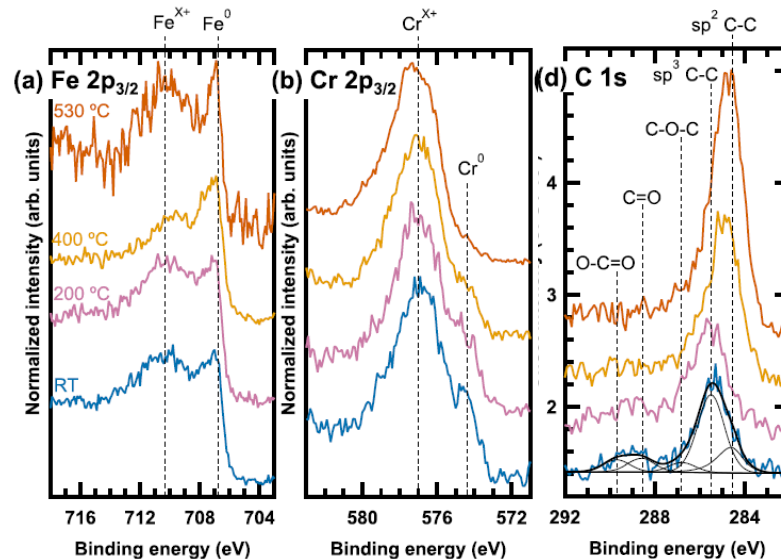
This work was supported by NSF–MRI DMR-1429765. *ACS Appl. Mater. Interfaces*, **2021**, 13, 14239

National Research Priority: NAE Grand Challenge–Making Solar Energy Economical

Molecular-scale oxidation of chromia-forming alloys in high-temperature CO₂

Owing to their oxidation resistance, chromia forming alloys have been applied for decades as construction materials in power plants, where they are exposed to high temperature CO₂. While Cr containing alloys tend to develop protective chromium-rich oxide layers, exposure to high temperature CO₂ is more corrosive to such steels than exposure to pure O₂. The development of alloys resistant to high temperature CO₂ corrosion is thus highly important for improving modern power systems.

Here, ambient pressure X-ray photoelectron spectroscopy revealed that chromium containing alloys experience selective Cr oxidation when exposed to CO₂ at high temperatures and high purity. CO₂ exposure in these systems leads to C accumulation, potentially altering the oxidation process. In contrast, low purity CO₂ exposure does not yield the same C accumulation, and leads to oxidation of additional alloy components that otherwise remain metallic in high purity CO₂. These findings provide previously inaccessible insights into the formation of protective Cr layers in materials crucial to modern power systems.



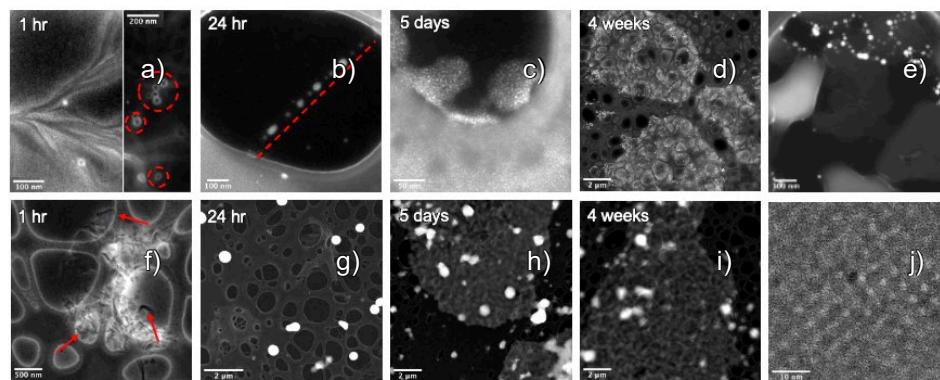
AP-XPS spectra of Fe²²Cr exposed to high purity CO₂: (a) Fe 2p_{3/2}. (b) Cr 2p_{3/2}. (d) C 1s.

R. P. Oleksak, R. Addou, B. Gwalani, J. P. Baltrus, T. Liu, J. T. Diulus, A. Devaraj, G. S. Herman, and Ö. N. Doğan, National Energy Technology Laboratory; NETL Support Contractor; CBEE, OSU; Physical and Computational Sciences Directorate, PNNL; National Energy Technology Laboratory. Work performed at Oregon State University's Ambient Pressure Surface Characterization Laboratory.

This work was supported by NSF-MRI DMR-1429765. *npj Mater. Degrad.*, **2021**, 5, 46.

Investigating the impact of nanoparticle size and surface chemistry on peptoid self-assembly

Utilizing peptoids (poly-N-substituted glycines) and quantum dots (QDs) allows for tunability of chemistry and sequence interactions to systematically study these interactions and target specific structures in a predictable manner. In this work, short chain peptoids with carboxylic acid groups are exchanged on to QDs at modest concentrations to result in partial ligand exchange. The impact of number of peptoids per QD, hydrophobicity of the QD surface, and size of the QD on the assembly pathway and final product were investigated. At low peptoid equivalence (0.33-5 eq. per QD), the final product remained the same with small peptoid sheets stitched together by QDs. Increasing the size of QDs led to large peptoid-QD hybrid sheets with the QDs in an ordered 2D lattice. Assemblies containing both small and large QDs generated large sheets with both QDs integrated into the structure. Increasing the hydrophobicity of the QD ligand shell, decreased the hybrid-unit solubility and generated amorphous, 3D structures that eventually phase segregated.



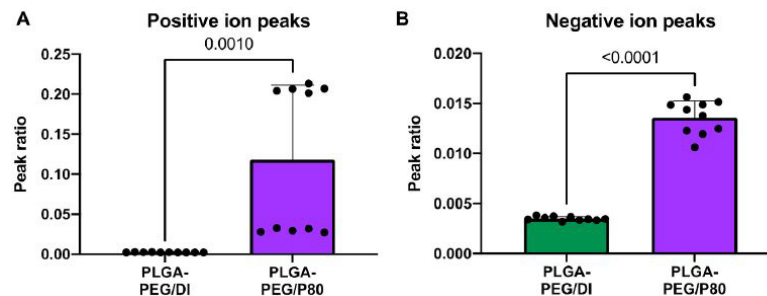
(a-d) 2.4 nm CdSe QDs assembling with 1 eq. Nbrpe₆Dig in H₂O/ACN forming large assemblies. Peptoid fibers and micelles form with QDs decorating the edges at early time points (a,b, red dashed lines) until small sheets evolve and stick together (c,d). (e) Small sheets with QDs on the edges inside the large assemblies from d. (f-i) 5.5 nm CdS QDs assembling with 1 eq Nbrpe₆Dig in DMSO/CHCl₃ forming large 2D sheets. At early times, peptoid sheets (red arrows) with QDs on the edges are observed (f) then hybrid sheets with integrated QDs appear and grow with time (g-i). (j) Ordered QDs lattices in a square close pack array inside the 2D sheets.

Madison Monahan, Renyu Zheng, Shuai Zhang, Micaela Homer, Chun-Long Chen, James De Yoreo, Brandi M. Cossairt
UW Chemistry, Materials Science and Engineering, and Chemical Engineering; PNNL Physical Sciences Division. Work performed at the University of Washington Molecular Analysis Facility.

This work was supported by DOE, Office of Science, Office of Basic Energy Sciences DE-SC0019288.

Surfactants influence polymer nanoparticle fate within the brain

This work focuses on the delivery of nanotherapeutics to the brain. Some surfactants used in nanoparticle synthesis have been shown to increase transport across the blood brain barrier. Understanding the role of surfactants in the nanoparticle fate is critical to designing effective therapeutics. Here we studied the role of several surfactants on nanoparticle transport to the brain. A crucial part of this work is verifying the presence of the surfactant on the nanoparticles. ToF-SIMS chemical specificity was able to verify the presence of P80 on PLGA-PEG nanoparticles. The PLGA-PEG nanoparticles showed enhanced uptake into the brain and localization within neurons and microglia.



ToF-SIMS peak ratio $A/(A + B)$ where A = sum of all P80 peaks and B = sum of all nanoparticle peaks for the positive ion (A) and negative ion (B) data. Green bar = PLGA-PEG control, purple bar = PLGA-PEG/P80.

Andrea Joseph, Georges Motchoffo Simo, Torahito Gao, Norah Alhindi, Nuo Xu, Daniel J. Graham, Lara J. Gamble, and Elizabeth Nance, Dept. of Chemical Engineering, Dept. of Biochemistry, National ESCA and Surface Analysis Center for Biomedical Problems, Dept. of Bioengineering, Center for Human Development and Disability, Dept. of Radiology UW. Work performed at the Northwest Nanotechnology Infrastructure.

This work was supported by NIH (#F31HD095572-03), NIH (EB-002027), NIGMS (#R35GM124677), and NSF (#1703438). *Biomaterials*, 2021, 277,121086.

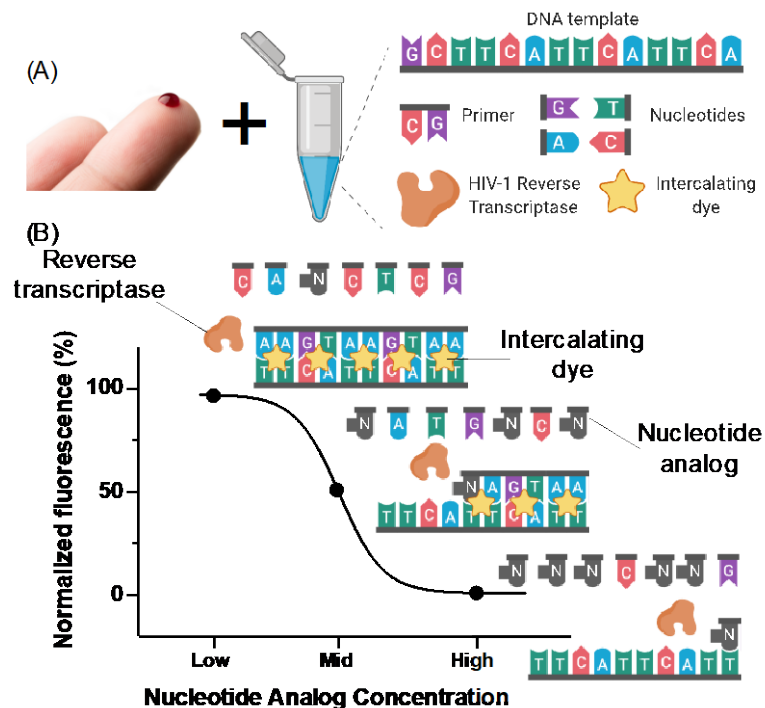
*National Research Priority: NSF–Understanding the Rules of Life and
NAE Grand Challenge–Engineer Better Medicines*

Rapid and User-Friendly Enzymatic Assays for Therapeutic Drug Monitoring

Rapid (<30 min) enzymatic assays measure medication concentration and can be used to improve medication adherence and prevent treatment failure.

Proof of concept measurement of nucleotide analog drugs used in human immunodeficiency virus (HIV) treatment and prevention (see Figure).

Extending assay strategy to support therapeutic drug monitoring of other infectious diseases (e.g., hepatitis, tuberculosis) and non-communicable diseases (cancer).



Ayokunle Olanrewaju, Mechanical Engineering, Univ. of Washington. Work performed at NNI.

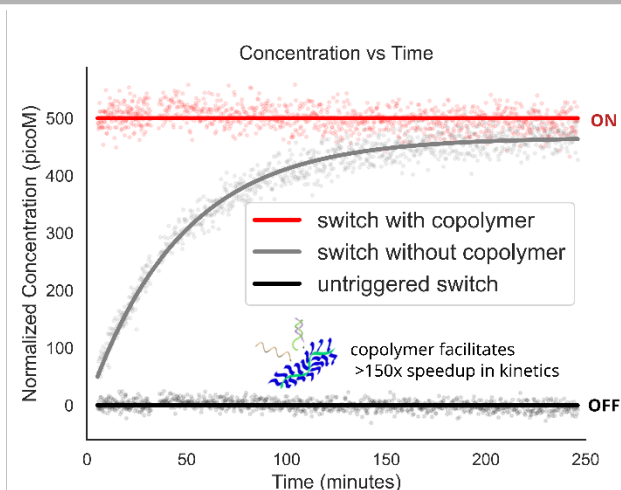
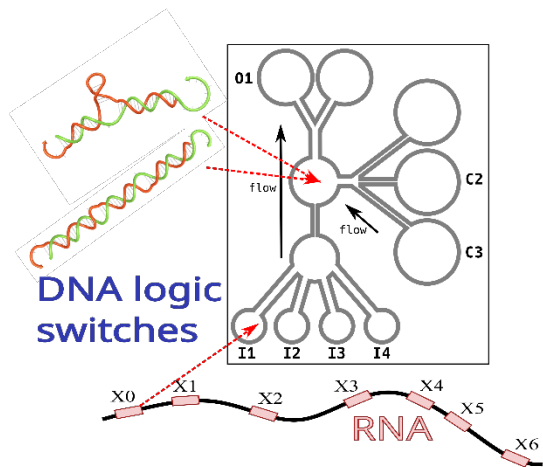
Supported by NIH (R01AI136648, R01AI157756), UW/Fred Hutch Center for AIDS Research, UW CoMotion Innovation Gap Fund, and the NIH-funded Atlanta Center for Microsystems Engineered Point-of-Care Technologies. *ACS Sensors* (2020) DOI:10.1021/acssensors.9b02198; *Virology Journal* (2021) DOI: 10.21203/rs.3.rs-104033/v2; Patent: Olanrewaju et al (2019) PCT/US2020/037609

National Research Priority: NSF–Understanding the Rules of Life and
NAE Grand Challenge–Engineer Better Medicines

Exquisite detection of molecular signals with enzyme-free, paper-based DNA circuits

Conventional tests for a variety of pathogens typically rely on the use of expensive enzymes, and require an intact cold-chain from point-of-distribution to point-of-use.

Enzyme-free, paper-based, DNA circuits are inexpensive, do not require refrigeration, and meet the requirements for point-of-care and low-resource diagnostics. They can be distributed as simply as mailing a letter, and can be made reconfigurable for different detection tasks once re-hydrated.



(Left) *Leakless* DNA circuits that incorporate exponential signal amplifiers are well suited for cheap diagnostics with exquisite detection in a paper-based device. Biological production of these circuits produces high fidelity components. (Right) A copolymer we refer to as the “magic buffer” speeds up the kinetics of these reactions by multiple orders of magnitude and could lead to rapid diagnostic applications. (Data collected by Cadence Pearce (UW CSE).)

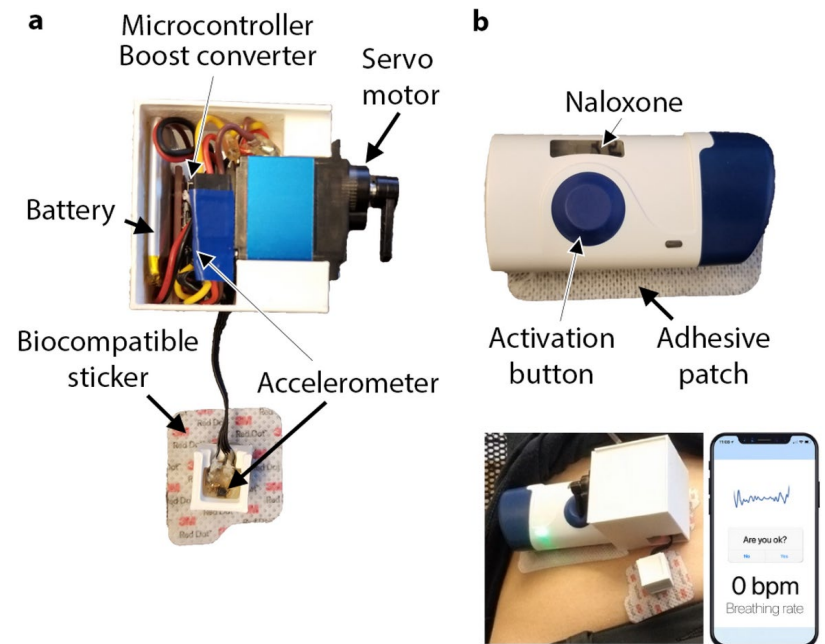
Chris Thachuk, Paul G. Allen School of Computer Science & Engineering, Univ. Washington. Work performed at the UW Institute for Nano-Engineered Systems (NanoES).

This work was supported by NSF (#2106695).

*National Research Priority: NSF–Understanding the Rules of Life and
NAE Grand Challenge–Engineer Better Medicines*

Closed-loop wearable naloxone injector system

Opioid overdoses can lead to respiratory failure, cardiac arrest, and death when left untreated. Opioid toxicity is readily reversed with naloxone, however there remains a critical need for technologies to administer naloxone in unwitnessed overdose events. We develop a closed-loop wearable injector system that measures respiration and apneic motion associated with an opioid overdose event using a pair of on-body accelerometers, and administers naloxone subcutaneously upon detection of an apnea. Our proof-of-concept system has been evaluated in both a supervised injection facility (SIF) and a hospital environment where we simulate opioid-induced apneas in healthy participants. A closed-loop naloxone injector system has the potential to complement existing evidence-based harm reduction strategies and help reduce opioid overdose deaths.



Overview of wearable auto-injector capable of detecting overdose events and injecting naloxone.

Justin Chan, Vikram Iyer, Anran Wang, Alexander Lyness, Preetma Kooner, Jacob Sunshine, and Shyam Gollakota. Work was performed at Northwest Nanotechnology Infrastructure.

This work was supported by NSF and West Pharmaceutical Services. *Scientific Reports*, 2021.

National Research Priority: NAE Grand Challenge—Engineer Better Medicines

Active Tuning of Hybridized Modes in a Heterogeneous Photonic Molecule

From fundamental discovery to practical application, advances in the optical and quantum sciences rely upon precise control of light-matter interactions. Systems of coupled optical cavities are ubiquitous in these efforts, yet the design and active modification of the hybridized mode properties remains challenging. Here, we demonstrate the design, fabrication, and analysis of a tunable heterogeneous photonic molecule consisting of a ring resonator strongly coupled to a nanobeam photonic crystal cavity. Leveraging the disparity in mode volume between these two strongly coupled cavities, we combine theory and experiment to establish the ability to actively tune the mode volume of the resulting supermodes over a full order of magnitude. As the mode volume determines the strength of light-matter interactions, this work illustrates the potential for strongly coupled cavities with dissimilar mode volumes in applications requiring designer photonic properties and tunable light-matter coupling, such as photonics-based quantum simulation.

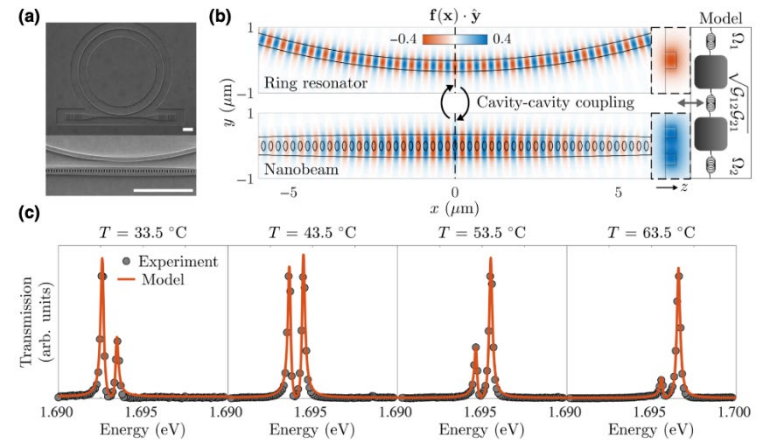


FIG. 1. (a) A SEM image of the SU-8 cladded coupled ring-resonator-nanobeam device with a 500-nm gap between the ring and the nanobeam at the point of closest separation. Scale bar: $5\ \mu\text{m}$. (b) The y component of the electric field profiles for the nanobeam-cavity mode (bottom) and the ring-resonator mode (top) studied. The system is modeled as a coupled oscillator, parametrized by an effective coupling strength $\sqrt{G_{12}G_{21}}$ and effective frequencies Ω_i distinct from the bare resonant frequencies ω_i . (c) Transmission spectra collected for four equally spaced temperatures (gray circles) with simultaneous least-squares fits to the model overlaid (red lines).

Yueyang Chen, Kevin Smith, David Masiello, Arka Majumdar, Physics, Chemistry, ECE, UW. Work performed in WNF, MAF.

Funding provided by NSF (QII-TAQS1936100; CHE-1836500; CHE-1836506)

National Research Priority: NSF–Quantum Leap

Nonvolatile Electrically Reconfigurable Integrated Photonic Switch Enabled by a Silicon PIN Diode Heater

Reconfigurability of photonic integrated circuits (PICs) has become increasingly important due to the growing demands for electronic–photonic systems on a chip driven by emerging applications, including neuromorphic computing, quantum information, and microwave photonics. Success in these fields usually requires highly scalable photonic switching units as essential building blocks. Current photonic switches, however, mainly rely on materials with weak, volatile thermo-optic or electro-optic modulation effects, resulting in large footprints and high energy consumption. As a promising alternative, chalcogenide phase-change materials (PCMs) exhibit strong optical modulation in a static, self-holding fashion, but the scalability of present PCM-integrated photonic applications is still limited by the poor optical or electrical actuation approaches. Here, with phase transitions actuated by in situ silicon PIN diode heaters, scalable nonvolatile electrically reconfigurable photonic switches using PCM-clad silicon waveguides and microring resonators are demonstrated.

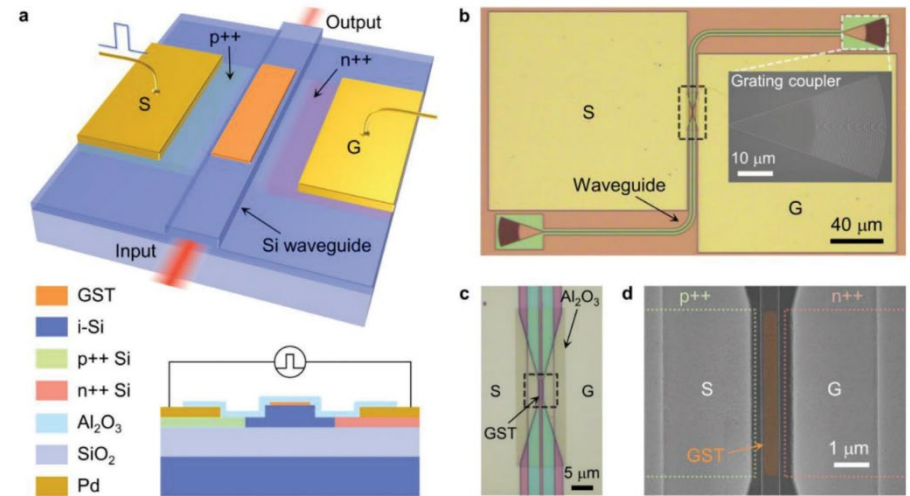


Figure 1. Nonvolatile electrically reconfigurable photonic switching units. a) Schematic of the device. For clarity, the top thin-film Al_2O_3 encapsulating layer is not displayed. Inset: cross-section of the device. b) Top-view optical microscope image of the switching unit on a waveguide with 10-nm-thick GST and a 5- μm -long active region. Inset: SEM image of the grating coupler. c) Optical microscope image of the black dashed area in (b). d) SEM image of the active region boxed in (c). False color is used to highlight the GST (orange). S (G), signal (ground) electrode. p++ (n++), heavily doped p (n)-type silicon region. i, intrinsic silicon region.

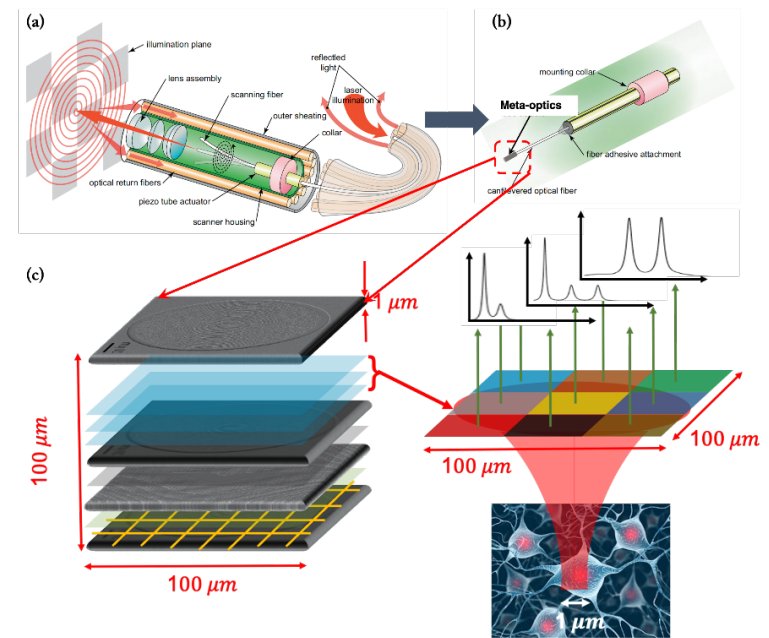
Jiajiu Zheng, Zhuoran Fang, Shifeng Zhu, Scott Dunham, Mo Li, Arka Majumdar, Physics, ECE, UW; collaborator: Intel, Stanford; Work performed in WNF, MAF.

Funding provided by NSF (EFRI-1640986, FA9550-17-C-0017)

National Research Priority: NSF–Quantum Leap

Meta-optical Angioscopes for Image-guided Therapies in Previously Inaccessible Locations

We aim to drastically miniaturize the state-of-the-art of forward viewing angioscopes using volumetric meta-optics and computational postprocessing and demonstrate **Spectrally Encoded Non-Scanning Endoscopy**, termed here as **SENSE**. Specifically, we aim to implement a spatial-spectral mapping using dispersive meta-optics, which can be computationally decoded to recover the images. By exploiting strong dispersion of the meta-molecules and the meta-optics, we aim to capture 2D images without any moving part, which will reduce the packaging complexity. The SENSE will have $\sim 250\mu\text{m}$ aperture and $\sim 100^\circ$ FOV with $\sim 10\mu\text{m}$ spatial resolution.



SENSE: (a) The current state-of-the-art scanning fiber endoscopes can be significantly miniaturized to create (b) spectrally encoded non-scanning endoscope. (c) The key will be volumetric meta-optics, which will (d) encode the spatial information to the spectrum via the dispersion of the meta-molecules and meta-optics.

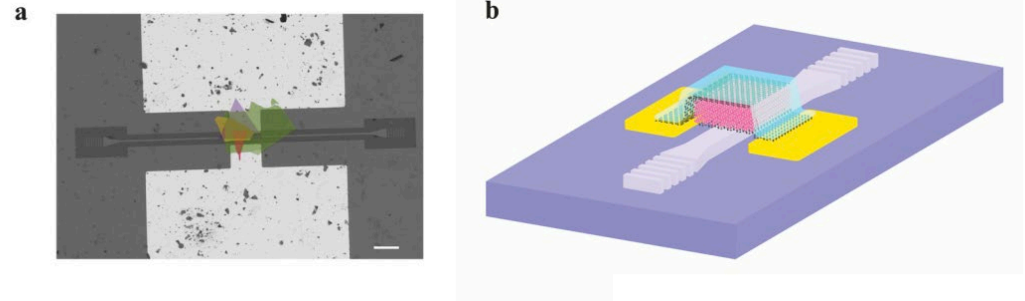
Arka Majumdar, Karl Böhringer, Eric Seibel, Steven Brunton, UW-Seattle with Swedish Medical, VerAvanti, Tunoptix.

This work was supported by NSF GCR award 2120774

*National Research Priority: NSF–Growing Convergence Research and
NAE Grant Challenge–Engineer Better Medicines*

Black Phosphorus Mid-Infrared Light-Emitting Diodes Integrated with Silicon Photonic Waveguides

Light-emitting diodes (LEDs) based on III-V/II-VI materials have delivered a compelling performance in the mid-infrared (mid-IR) region, which enabled wide-ranging applications in sensing, including environmental monitoring, defense, and medical diagnostics. Continued efforts are underway to realize on-chip sensors via heterogeneous integration of mid-IR emitters on a silicon photonic chip, but the uptake of such an approach is limited by the high costs and interfacial strains, associated with the processes of heterogeneous integrations. Here, the black phosphorus (BP)-based van der Waals (vdW) heterostructures are exploited as room-temperature LEDs.



The waveguide-integrated BP LED. (a) A false-color SEM image of the waveguide-integrated BP LED. The emitter is composed of the vertically stacked hBN (green)/GrT (red)/BP (yellow)/GrB (purple) heterostructures. The used BP flake is 65 nm thick. Scale bar, 50 μm .

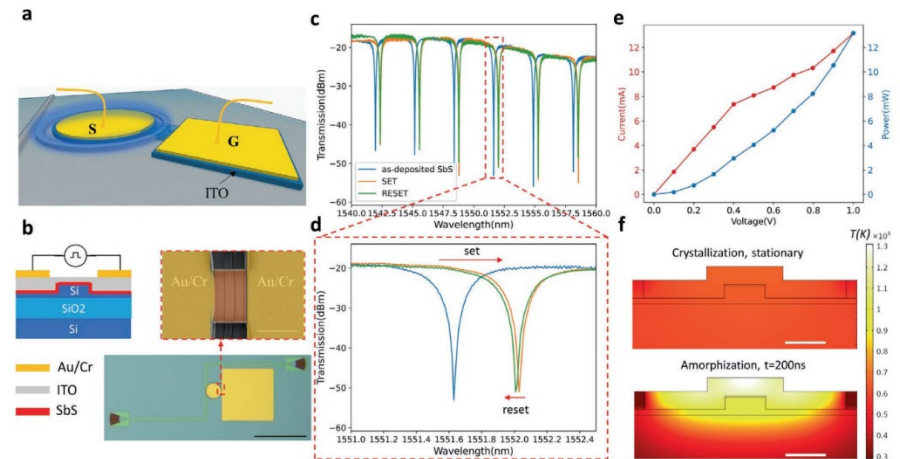
Yueyang Chen, Mo Li, Arka Majumdar, Physics, ECE, UW with collaborator NTSU.

Funding supported by NSF-1845009, and NSF-ECCS-1708579.

National Research Priority: NAE Grand Challenge—Engineer the Tools of Scientific Discovery

Non-Volatile Reconfigurable Integrated Photonics Enabled by Broadband Low-Loss Phase Change Material

In recent years, integration of PCMs with nanophotonic structures has introduced a new paradigm for non-volatile reconfigurable optics. However, the high loss of the archetypal PCM GST in both visible and telecommunication wavelengths has fundamentally limited its applications. SbS has recently emerged as a wide-bandgap PCM with transparency windows ranging from 610 nm to near-IR. In this paper, the strong optical phase modulation and low optical loss of Sb₂S₃ are experimentally demonstrated for the first time in integrated photonic platforms at both 750 and 1550 nm.



Electrical switching of SbS. a) Schematic of integrated photonic microring switch based on SbS. b) Cross-section of the device, optical micrograph (scale bar: 200 μm) and false color SEM (scale bar: 3 μm) of the fabricated device. c, d) Transmission spectrum showing the SET and RESET operation as red and blue shift of the resonance dip. e) I-V curve (red) and power (blue) during a 0–1 V DC sweep that triggered the SET operation. f) Temperature distribution under stationary heating at 1 V (top) and after 200 ns pulse at 6 V (bottom). Scale bar is 500 nm.

Zhuoran Fang, Jiajiu Zheng, Abhi Saxena, James Whitehead, Yueyang Chen, and Arka Majumdar, Physics, ECE, UW

Funding support from ONR-YIP, NSF-1640986, NSF-2003509.

National Research Priority: NAE Grand Challenge—Engineer the Tools of Scientific Discovery

1D Self-Healing Beams in Integrated Silicon Photonics

Since the first experimental observation of optical Airy beams, various applications ranging from particle and cell micromanipulation to laser micromachining have exploited their nondiffracting and accelerating properties. The later discovery that Airy beams can self-heal after being blocked by an obstacle further proved their robustness to propagate under a scattering and disordered environment. Here, we report the generation of an Airy-like accelerating beam on an integrated silicon photonic chip and demonstrate that the on-chip 1D Airy-like accelerating beams preserve the same properties as the 2D Airy beams.

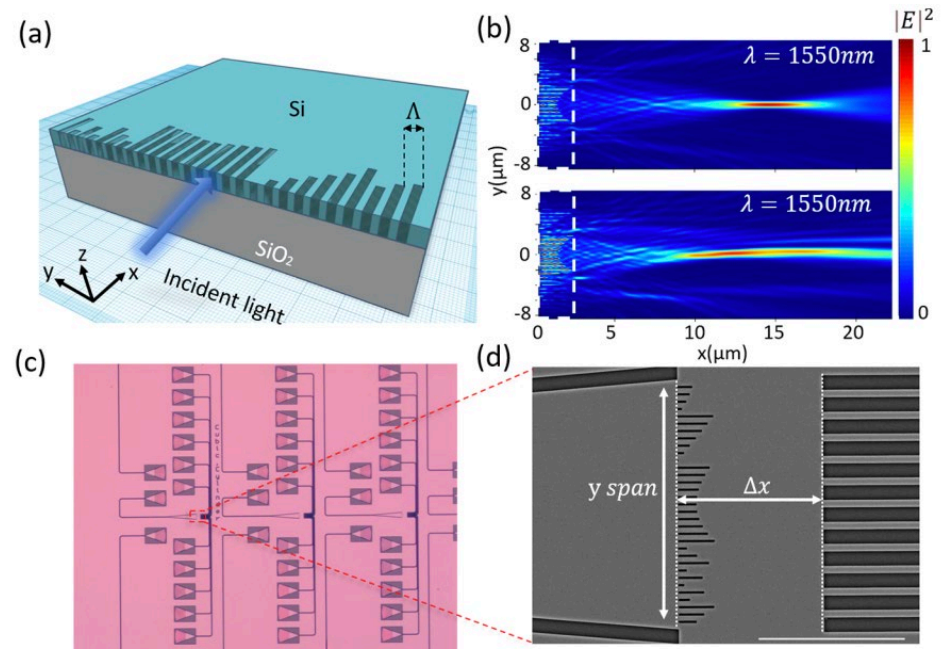


Figure 1. Design of on-chip synthetic-phase meta-optics. (a) Schematic showing the structure of 1D synthetic-phase meta-optics. The blue arrow indicates the direction in which the light is launched into the metalens. (b) Simulated electric field intensity of light focused by a quadratic meta-optics (top) and synthetic-phase meta-optics (bottom). The focal length is $15 \mu\text{m}$ for both metasurfaces, and α of the synthetic-phase meta-optics is 0.025. The white dashed boxes highlight where the phase masks are. (c) Optica micrograph showing three synthetic-phase meta-optics of increasing Δx . Grating couplers that are used to extract the light intensity at each port are also visible. (d) SEM image of a synthetic-phase meta-optics on SOI (scale bar: $10 \mu\text{m}$).

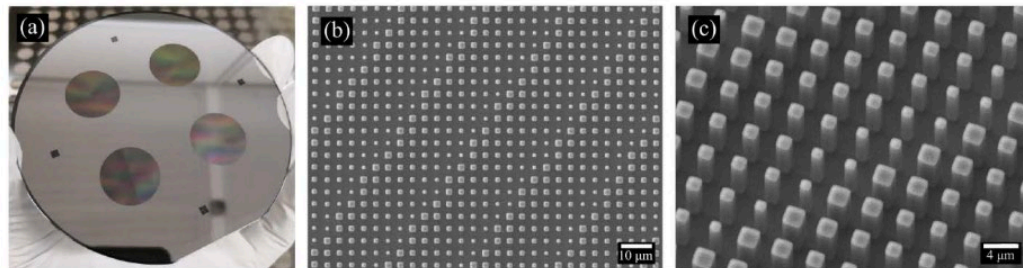
Zhuoran Fang, Rui Chen, Albert Ryou and Arka Majumdar, Physics, ECE, UW.

Funding provided by ONR-YIP, NSF-1640986, NSF-2003509.

National Research Priority: NAE Grand Challenge—Engineer the Tools of Scientific Discovery

Long wavelength infrared imaging under ambient thermal radiation via an all-silicon metalens

Further miniaturization of imaging systems is prevented by the prevalent, traditional bulky refractive optics today. Meta-optics have recently generated great interest in the visible wavelength as a replacement for refractive optics thanks to their low weight, small size, and amenability to high-throughput semiconductor manufacturing. Here, we extend these meta-optics to the long-wave infrared (LWIR) regime and demonstrate imaging with a 2 cm aperture $f/1$ all-silicon metalens under ambient thermal emission. We showed that even with the strongly chromatic nature of the metalenses, we can perform ambient light imaging, primarily due to the lack of wavelength discrimination in the sensor, as is the norm for an RGB-camera in the visible.



Fabricated devices: (a) Image taken with a cellphone camera, (b) scanning electron microscope (SEM) images of the fabricated structures, and (c) a zoomed-in view of the device.

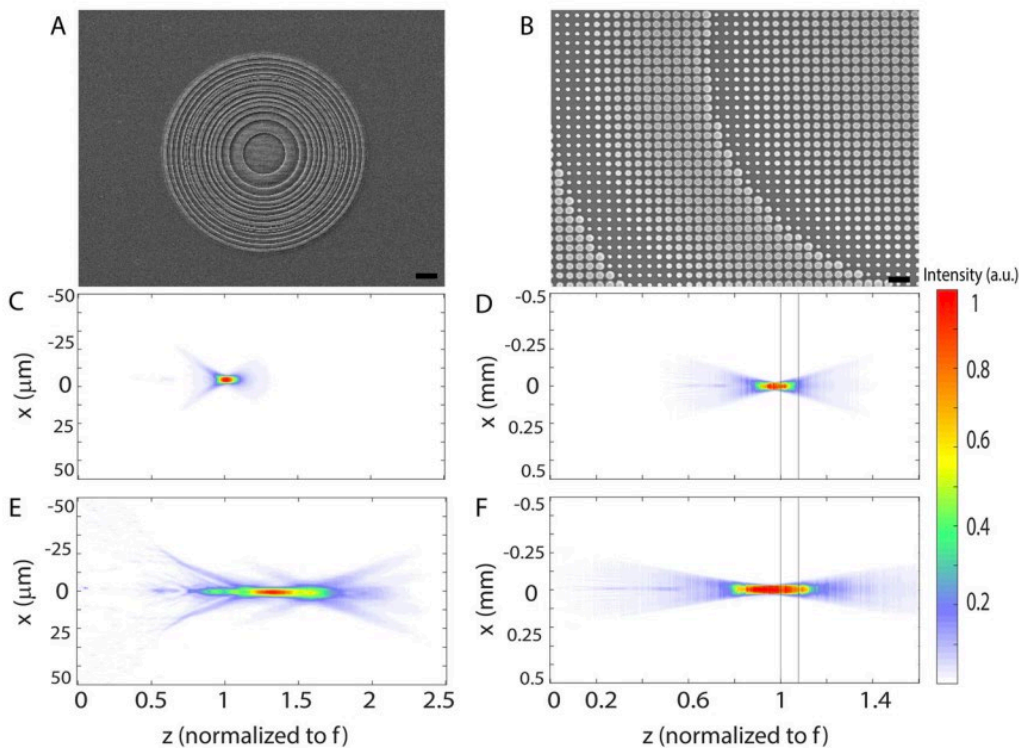
Luocheng Huang, Zheyi Han, Karl Böhringer and Arka Majumdar, Physics, ECE, UW with collaborator CFDRG.

Funding provided by ARO.

National Research Priority: NAE Grand Challenge—Engineer the Tools of Scientific Discovery

Inverse designed extended depth of focus metaoptics for broadband imaging in the visible

We report an inverse-designed, high numerical aperture (~ 0.44), extended depth of focus (EDOF) metaoptic, which exhibits a lens-like point spread function (PSF). The EDOF meta-optic maintains a focusing efficiency comparable to that of a hyperboloid metalens throughout its depth of focus. Exploiting the extended depth of focus and computational post processing, we demonstrate broadband imaging across the full visible spectrum using a 1 mm, f/1 meta-optic. Unlike other canonical EDOF metaoptics, characterized by phase masks such as a log-asphere or cubic function, our design exhibits a highly invariant PSF across ~ 290 nm optical bandwidth, which leads to significantly improved image quality, as quantified by structural similarity metrics.



SEM of the fabricated meta-optics and the measurement showing extended depth of focus.

Elyas Bayati, Shane Colburn and Arka Majumdar, Physics, ECE, UW with collaborator MIT.

Funding provided by DARPA

National Research Priority: NAE Grand Challenge—Engineer the Tools of Scientific Discovery

Research Triangle Nanotechnology Network (RTNN)

Preventing lead leakage with built-in resin layers for sustainable perovskite solar cells

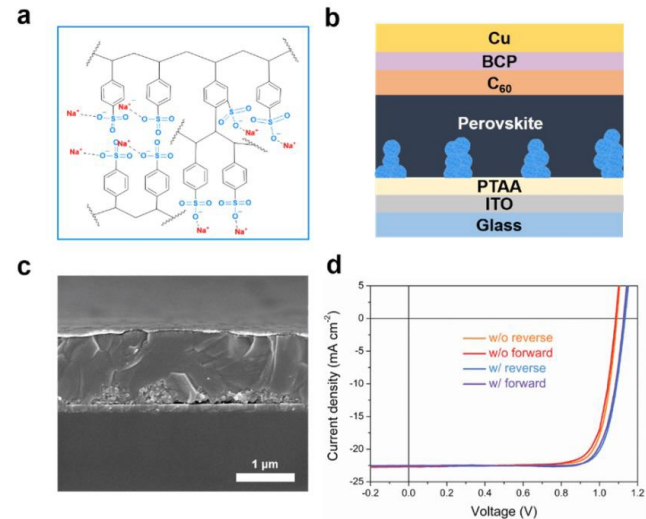
New materials and structures can help reduce lead leakage from damaged solar cells during rainfall.

A new device structure was designed which incorporates a scaffold of low-cost mesoporous sulfonic acid-based lead-adsorbing resin, which immobilizes lead ions.

Insulating scaffold design shown is scalable up to large-area modules and does not decrease device efficiency.

This structure proves more effective in preventing lead leakage than alternative configurations like coatings on glass surfaces.

Lead contamination from damaged perovskite modules was reduced to 11.9 parts per billion using this configuration.



(a) Chemical structure of the mesoporous lead-adsorbing resins. Device structure (b) and cross-sectional SEM image (c) of the blade-coated MAPbI₃ solar cells with embedded mesoporous lead-adsorbing resins. (d) J-V curves of the blade-coated MAPbI₃ solar cells with and without mesoporous lead-adsorbing resins.

Shangshang Chen, Yehao Deng, Xun Xiao, Shuang Xu, Peter N. Rudd, and Jinsong Huang; University of North Carolina at Chapel Hill. Work performed at UNC's Chapel Hill Analytical and Nanofabrication Laboratory.

This work was supported by NSF Award # DMR-1903981. *Nat Sustain* 4, 636-643 (2021).

National Research Priority: NAE Grand Challenge—Make Solar Energy Economical

Understanding role of ion migration in perovskite LEDs by transient measurements

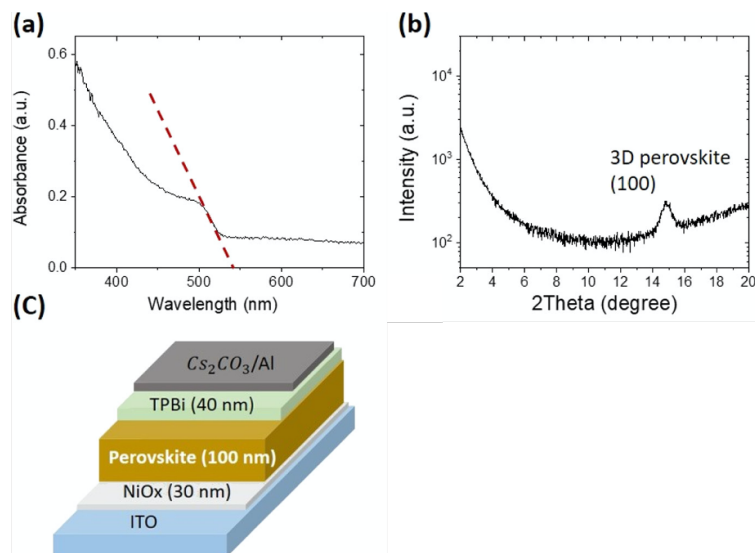
Perovskite light-emitting diodes (LEDs) have high efficiencies, though effect of ion migration is not well understood.

Slow current response is due to slow hole injection attributed to Br ions at the anode interface.

Electron injection is not affected by ion migration; such a different effect of ion migration on electron and hole injection leads to a strong charge imbalance.

To enhance device efficiency, electron injection needs to be enhanced to compensate for enhanced hole injection facilitated by halide ion migration.

Slow efficiency response is attributed to the enhanced charge injection which causes increased carrier density favoring bimolecular radiative recombination.



(a) Absorption and (b) X-ray diffraction of the perovskite film. (c) Schematic diagram of the device structure.

Qi Dong, Juliana Mendes, Lei Lei, Dovletgeldi Seyitliyev, Liping Zhu, Siliang He, Kenan Gundogdu, and Franky So, NC State University. Work performed at NC State's Analytical Instrumentation Facility.

This work was supported by NSF Award # ECCS-1542015. *ACS Appl Mater Interfaces* 12(43) 48845-48853 43 (2020).

National Research Priority: White House FY2022, Administration R&D Budget Priorities-Energy

Solution-processing of $\text{Cu}_2\text{BaSn}(\text{S},\text{Se})_4$ films for solar cell applications

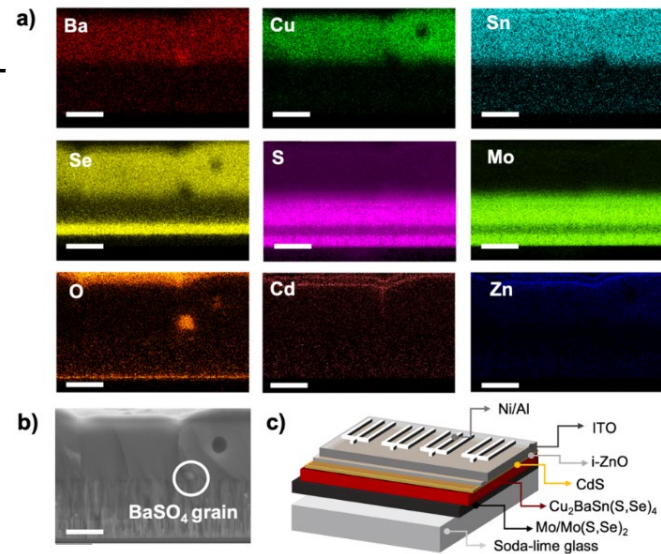
Copper barium thioselenostannate (CBTSSe) is an exciting new absorber material for solar cells since they employ low-toxicity and are made with abundant metals at low-cost, controllable stoichiometry and band gap tunability.

Charge carrier mobility found to be comparable to values in currently used commercial materials.

Longer lifetime can be achieved through bulk recombination, though strong recombination at the surface leads to a lifetime inferior to state-of-the-art absorbers.

This study shows best performance observed from solution processed CBTSSe photovoltaic (PV) devices compared to other research.

Reactivity was detected between the CBTSSe film and the Mo substrate; this should be addressed in further research.



(a) Energy dispersive spectroscopy cross-sectional mapping of PV device presented with SEM cross section image in (b) and device schematic in (c). EDS mapping collected at an accelerating voltage of 10 kV and 0.8 nA current. Mo plot contains contributions from S due to X-ray line partial overlap. The scale bar indicates 1 micron.

Betul Teymur, Sergiu Levcen, Hannes Hempel, Eric Bergmann, José A. Márquez, Leo Choubra, Ian G. Hill, Thomas Unol, David B. Mitzi, Duke University, Helmholtz-Zentrum Berlin für Materialien und Energie GmbH, Dalhousie Univ. Work performed at Duke University's Shared Materials Instrumentation Facility (SMIF).

This work was supported by DOE (#DE-SC0020061) and Horizon 2020 Award (#H2020-NMBP-03-2016-720907). *Nano Energy* 80, 105556 (2021).

Roll-to-roll nanoimprint lithography using nanopatterned seamless cylindrical mold

Nanocoating process was used for seamless nanopatterning of a cylinder mold at speeds that are hundreds of times faster than electron-beam lithography.

This Cylinder mold was then used in a Roll-to-roll (R2R) nanoimprint lithography (NIL) process to pattern a large area of a polymer film that would be prohibitively slow and expensive compared to other traditional photolithography with submicron feature sizes that can enhance optical and wetting properties.

This scalable process offers the potential to transfer exciting lab-scale demonstrations to industrial-scale manufacturing without the prohibitively high cost usually associated with the fabrication of a master mold.

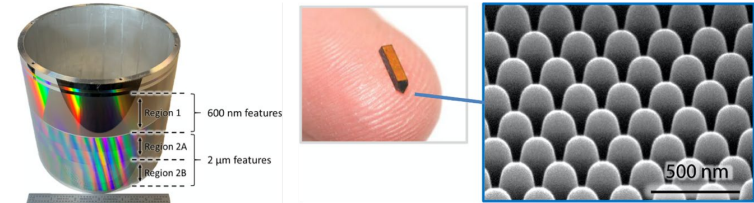


Photo of the 6.5" diameter master mold used in the work (left). Photo of a diamond die (middle). SEM of feature patterned into the tip of the diamond die (right). The first step of the nanocoating process is the nanopatterning of the tip of a diamond die using FIB milling in AIF.

Nichole Cates, Vincent J Einck, Lauren Micklow, Jacobo Morère, Uzodinma Okoroanyanwu, James J Watkins, and Stephen Furst, Smart Material Solutions, Inc., Univ. Massachusetts at Amherst. Work performed at NC State's Analytical Instrumentation Facility and Nanofabrication Facility.

This work was supported by NSF (SBIR #1738387). *Nanotechnology* 32(15), 155301 (2021).

National Research Priority: NAE Grand Challenge—Make Solar Energy Economical and White House FY2022, Administration R&D Budget Priorities-Energy

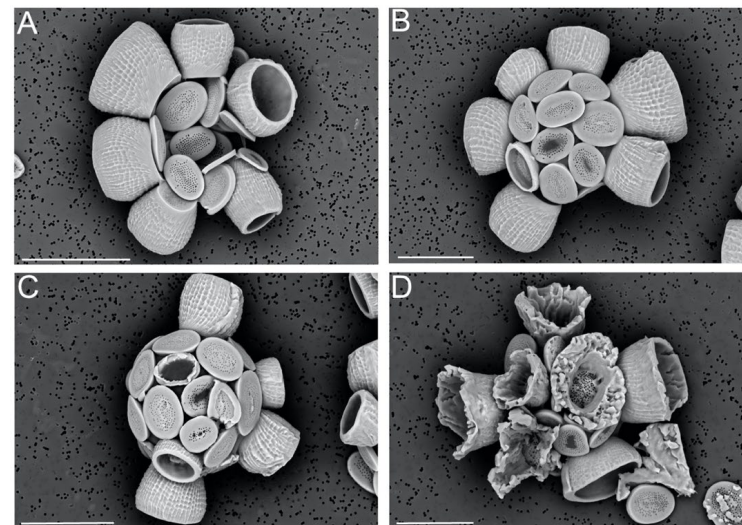
Investigating trace element incorporation during biomineralization of the alga *S. apsteinii*

These coccoliths are known to have higher Sr/Ca ratios and partitioning coefficients (D_{Sr}) when compared to any other species, but this phenomenon had not been studied.

Coccolithophores were grown in deplete Sr/Ca and did not exhibit disrupted calcification; others which were grown in higher Sr/Ca conditions displayed significantly more aberrant morphologies.

Differential Sr- and Ca-binding capacities and a less selective Ca^{2+} transport pathway may account for the high Sr incorporation.

Understanding how biomineralization affects trace metal incorporation among species is important because the trace element composition of microfossil coccoliths is used to understand physiochemical properties of the surface oceans.



SEM images acquired with an electron backscatter detector showing the effects of (A) deplete, (B) ambient, and (C, D) high (36 mmol/mol Sr/Ca and 72 mmol/mol Sr/Ca, respectively) Sr on *S. apsteinii* coccolith morphology. Scale bars represent 20 μ m.

Erin Meyer and Alison Taylor; Dept. of Biology and Marine Biology, UNC at Wilmington. Work performed at NC State's Analytical Instrumentation Facility and Joint School of Nanoscience and Nanoengineering (SENIC).

The work was supported by NSF (GEO-NERC 1638838), European Research Council (ERC-ADG-670390), and Natural Environment Research Council (NE/N011708/1). *Geochimica et Cosmochimica Acta*, 285, 41-54 (2020).

National Research Priority: NSF–Understanding the Rules of Life

Distribution of rubber particles in FFF-ABS and its impact on weld strength

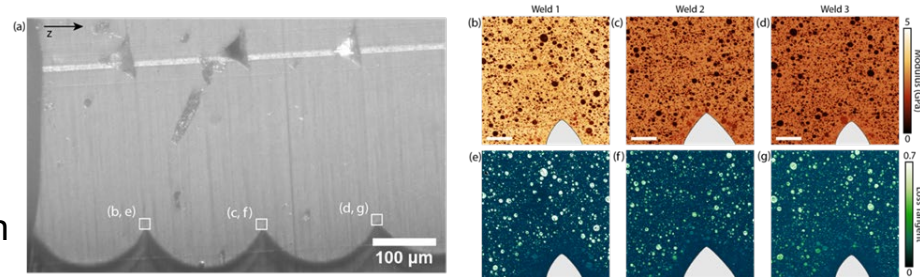
Fused Filament Fabrication (FFF) is commonly used in additive manufacturing of polymers due to low cost and ease of use, although mechanical properties are poor at weld regions between fibers.

Atomic force microscopy (AFM) was used to obtain nanomechanical maps of the polybutadiene domain morphology around weld interfaces of acrylonitrile butadiene styrene (ABS).

Decreases in average size/density of the polybutadiene particles were observed within 5-10 μm regions across multiple welds.

Polybutadiene particles within the weld zone seem to promote brittle fracture between printed fibers.

These results suggest that improving migration of polybutadiene particles into weld regions can improve fracture toughness.



(a) Optical image of the FFF-ABS cross-section prepared for imaging with AFM. The locations used for AFM imaging are indicated with white squares. The vertical print orientation (z-axis) is indicated with a black arrow. (b-d) Punch moduli and (e-g) loss tangent of welds 1-3. Scale bar indicates 4 μm . The air gap between filaments is indicated in grey and is not included in subsequent analysis.

David Collinson, Pavan Kollor, Natalia von Windheim, and L. Catherine Brinson, Northwestern University, Texas A&M University, Duke University. Work was performed at Shared Materials Instrumentation Facility (SMIF) and NUANCE (SHyNE).

This work was supported by NSF (CMMI-1818574, BCS-1734981, DMR-1720139). *Addit Manuf* 41, 101964 (2021).

National Research Priority: DoD Additive Manufacturing Strategy 2021-Expand proficiency in AM

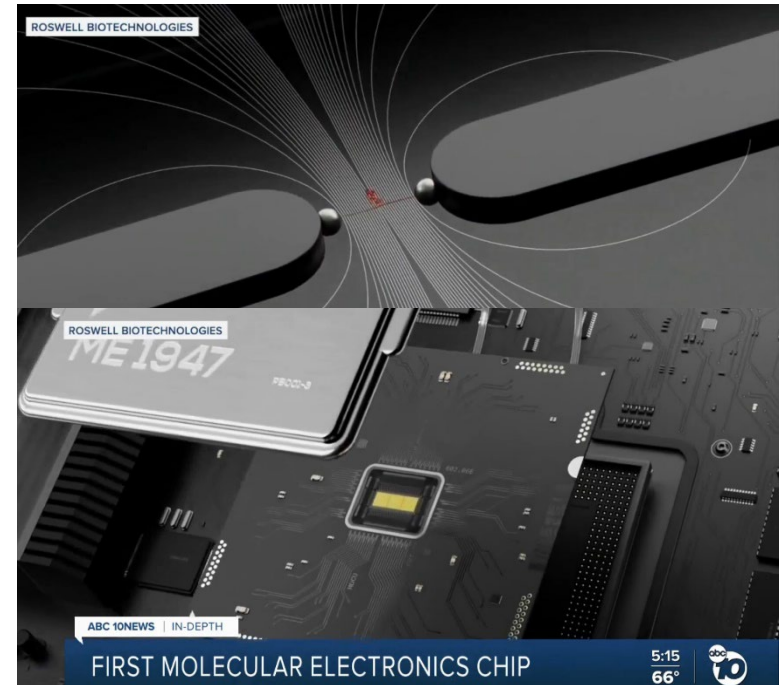
San Diego Nanotechnology Infrastructure (SDNI)

Molecular Electronics Chip with Single Molecule Sensitivity

Roswell Biotechnologies has developed a CMOS integrated molecular biochip with 16,000 individual sensors for single molecule detection that can be a platform to be used for a wide range of medical applications. The first commercial market the company is targeting is in drug discovery, but the chips could also dramatically lower the cost of whole-genome sequencing.

The electric field generated by the sensor nano-electrodes (10nm gap), through dielectrophoresis, pulls molecules to the vicinity of the electrode gap, increasing the limits of sensitivity to single molecule levels.

Staff at SDNI's Nano3 facility, especially in the area of electron-beam lithography, has been instrumental in enabling the development of the chip.



Roswell Biotechnology's molecular electronics chip with single molecule detection sensitivity.

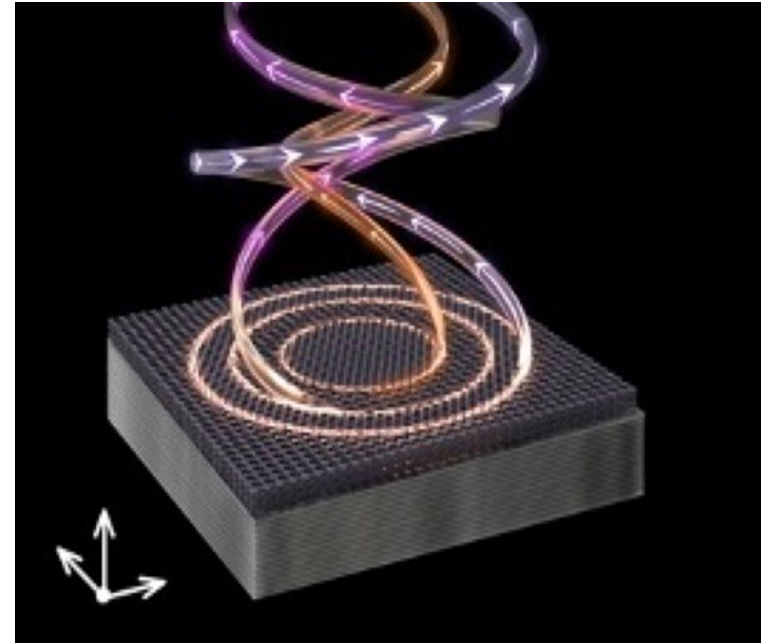
Roswell Biotechnologies. This company has been supported by staff at SDNI's Nano3 facility since its inception.

National Research Priority: NSF–Understanding the Rules of Life

Photonic Quantum Hall Effect Light Sources of Controlled Orbital Angular Momenta

The photonic quantum Hall effect enables the direct and integrated generation of coherent orbital angular momenta beams of large quantum numbers from light travelling in leaky circular orbits at the interface between two topologically dissimilar photonic structures. The work by the Kante group gives direct access to the infinite number of orbital angular momenta basis elements and will thus enable multiplexed quantum light sources for communication and imaging applications.

The work requires challenging heterogeneous integration of structured semiconductors on a magnetic substrate to nanofabricate photonic quantum Hall rings via circular boundaries between topologically dissimilar photonic crystals.



Photonic QH rings and integrated OAM of large quantum numbers.

Babak Bahari, Liyi Hsu, Si Hui Pan, Daryl Preece, Abdoulaye Ndao, Abdelkrim El Amili, Yeshaiahu Fainman & Boubacar Kanté, Dept. of Electrical Engineering and Computer Sciences, University of California-Berkeley. Electron-Beam Lithography Fabrication performed at UCSD's SDNI Nano3 facility.

Nature Physics 17, 700–703 (2021)

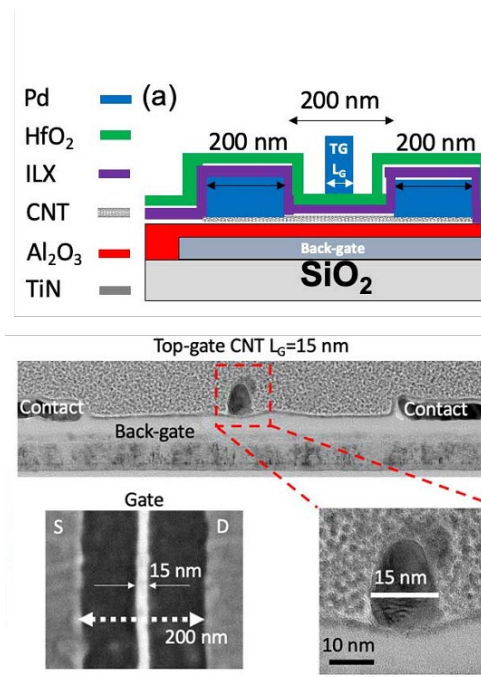
National Research Priority: NSF–Quantum Leap

Nanofog Technology for Scaled-Down Carbon Nanotube Transistors

This collaborative work between TSMC and US research institutions (Stanford, UCSD) focuses on post Moore's law semiconductor technologies to produce fully turn-off CNT transistors.

A lack of compatible high-k dielectric gate oxide to allow full turn off has made single wall carbon nanotube transistors highly.

SDNI's Nano3 staff provided crucial supports (ALD Al₂O₃ and HfO₂ deposition, TEM characterization, etc.) for the invention and development of a "Nanofog" process, enabling high K gate oxide deposition on CNT to make transistors that can be fully turned off.



"Nanofog" ALD processing enables intermediate high-k gate oxide deposition on single wall carbon nanotube based transistors.

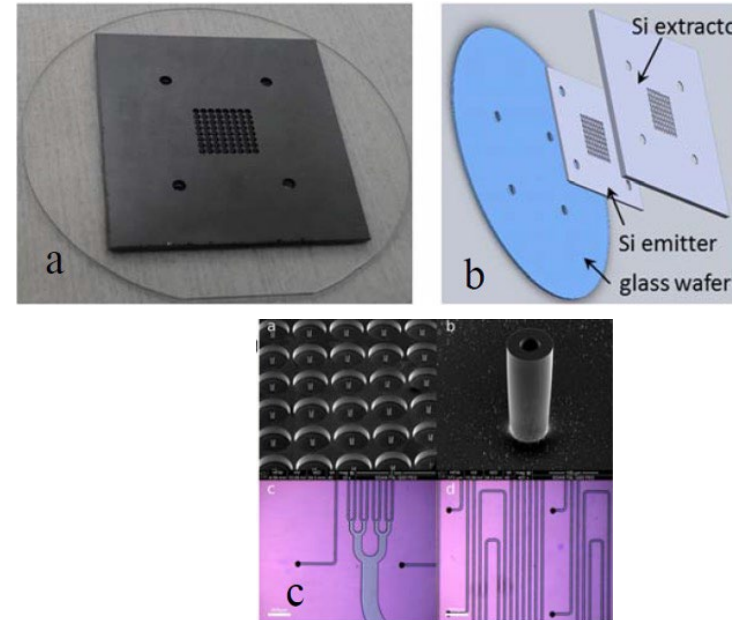
TSMC/Stanford/UCSD team; Atomic Layer Deposition, Transmission Electron Microscopy characterization performed at SDNI's Nano3 facility.

National Research Priority: NSF–Growing Convergence Research

Variable Specific Impulse Electro Spray Thrusters for SmallSat Propulsion

This work supports NASA Small Satellite Missions. Small spacecraft and satellites help NASA advance scientific and human exploration, reduce the cost of new space missions, and expand access to space. Through technological innovation, small satellites enable entirely new architectures for a wide range of activities in space with the potential for exponential jumps in transformative science.

Low thrust electro spray propulsion (ESP) systems are developed for SmallSats and CubeSats to advance the technology from low TRL to TRL 5. SDNI's Nano3 technical staff have provided full services of device fabrication and integration in close interactions with the team.



“Nanofog” ALD processing enables high-k gate oxide deposition on single wall carbon nanotube based transistors.

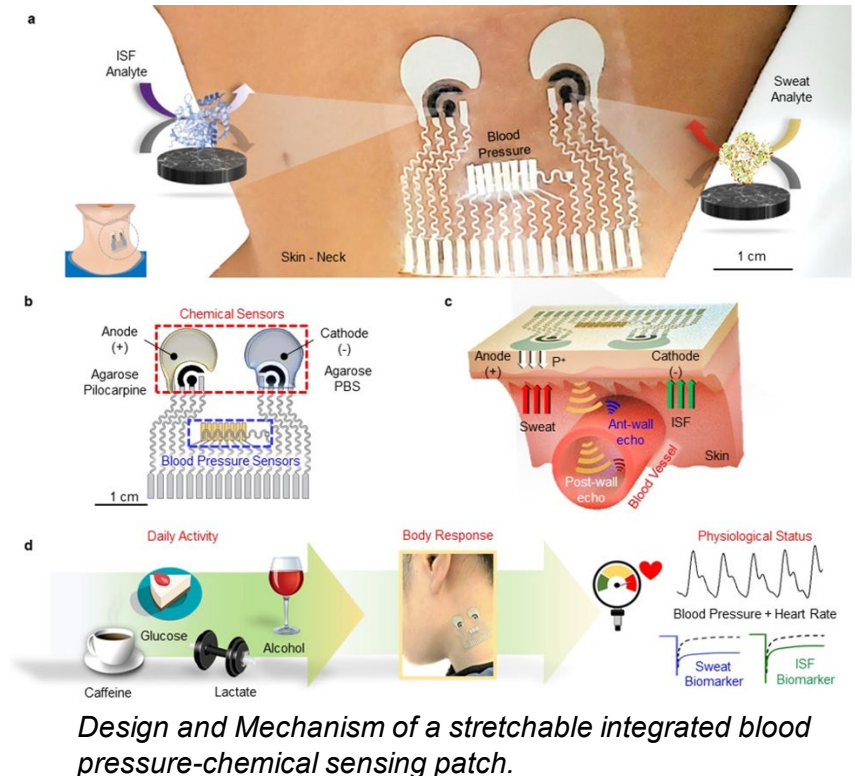
Research team of JPL, UCI, UCLA and Cal Poly, led by Prof. Manuel Gamero-Castaño at UC Irvine. SDNI's Nano3 facility provides crucial support in device fabrication and integration.

National Research Priority: NSF–Windows on the Universe

Integrated Blood Pressure-Chemical Sensing Epidermal Patch

UCSD faculty Joseph Wang and Sheng Xu, collaboration with the companies affiliated with the Center for Wearable Sensors, have developed a multimodal wearable sensor to simultaneously sense hemodynamics and metabolic signals from the human body. The work presents the first demonstration of an integrated wearable sensor that monitors the blood pressure and heart rate via ultrasonic transducers, along with parallel non-invasive electrochemical detection of biomarker levels, such as glucose, lactate, caffeine, and alcohol, in sweat and interstitial fluid.

The fabrication, heterogeneous integration, and assembly of the devices were produced in the SDNI facilities, with the assistance of the SDNI equipment and engineering team.



Design and Mechanism of a stretchable integrated blood pressure-chemical sensing patch.

Joseph Wang, Sheng Xu, Nanoengineering, UCSD. Work performed at SDNI's Nano3 facility.

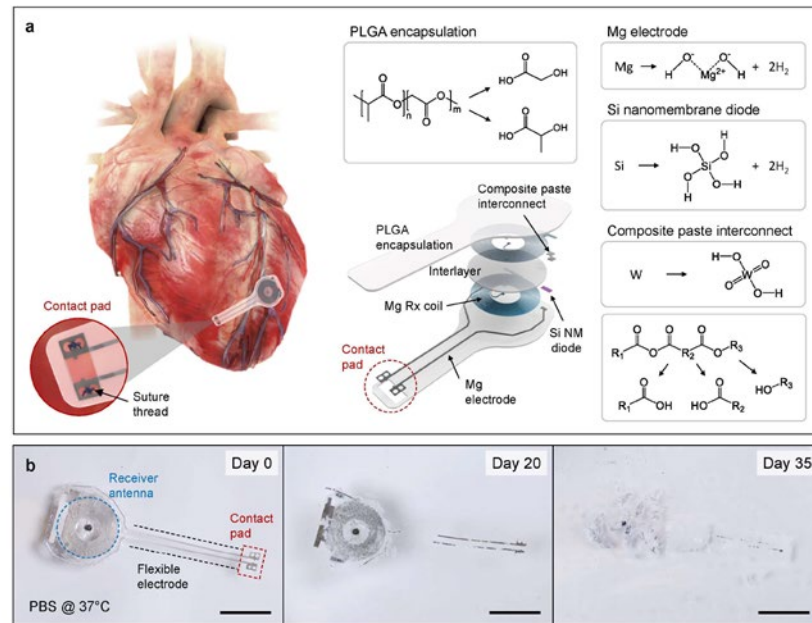
Nature Biomedical Engineering 5, 737–748 (2021)

National Research Priority: NSF–Understanding the Rules of Life

Soft and Hybrid Nanotechnology Experimental (SHyNE) Resource

Materials and Device Designs for Bioresorbable, Wireless Pacemakers

Temporary cardiac pacemakers provide critical functions in pacing through periods of need during post-surgical recovery. The percutaneous leads and externalized hardware associated with these systems represent, however, risks of infection and for myocardial damage and perforation during lead removal. Our advances in bioresorbable electronic materials serve as the basis for wireless and fully implantable cardiac pacemakers capable of post-operative control of cardiac rate and rhythm during a stable operating timeframe, followed by complete dissolution and clearance via natural biological processes. A combined set of studies across mouse, rat, rabbit, canine, and human cardiac models demonstrate that these devices provide an effective, battery-free means for pacing as a new type of biomedical device technology.



(a) Schematic illustration of a device mounted on the myocardial tissue, the device configuration and the materials chemistry. (b) The device dissolves via hydrolysis in simulated biofluids.

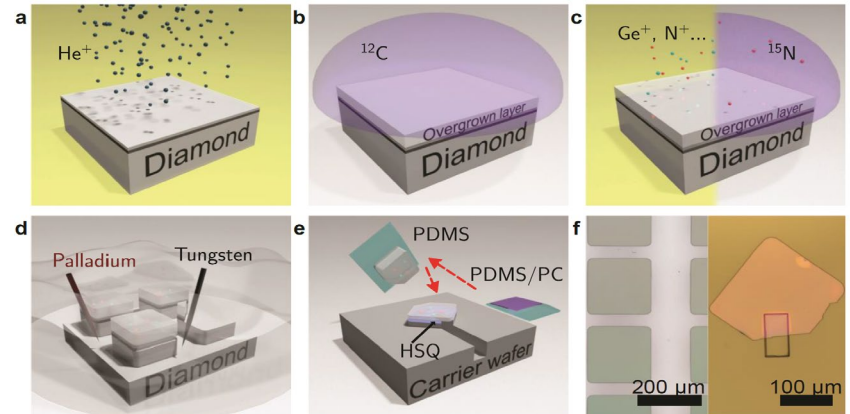
John A. Rogers and co-workers, Northwestern University. Work was performed at SHyNE Resource.

Nature Biotechnology 39, 1228-1238 (2021).

National Research Priority: NSF–Understanding the Rules of Life

Tunable Diamond Membranes for Integrated Quantum Technologies

Color centers in diamond are widely explored as qubits in quantum technologies. However, challenges remain for the effective and efficient integration of these diamond-hosted qubits in device hetero-structures. Here, nanoscale-thick uniform diamond membranes are synthesized via “smart-cut” and isotopically purified overgrowth. These membranes have tunable thicknesses, are deterministically transferable, have bilaterally atomically flat surfaces and bulk-diamond-like crystallinity. Color centers are synthesized via both implantation and in-situ overgrowth incorporation. Individual Ge-vacancy centers exhibit stable photoluminescence. The spin coherence of individual nitrogen-vacancy centers shows coherence times as long as 400 μs . This platform enables the straightforward integration of diamond membranes that host coherent color centers into quantum technologies.



Schematic of the diamond membrane fabrication process. (a) He⁺ implantation with subsequent annealing to form the membrane (light gray on the top) and the graphitized layer (dark grey underneath). (b) Isotopically purified PE-CVD diamond overgrowth. (c) Color center incorporation via ion implantation (left) or in-situ doping (right). (d) Diamond membrane undercut via EC etching. (e) Membrane transfer and back etching. The membrane is picked up by the PDMS/PC stamp (green/purple), flipped onto another PDMS stamp (green), and bonded to the carrier wafer by HSQ resist. (f) Microscope images of patterned overgrown membranes (left) and a transferred and multi-step etched membrane on a fused silica wafer (right).

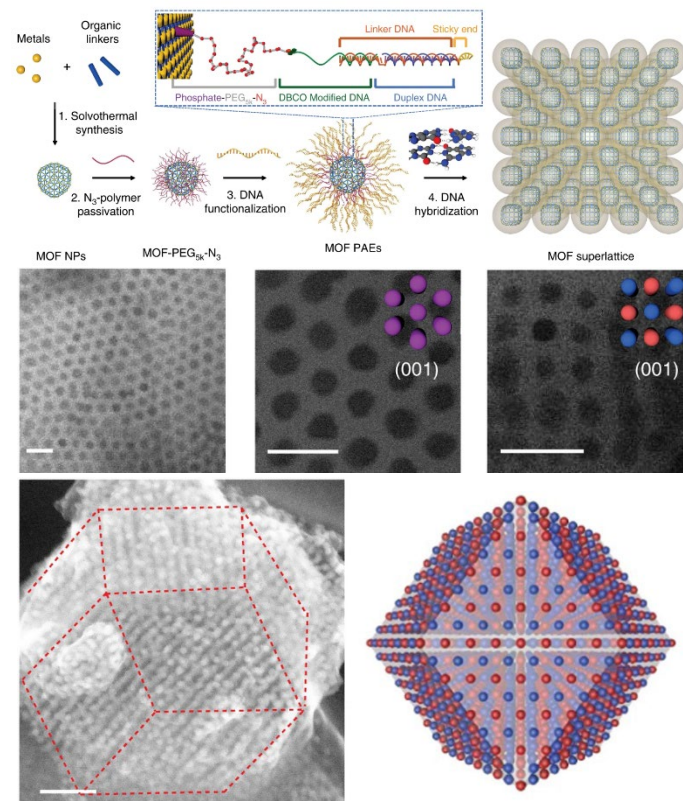
X.H. Guo, N. Deegan, J.C. Karsch, Z.X. Li, T.L. Liu, R. Shreiner, A. Butcher, D/ D. Awschalom, F.J. Heremans, A.A. High, Pritzker School of Engineering, University of Chicago. Work performed at SHyNE Resources.

This work was supported by DOE, NSF MRSEC, and NSF NNCI. *arXiv* 2109.11507

National Research Priority: NSF–Quantum Leap

Colloidal crystal engineering with metal-organic framework nanoparticles and DNA

Colloidal crystal engineering with nanoparticles (NPs) has emerged as a powerful tool to design materials from the bottom up. When NP building blocks are combined with nucleic acids, they may behave as programmable atom equivalents (PAEs) and can be assembled in a sequence-specific fashion into crystalline arrangements driven by a combination of DNA complementarity and their unique nanoscale architectural features. Colloidal crystal engineering with nucleic acid-modified nanoparticles is a powerful way for preparing 3D superlattices, which may be useful in many areas, including catalysis, sensing, and photonics. Here, we show that metal-organic framework nanoparticles (MOF NPs) densely functionalized with oligonucleotides can be programmed into a diverse set of superlattices. to crystallize into a diverse set of superlattices with well-defined crystal symmetries and compositions.



Shunzhi Wang, Sarah S. Park, Cassandra T. Buru, Haixin Lin, Peng-Cheng Chen, Eric W. Roth, Omar K. Farha & Chad A. Mirkin, Northwestern Univ. Work was performed at SHyNE Resources

Nature Communications volume 11, Article number: 2495 (2020)

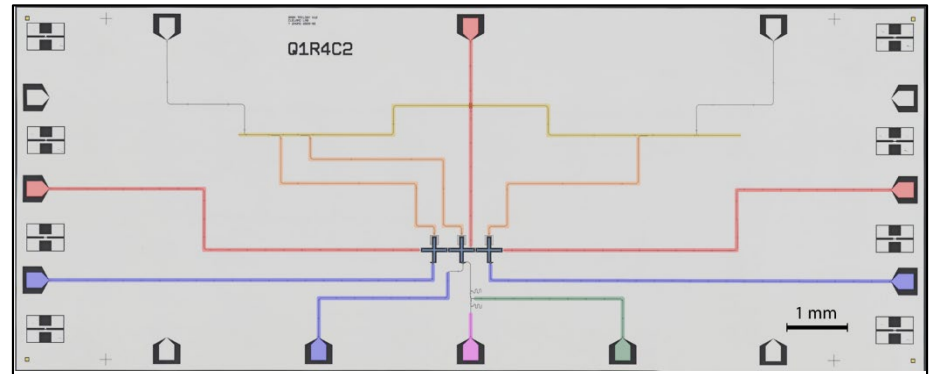
National Research Priority: NSF–Understanding the Rules of Life

Generation and Transmission of Complex Quantum Photon States

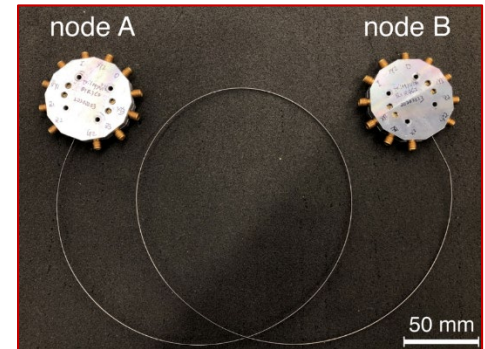
Quantum communication relies on high fidelity transfer of quantum information, processed at the sending and receiving nodes by high fidelity qubits. This work demonstrates the generation of complex 3-qubit entangled states in one superconducting qubit node, followed by transmission through a cable to a second superconducting qubit node. Another experiment used the same device to entangle one qubit in each node, followed by expansion of the entangled state to include all six qubits in the system. This experiment demonstrates a significant breakthrough for the generation and transmission of complex quantum states, pointing to new opportunities for quantum-enabled encryption and data compression.

Y.P. Zhong, H.-S. Chang, A. Bienfait, É. Dumur, M.-H. Chou, C. R. Conner, J. Grebel, R.G. Povey, H.X. Yan, D. I. Schuster, A. N. Cleland, Pritzker School of Engineering, University of Chicago. Work performed at SHyNE Resource.

This work was supported by ARO, DOE, NSF MRSEC, and NSF NNCI. *Nature* **590**, 571-575 (2021)



Top image shows an integrated quantum circuit with three superconducting qubits, each with its integrated control and readout circuitry. The circuit also includes special tunable coupling to a cable (see image to right), allowing the qubit circuit to be coupled in the time-domain to emit or receive photonic quantum states.

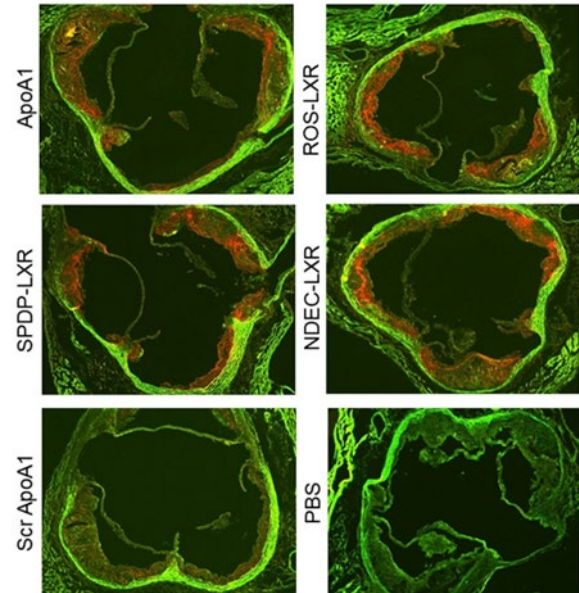


Right image shows two-node assembly, where each node A and B contains the integrated circuit shown in the top image. The middle qubit in each node is coupled to the 1 meter long cable linking the two nodes. Quantum states are sent through the cable, entangling the qubits in the two nodes and supporting the transmission of quantum information between the two nodes.

National Research Priority: NSF–Quantum Leap

Niche-responsive Nanocarriers Target Atherosclerotic Plaque

SQI and **NUANCE** helped support this study aimed to develop a minimally invasive, injectable nanocarrier that could target plaque and release therapeutics in response to the diseased microenvironment using self-assembled peptide amphiphile (PAs) nanofibers. Three linkages were evaluated for tethering a therapeutic to PA monomers and after 24 hours of treatment with physiological levels of stimuli, all therapeutic was released *in vitro*. Therapeutic PAs were then co-assembled with PAs that target atherosclerotic plaque and localization was confirmed in a low-density lipoprotein knockout mice *in vivo*. These results demonstrate the potential for controlled drug delivery to atherosclerotic lesions and supports the use of PA nanofibers for atherosclerosis nanomedicine.



Targeted PA nanofibers (red in top 4 images) localize to plaque in the aortic root of atherosclerotic mice compared to controls (bottom 2 images).

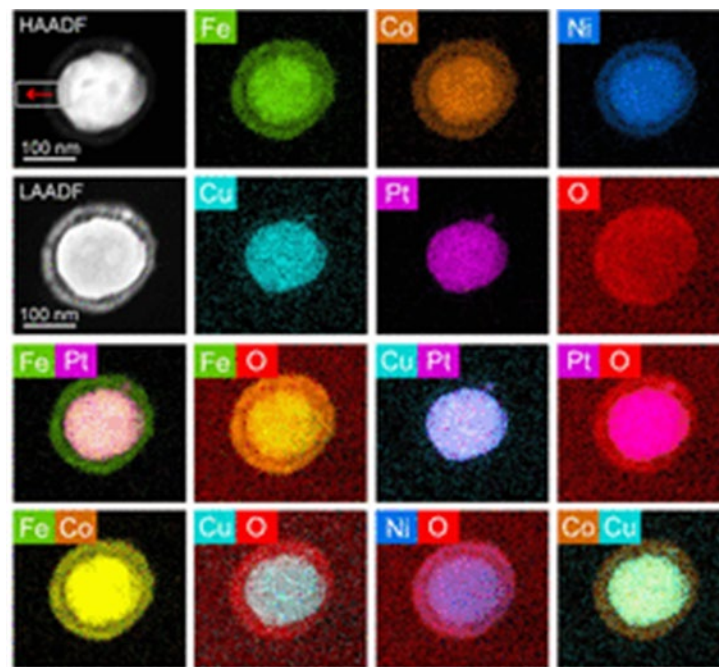
Work by the lab of Prof. Melina Kibbe (Dept. of Surgery, University of North Carolina) in collaboration with the lab of Prof. Samuel Stupp (Dept. of Materials Science and Engineering, Northwestern University). Work was performed at SQI and NUANCE at SHyNE.

This work was supported by NSF (ECCS-2025633). *Advanced Therapeutics* 4(9), (2021) 2100103.

National Research Priority: NSF–Understanding the-Rules of Life

High-Temperature Reduction Dynamics of High-Entropy Alloy Nanoparticles

Understanding the behavior of high-entropy alloy (HEA) materials under hydrogen (H₂) environment is of utmost importance for their promising applications in structural materials, catalysis, and energy-related reactions. In this work, reduction behavior of oxidized FeCoNiCuPt HEA nanoparticles (NPs) in atmospheric pressure H₂ environment was investigated by *in situ* gas-cell transmission electron microscopy (TEM). During reduction, the oxide layer expanded and transformed into porous structures where oxidized Cu was fully reduced to Cu NPs while Fe, Co, and Ni remained in the oxidized form. In situ chemical analysis showed that the expansion of the oxide layer resulted from the outward diffusion flux of all transition metals (Fe, Co, Ni, Cu).



Scanning TEM image and associated EDS maps of the HEA nanoparticles after the *in situ* reduction

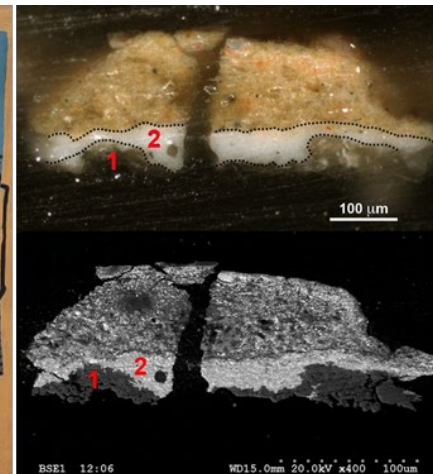
Boao Song et al, Dept. of Mechanical and Industrial Engineering, University of Illinois at Chicago. This work utilized the NUANCE Center at SHyNE.

Work was supported by NSF (DMR-1809439). *Nano Letters* 2021,21, 4, 1742-1748.

National Research Priority: NSF–Quantum Leap

Scenes from the life of Picasso's Still Life (1922)

Scenes from the life of Picasso's *Still Life* (1922): history, materials, and conservation. Discolored surface coatings and overpaint from an early restoration treatment posed challenges to the understanding and conservation treatment of the work. Picasso used a lead-white-based priming layer over the first composition before painting the linear abstract *Still Life* dated February 4, 1922. SEM-EDS spectrometry analysis of paint samples and restoration coatings from past treatments helped to clarify our understanding of the painting and supplement previously published analytical results.



Pablo Picasso, *Still Life*, February 4, 1922. Oil on canvas. The image shows the painting after the most recent treatment was completed. Cross section of paint and ground layers from the yellow area in the upper right corner in reflected light (top) and backscattered electron image (bottom); 1. Calcium carbonate layer. 2. Lead white layer

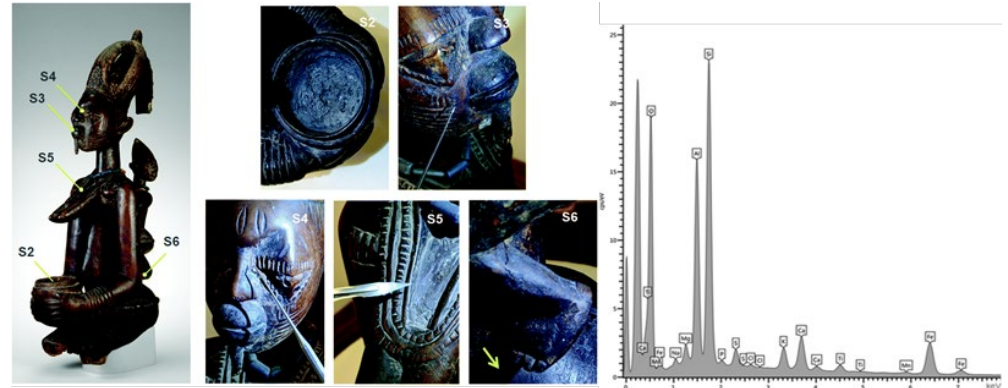
Allison Langley, Kimberley Muir, Ken Sutherland, Art Institute of Chicago. Utilized the NUANCE EPIC-SEM facility Hitachi S-3400N SEM and Oxford EDS system.

SN Appl. Sci. 2, 1384 (2020).

National Research Priority: NSF–Growing Convergence Research

Characterization of surface materials on African sculptures

Multiple analytical techniques were used to characterize materials from the surfaces of two African sculptures in the collection of the Art Institute of Chicago: a Bamana power object (*boli*), and a Yoruba wooden sculpture of a female figure. Surface accretions on objects are made with complex mixtures of natural materials. SEM-EDS was used to understand the composition and surface morphology. The presence of plant resins, oils, polysaccharides, and inorganic (clay or earth) compounds, as well as sacrificial blood, and more specifically, blood from chicken, goat, sheep and dog (discovered through EDS and proteomics analysis).



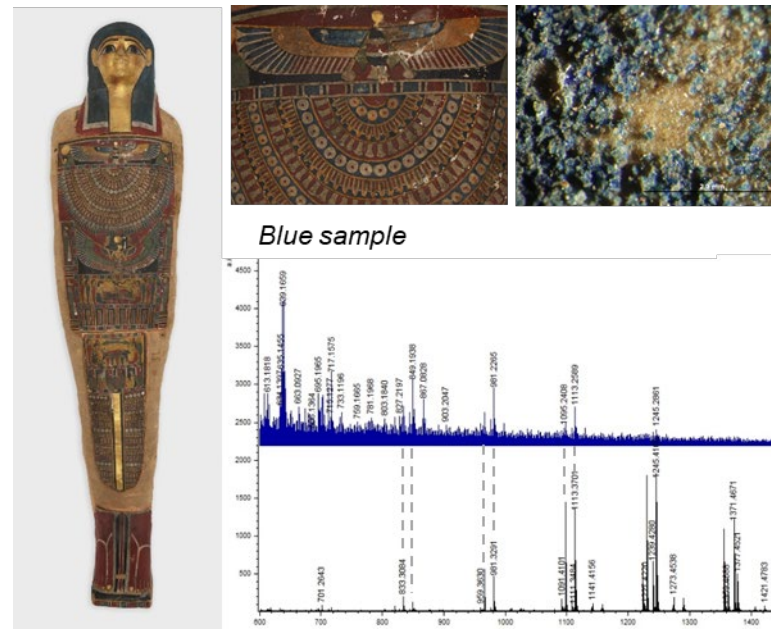
Female Figure with Bowl (AIC #1988.21), late 19th century, 62.2 × 19 × 31.7 cm (24½ × 7½ × 12½ in.) with sampling locations indicated (left) and the corresponding detail images (right). DS spectrum of sample S4 from the female figure ariable amounts of Ca, Mg, K, S and Fe, and traces of other elements including Mn, Ti and P. This composition suggests the presence of aluminosilicates and other inorganic compounds consistent with the expected presence of clay.

Clara Granzotto, Ken Sutherland, Young Ah Goo, and Amra Aksamija, Art Institute of Chicago, Proteomics Center of Excellence, and Center for Scientific Studies in the Arts, Northwestern University. Utilized the NUANCE EPIC-SEM facility Hitachi S-3400N SEM and Oxford EDS system.

National Research Priority: NSF–Growing Convergence Research

Study of a cartonnage from ancient Egypt: MALDI-MS analysis of the paint binder

This ancient Egyptian cartonnage, a papier-mâché-like material, was analyzed to determine the nature of the paint medium. Micro-samples obtained from different colors were digested with a specific enzyme, which releases oligosaccharides characteristic of polysaccharide-based materials, and analyzed by MALDI-MS. This strategy allows to discriminate plant gums from different species and showed evidence for the use of *Acacia tortilis* as paint binder, a native species in Egypt but less common than the most known and used gum arabic (*A. senegal*). Research continues to extend the library of plant gums mass fingerprints that will facilitate reliable identification and differentiation of plant gums in samples from various works of art. Results will shed light on plant sources, trade, and selection of materials by artists.



Nanomechanical Sensors for Non-Invasive Diagnostics

RT-PCR-gold standard in COVID-19 detection (takes 2-3 hours)

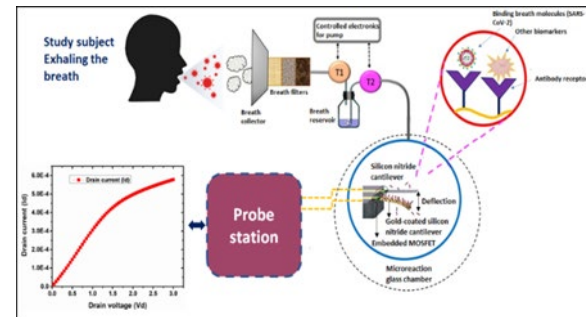
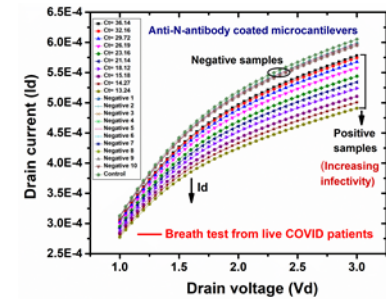
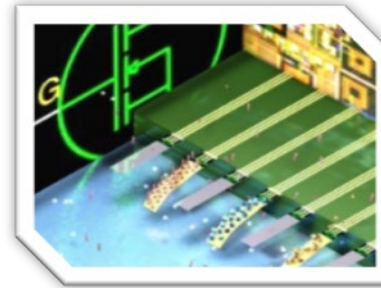
Antigen tests are available-produce false positives/negative data

SHyNE *in-house* developed integrated diagnostics detection technology allows:

Rapid detection (swab/Breath to signal <3 min)

Multiplexing (simultaneous detection of multiple viral moieties)

Differential readout allows zero false positives, Wireless compatibility



Breath based detection of COVID through current modulation (I_d - V_d) measurement of the MOSFET device, (a) I_d - V_d measurement data from 24 positive patients, (b) I_d - V_d measurement data from COVID positive and negative patients.

Gajendra Shekhawat, Dilip Agarwal, Vikas Nandwana and Vinayak Dravid, Dept. of Material Science and Engineering and NUANCE Center, Northwestern University. Work performed in part at SHyNE Resource.

This work was supported by NIH (#3U54HL119810-07S1). *Biosensors and Bioelectronics* 195, 113647 (2021).

National Research Priority: NSF–Understanding the Rules of Life

Electron Emission and Gas Breakdown Experiments for Nanoscale Gaps

Typically, gas breakdown is driven by Townsend avalanche and predicted mathematically by Paschen's law. For microscale gaps at atmospheric pressure, the applied voltage creates a sufficiently strong electric field to strip electrons from the cathode by field emission, resulting in a lower breakdown voltage than predicted by Paschen's law. The importance of field emission in microscale gas breakdown raises the question about the implications of further reducing gap distance to nanoscale. To understand the effects of gap distance and pressure on breakdown voltage and the transitions between different electron emission mechanisms (Fowler-Nordheim, Child-Langmuir, and Mott-Gurney) before breakdown occurs, we measured current as a function of voltage for nanoscale gaps ranging from 20 nm to 800 nm with different protrusion aspect ratio in both atmospheric air and vacuum (see figure to right). We then developed Fowler-Nordheim curves to assess the electron emission mechanism prior to breakdown.

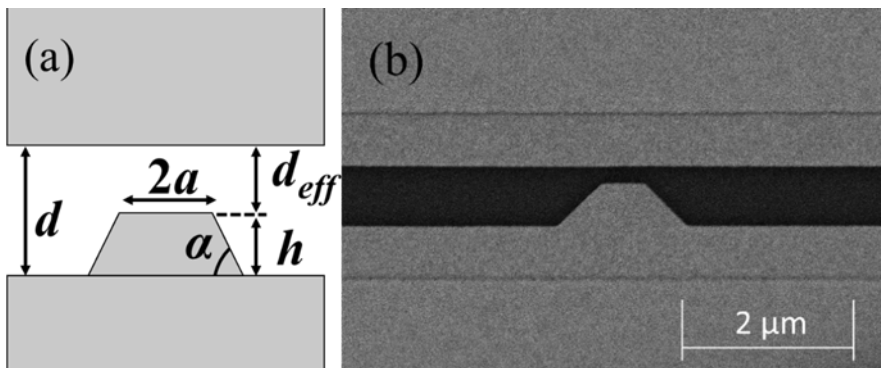


Image left shows the device schematic and image right shows an SEM photo of a representative device with $d_{eff} = 250 \text{ nm}$ and $2a = 500 \text{ nm}$, fabricated in the PNF at the University of Chicago.

H.Wang, A.L. Garner, et al, School of Nuclear Engineering, Purdue University. Devices fabricated at the Pritzker Nanofabrication Facility, University of Chicago.

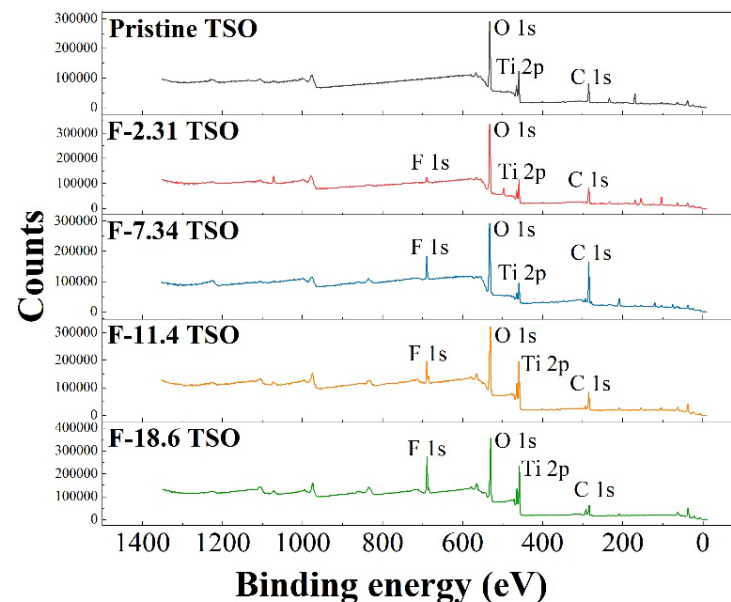
Work supported by Office of Naval Research.

National Research Priority: NSF–Growing Convergence Research

Southeastern Nanotechnology Infrastructure Corridor (SENIC)

Treatment of per- and polyfluoroalkyl substances (PFASs) using novel reactive electrochemical membrane (REM) systems based on titanium suboxide (TSO) materials

The objective of this work is to provide a basis for design and optimization of the TSO-based REM systems for electrochemical treatment of PFAS-contaminated waters. Porous Magnéli phase TSO have been used as anode to degrade PFASs in electrochemical oxidation. Modification of the TSO materials by manipulating their porous structure and doping with selected elements using sintering and surface modification approaches can further improve its efficiency towards PFAS degradation in REM processes and minimize its reactivity towards chloride to inhibit the formation of unwanted chlorate and perchlorate. Material characterizations performed at SENIC along with molecular simulations help to guide the design of the materials and explore the interactions of PFAS and chloride on the anodes.



XPS full scan of pristine and surface fluorinated TSO anode.

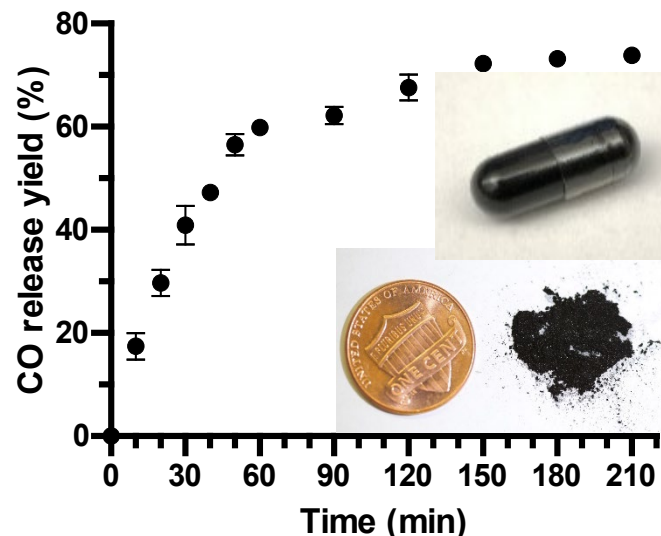
Qingguo Huang, College of Agricultural and Environmental Sciences, Department of Crop and Soil Sciences, University of Georgia. This work was partially performed at Georgia Tech's Institute for Electronics and Nanotechnology.

This work was supported by DoD SERDP ER-2717 and ER-1320 and EPA National Priorities Program Grant 840080. *Science of The Total Environment*, 788, 147723, 2(021).

National Research Priority: NAE Grand Challenge—Provide Access to Clean Water

Activated Charcoal-based Formulation for Oral Delivery Carbon Monoxide

A unique orally bioavailable formulation of carbon monoxide (CO) prodrug was developed by adsorbing oxalyl saccharin, a newly developed organic CO prodrug, in the activated charcoal (AC). The formed solid dispersion formulation addressed key developability issues of this CO prodrug. By taking advantage of the large surface area of AC, the paradox in the low water solubility of the prodrug and the requirement of hydrolysis to release CO is resolved, and the need for undesirable organic cosolvent is completely circumvented. The AC formulation also mitigates the adverse effect of low pH on the CO release yield, allowing steady CO release in simulated gastro and intestine fluid. It allows feasible encapsulation in normal and enteric-coated gel capsules, which enables controllable CO delivery to the upper or lower GI system. It also features an advantage of trapping CO prodrug and release product in the AC, therefore lowering systemic absorption of these chemicals. Through in-vivo pharmacokinetic study in mice, the AC formulation showed better CO delivery efficiency of delivering CO through oral administration compared to the prodrug dosed with organic cosolvent at the same dose. The formulation method has also been applied to address similar developability issues of a reported Diels-Alder reaction-based CO prodrug. We envision this formulation approach to facilitate the future development of CO therapeutics.



CO release yield of cellulose capsule loaded with the activated charcoal formulation of the CO prodrug (insert images) in simulated gastric fluid.

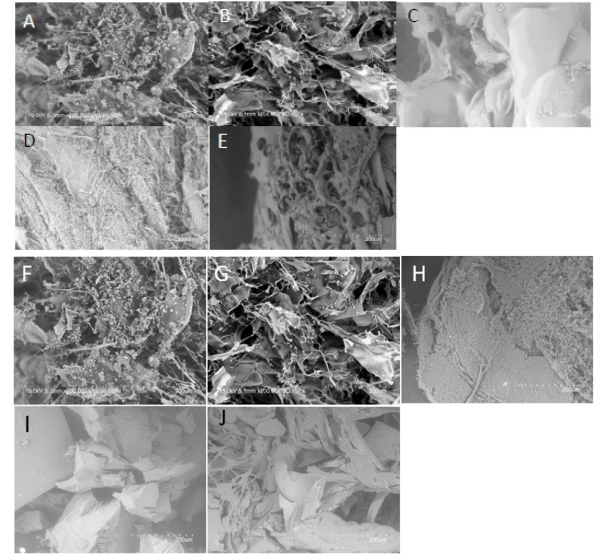
Xiaoxiao Yang, Wen Lu, Ladie Kimberly De La Cruz, and Binghe Wang, Department of Chemistry and Center for Diagnostics and Therapeutics, Georgia State University. Work was partially performed at Georgia Tech's Institute for Electronics and Nanotechnology.

This work was supported by National Institutes of Health (R01DK119202).

National Research Priority: NAE Grand Challenge—Engineer Better Medicines

Morphological evaluation of graft and crosslinked hydrogel using SEM

This work involves preparation of thermosensitive hydrogels with a variety of therapeutic nutraceuticals and characterization using SEMs. The development of biomaterials that retain structure/function properties, in addition a protective cellular approach via simultaneously controlling cell fate and ECM production is critical for advancing the new knowledge in improving tissue engineering strategies. We have used SEM at the SENIC facility for our research. The SEM images reveal that the morphology of pure PVCL hydrogel, and meHA200K have porous microstructure, and PVCL-g-meHA200K(AM), PVCL-g-meHA200K-g-ATP (AM) and PVCL-g-meHA200K-g-CURC(AM) has a denser microstructure and smaller pore size that characterize the completion of graft reaction. Sheet-like microstructure of PVCL-c-meHA200K-c-ATP (AM) and PVCL-c-meHA200K-c-CURC(AM) images reveal crosslinking results more compact and interlocking of reacting molecules.



SEM Images of lyophilized samples A. PVCL, B. meHA200K, C. PVCL-g-meHA200K(AM), D. PVCL-g-meHA200K-g-ATP(AM), E. PVCL-g-meHA200K-g-CURC(AM), F. PVCL, G. meHA200K, H. PVCL-c-meHA200K(AM), I. PVCL-c-meHA200K-c-ATP(AM), J. PVCL-c-meHA200K-c-CURC(AM) at 200-micron scale bar.

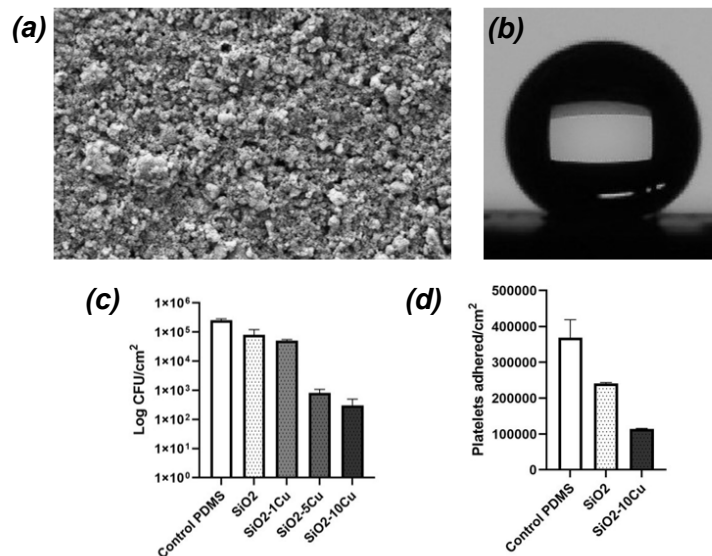
Samina Yasmeen and Juana Mendenhall, Department of Chemistry, Morehouse College. Work performed at Georgia Tech's Institute for Electronics and Nanotechnology.

This work was supported by NSF (EiR 1900806).

National Research Priority: NSF—Understanding the Rules of Life

Superhydrophobic NO-Generating Coating

This work is the result of research into multifunctional superhydrophobic coatings to prevent biofouling in blood-contacting biomedical devices. A polymeric nanocomposite utilizes hydrophobic-modified nanoparticles to provide low surface energy micro-/nano-structures that yield a superhydrophobic state, where water droplets do not adhere. The inclusion of a copper catalyst gives the coating the ability generate nitric oxide, a therapeutic gasotransmitter with antimicrobial and antithrombotic potential, from molecules naturally endogenous to blood. The resulting coating reduced bacterial and platelet adhesion.



(a) SEM image of Coating (b) Contact Angle Image of Water Droplet on Superhydrophobic Coated Surface (c) *E. coli* adhesion of Coatings with Various Concentrations of Copper Catalyst (d) Platelet adhesion study of Coatings with/without Copper Catalyst

Divine Francis and Hitesh Handa, School of Chemical, Materials and Biomedical Engineering, University of Georgia. Work performed at Georgia Tech's Institute for Electronics and Nanotechnology.

This work was supported by NIH (R01HL134899 and R01HL151473).

National Research Priority: NAE Grand Challenge—Engineer Better Medicines

Powering Internet-of-Things using the 5G Network

Researchers led by Prof. Manos Tentzeris at Georgia Tech have developed a method to use 5G networks as a “wireless power grid” for IoT devices that typically use battery power. The device is based on a flexible Rotman lens-based rectifying antenna (rectenna) for energy harvesting in the 28-GHz band.



Manos Tentzeris et al., School of Electrical and Computer Engineering, Georgia Institute of Technology. Work performed at Georgia Tech's Institute for Electronics and Nanotechnology.

This research was supported by the Air Force Research Laboratory and the NSF-Emerging Frontiers in Research and Innovation program. *Scientific Reports*, 11, 636, 2021.

National Research Priority: NSF–Growing Convergence Research

Low-cost, Fast Production of Solid-state Batteries for Electric Vehicles

Materials science researchers at Georgia Tech, led by Prof. Gleb Yushin, have developed a melt-infiltration technology to produce high-density composites for solid-state automotive lithium-ion batteries. At the lower temperatures for this procedure, fabrication is much faster and easier.

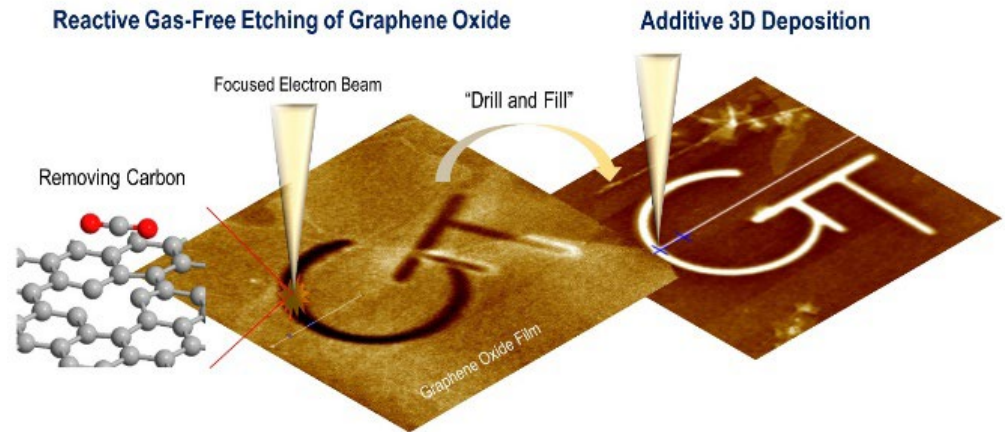


Gleb Yushin et al., School of Materials Science and Engineering, Georgia Institute of Technology. Characterization of the materials was performed at the Georgia Tech Materials Characterization Facility.

This research was supported by Sila Nanotechnologies Inc., a Georgia Tech startup company. *Nature Materials*, 2021.

E-Beam Process for Quantum Nanodevices

A team at Georgia Tech led by Andrei Fedorov has developed a technique for etching and depositing high-resolution nanoscale patterns on two-dimensional layers of graphene oxide using focused electron beam-induced (FEBID) processing. This direct-write method with atomic-scale resolution may be used to produce 2D and 3D structures for quantum communications and sensing, among other applications.



Andrei Fedorov et al., School of Mechanical Engineering, Georgia Institute of Technology. Work performed at Georgia Tech's Institute for Electronics and Nanotechnology.

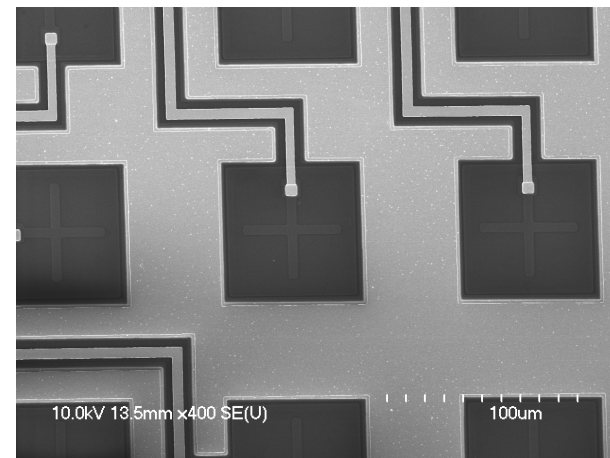
The research was supported by the DOE, Office of Science, Basic Energy Sciences and the National Research Foundation of Korea. *ACS Applied Materials & Interfaces*, 12, 39595–39601, 2020.

National Research Priority: NSF–Quantum Leap

Development of Micro UV LED Array for Compact DNA Data Storage Device

The goal of this project is to fabricate Micro LED device with UV light emission at wavelength of 365nm for medical applications, specifically for DNA synthesis. This project aims at developing a UV Micro LED, which can effectively serve as manipulation method on oligonucleotide (oligo) synthesis.

A GaN-based Micro LED array on sapphire substrate was fabricated. Ion implantation was used as device isolation and leakage suppress technique. ICP etching was used to form mesa structures. The device was passivated with Spin-on-Glass (SOG). The Micro LED array overall gains uniformity with 32 out of 36 devices achieve uniform forward IV curves in a 6-by-6 array with mesa size of $60\mu\text{m} \times 60\mu\text{m}$.



SEM image of Micro LED array devices

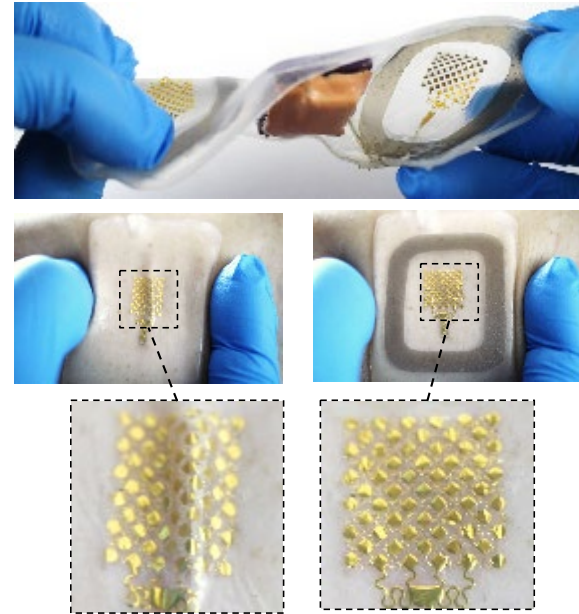
Zhiyu Xu, Minkyu Cho and Shyh-Chiang Shen, School of Electrical and Computer Engineering, Georgia Institute of Technology. Work was performed at Georgia Tech's Institute for Electronics and Nanotechnology.

This work was partially supported by a SENIC Seed Grant (NSF ECCS-2025462).

National Research Priority: NSF–Harnessing the Data Revolution

Skin-Conformal, Wireless, Wearable ECG Biopatch with Minimized Motion Artifacts

The miniaturization of electronics continues to incorporate wearable devices into our daily lives to improve health and fitness monitoring. The benefit of this progress is that a smaller device is less cumbersome, enabling freedom of movement without restriction. A simultaneous limitation is that more movement increases the opportunity for noise in the signal. Most wearable electronics measure signals through contact with the skin's surface, which stretches and flexes during movement. Here, we show a non-invasive device with measurable increased integration between the sensor and the skin. Limiting skin strain and electrode deformation is shown to reduce motion artifacts by 20% in ECG recordings during heavy jogging. Further developing wearable systems that conform to the skin will move wireless monitoring beyond the currently popular wrist-strap paradigm.



ECG device using skin friendly soft materials for long-term signal monitoring. Strain isolation layers shield electrodes from buckling and deformation that causes signal noise.

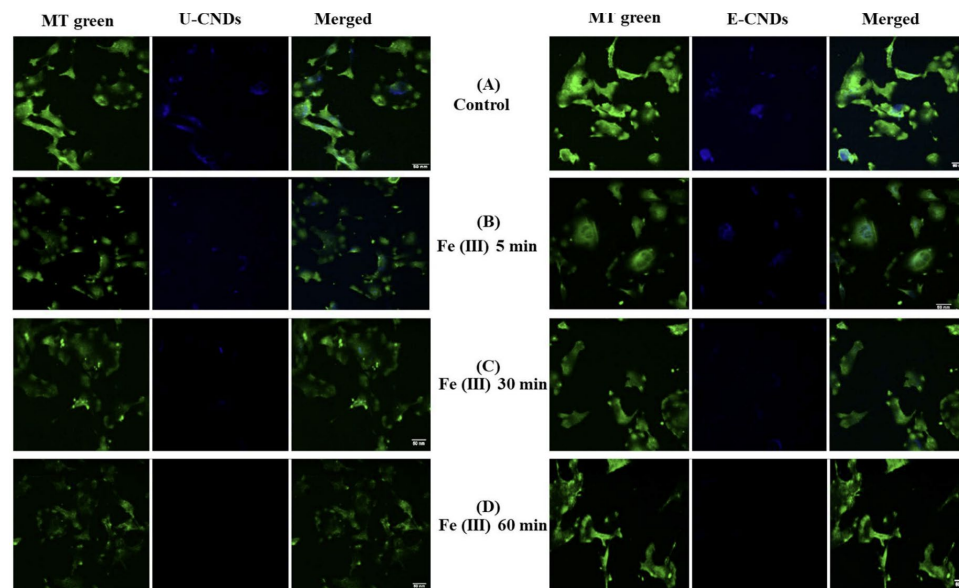
Nathan A. Rodeheaver and W. Hong Yeo, School of Mechanical Engineering, Georgia Institute of Technology
Work performed at Georgia Tech's Institute for Electronics and Nanotechnology

This work was partially supported by a SENIC Seed Grant (NSF ECCS-2025462).

National Research Priority: NAE Grand Challenge—Advance Health Informatics

High quantum yield fluorescent carbon nanodots for detection of Fe (III) ions

In this work, two types of fluorescent carbon nanodots (CNDs) are synthesized economically from ethylene diamine (E-CNDs) or urea (U-CNDs) in a single step microwave process. Both E-CNDs and U-CNDs demonstrate high selectivity towards Fe (III) ions among different metal ions, by fluorescence quenching in a dose dependent manner. The limit of detection of E-CNDs and UCNDs is observed to be 18 nM and 30 nM, respectively, in the linear response range of 0-2000 μM . Cellular internalization studies confirm the localization of the CNDs and the optical imaging sensing of Fe (III) ions inside living cells. In overall characteristics, E-CNDs provides a sensing platform for highly sensitive and selective detection of Fe (III) ions.



Fluorescence images of EA. hy926 cells incubated with E-CNDs (0.1mg mL^{-1} , right) and U-CNDs (0.3mg mL^{-1} , left) in the absence of Fe (III) ions and in the presence of $10\mu\text{M}$ of Fe (III) for different time intervals of 5 min (B), 30 min (C) and 1 hour (D)

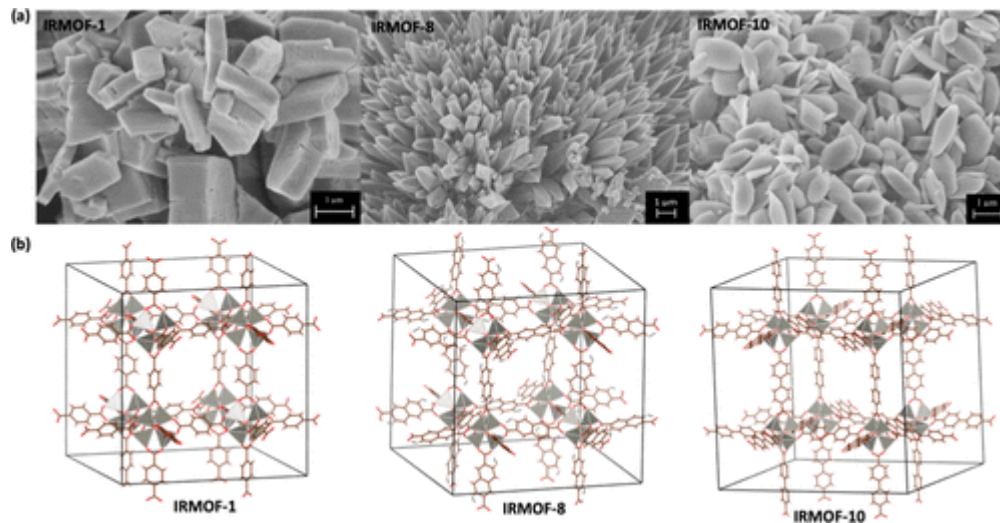
Durga Arvapalli, Jianjun Wei et al., Department of Nanoscience, University of North Carolina at Greensboro. Work was performed at the Joint School of Nanoscience and Nanoengineering (JSNN).

This work was supported by NSF Award #1832134. *Talanta*, 209, 120538, 2020.

National Research Priority: NSF–Growing Convergence Research

Semiconducting MOFs using Bloch mode analysis and spectroscopic measurements

A rapid and simple analytical approach is developed to screen the semiconducting properties of metal organic frameworks (MOFs) by modeling the band structure and predicting the density of state of isorecticular MOFs (IRMOFs). By solving Schrödinger's equation with a Kronig–Penney periodic potential and fitting the computed energy spectra to IRMOFs' experimental spectroscopic data, we model electronic band structures and obtain densities of state. The band diagram of each IRMOF reveals the nature of its electronic structures and density of state. This novel analytical approach serves as a predictive and rapid screening tool to search the MOF database to identify potential semiconducting MOFs.



(a) SEM images of microstructures of IRMOF-1, IRMOF-8, and IRMOF-10. (b) Crystal structures of the three IRMOFs. (Crystal structures were retrieved from CCDC and rendered using VESTA.)

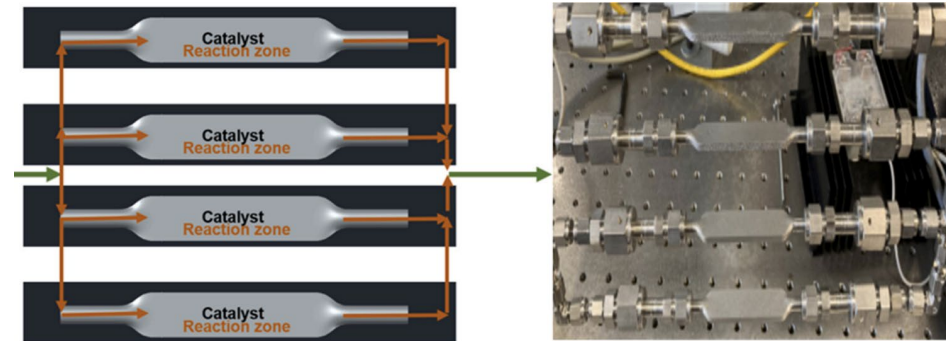
Hemali Rathnayake, Sujoy Saha, Sheeba Dawood, Shane Loeffler, Joseph Starobin, Department of Nanoscience, University of North Carolina at Greensboro. Work was performed at the Joint School of Nanoscience and Nanoengineering.

The Journal of Physical Chemistry Letters, 12(2), 884-891, 2021.

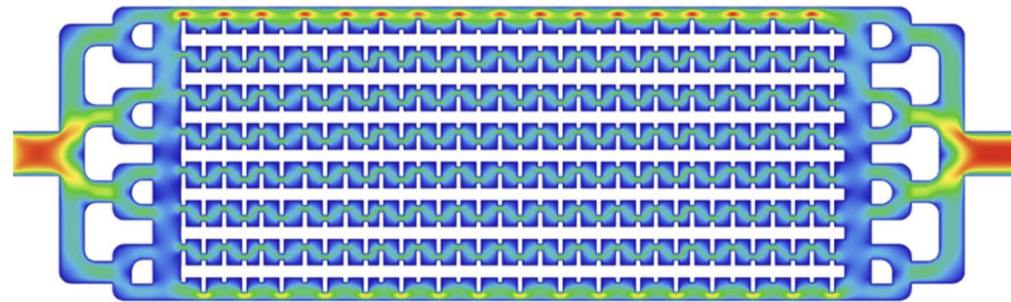
National Research Priority: NSF–Quantum Leap

Scale-up of high-pressure F-T synthesis in 3D printed microchannel microreactors

Scale-up of Fischer-Tropsch (F-T) synthesis using microreactors is very important for a paradigm shift in the production of fuels and chemicals. The scalability of microreactors for F-T Synthesis was experimentally evaluated using 3D printed stainless steel microreactors. The performance of catalysts was evaluated for three different scale-up configurations (stand-alone, two, and four microreactors assembled in parallel) at both atmospheric pressure and 20 bar at F-T operating temperature of 240 °C using a syngas molar ratio (H₂:CO) of 2. A CFD model was used to investigate the effect of different design features and numbering up approaches on the performance of the microchannel reactor.



Schematic and actual reactor assembly of scale-up experiments.



CFD results of effect of microreactor with a straight inlet, original mixing internals and channel design 3:: velocity contour

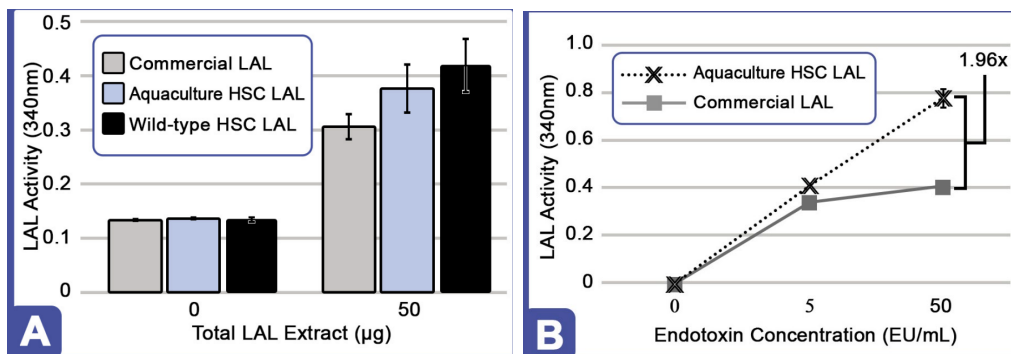
Nafeezuddin Mohammad, Debasish Kuila, Department of Chemistry, North Carolina A&T State University.
Work was performed at the Joint School of Nanoscience and Nanoengineering.

This work is supported by NSF-CREST Award #260326. *Catalyst Today*, 2021.

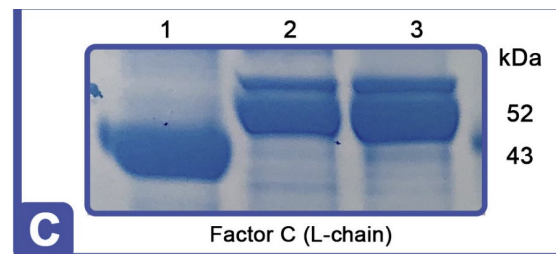
National Research Priority: NSF–Growing Convergence Research/Sustainable Nanomanufacturing

Horseshoe crab aquaculture as a sustainable endotoxin testing source

Horseshoe crab (HSC) hemolymph is the source of Limulus ameobocyte lysate (LAL), a critical component in sterility testing that ensures drug and medical device safety for millions of patients every year. We designed a controlled aquaculture habitat to husband HSCs and evaluated the effects of captivity on health markers (e.g., ameobocyte density, hemocyanin levels, and LAL activity). We found HSC aquaculture to be practicable, with routine hemolymph harvesting resulting in high LAL quality, while safeguarding animal well-being with 100% HSC survival. We report the development of a new LAL-based assay that can detect gram-negative bacteria and endotoxins in human blood without interference using aquaculture-derived LAL.



Evaluation & protein analysis of aquaculture-derived LAL at Day 88. A) Degree of gel clot formation - total protein of ameobocyte extracts. B) Degree of clot formation of aquaculture HSC and commercial LAL.



Coomassie blue staining of crude protein lysate, commercial LAL (Lane 1), aquaculture LAL (Lane 2), and wild-type LAL.

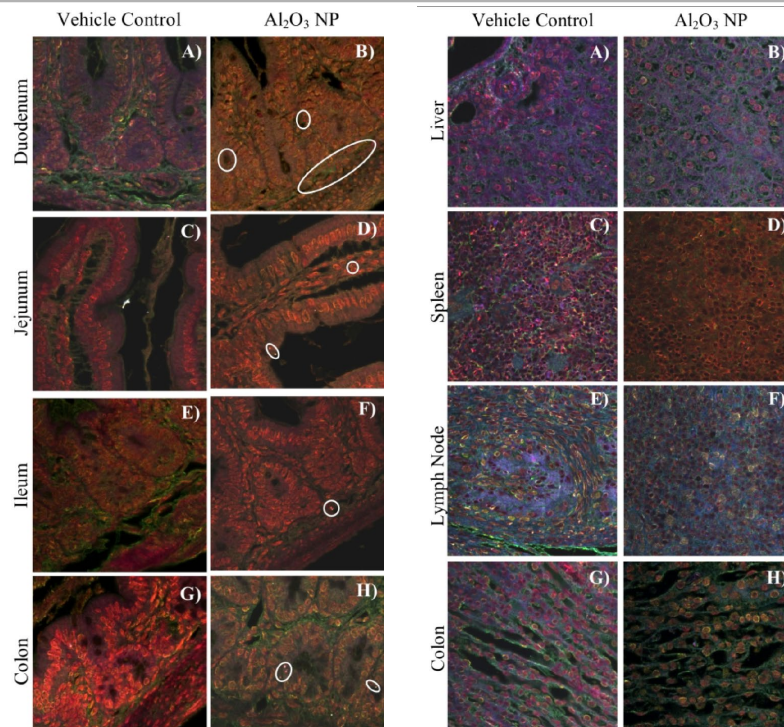
Rachel Tinker-Kulberg, Anthony Dellinger et al, Kepley Biosystems. Partial work was performed at the Joint School of Nanoscience and Nanoengineering.

This work is supported by NSF (SBIR #1819562). *Frontiers in Marine Science*, 7, 153, 2021.

National Research Priority: NSF–Growing Convergence Research/Sustainability

Response of aluminum oxide nanoparticles in juvenile rats following oral administration

Little is known about the uptake, biodistribution, and biological responses of nanoparticles (NPs) and their toxicity in developing animals. Here, male and female juvenile Sprague–Dawley rats received four consecutive daily doses of 10 mg/kg Al₂O₃ NP or vehicle control (water) by gavage between postnatal days (PNDs) 17–20. The biodistribution of Al₂O₃ NP in tissue sections of the intestine, liver, spleen, kidney, and lymph nodes were evaluated using enhanced dark-field microscopy (EDM) and hyperspectral imaging (HSI). EDM/HSI indicates intestinal uptake of Al₂O₃ NP. Al₂O₃ NP altered neurotransmitter/metabolite concentrations in juvenile rats' brain. These data suggest that orally administered Al₂O₃ NP interferes with the brain biochemistry in both female and male pups.



Hyperspectral images of H&E stained vehicle control and Al₂O₃ NP dosed (left) A-B) duodenum, C-D) jejunum, E-F) ileum, and G-H) colon. (right) A-B) liver, C-D) spleen, E-F) lymph node, and G-H) kidney

Mortensen, Fennell et al., RTI International, Research Triangle Park, NC. Partial work was performed at the Joint School of Nanoscience and Nanoengineering.

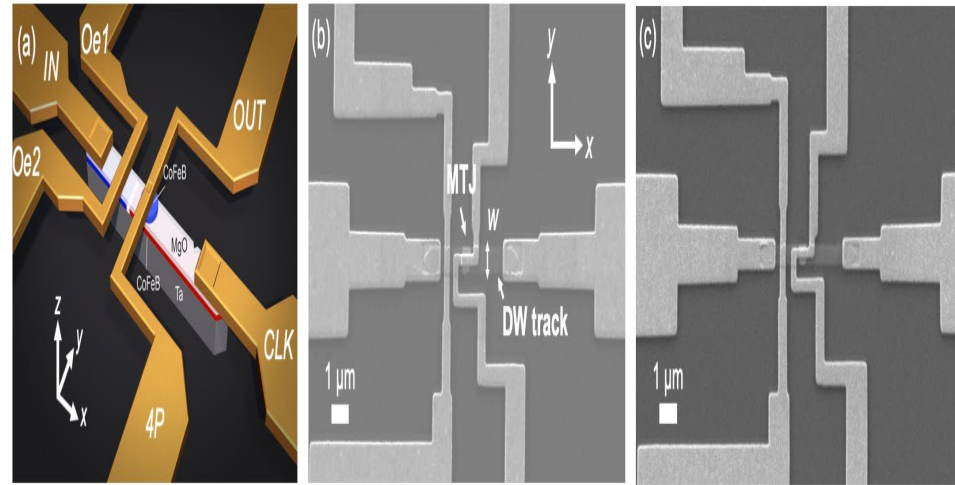
This work was supported by NIH (U01ES027254) and NSF (CBET 1604647). *J. Appl. Toxicol.* 41, 1316, 2021.

National Research Priority: NAE Grand Challenge—Engineer Better Medicines

Texas Nanofabrication Facility (TNF)

Spintronics Based on Domain Wall Logic

There are pressing problems with traditional computing, especially for accomplishing data-intensive and real-time tasks, that motivate the development of in-memory computing devices to both store information and perform computation. Magnetic tunnel junction memory elements can be used for computation by manipulating a domain wall, a transition region between magnetic domains, but the experimental study of such devices has been limited by high current densities and low tunnel magnetoresistance. Here, we study prototypes of three-terminal domain wall-magnetic tunnel junction in-memory computing devices that can address data processing bottlenecks and resolve these challenges by using perpendicular magnetic anisotropy, spin-orbit torque switching, and an optimized lithography process.



Domain wall-magnetic tunnel junction spin orbit torque device and circuit prototypes for in-memory computing

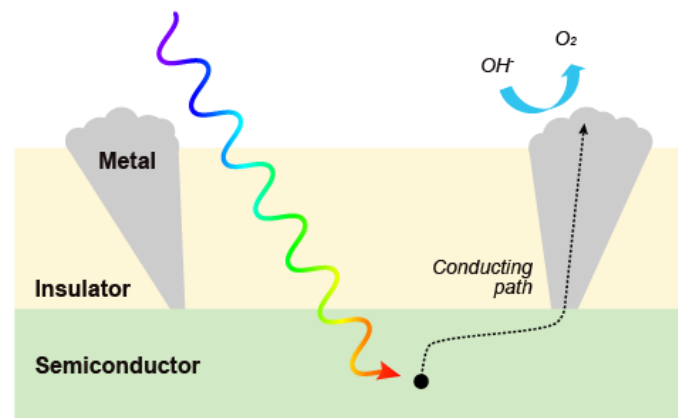
M. Alamdar, T. Leonard, C. Cui, B. P. Rimal, L. Xue, O. G. Akinola, P. Xiao, J. S. Friedman (UTD), C. H. Bennett, M. J. Marinella (Sandia), and J. A. C. Incorvia, Electrical and Computer Engineering, University of Texas at Austin. Work performed at Texas Nanofabrication Facility.

This work was supported by DOE NNSA (DE-NA0003525). *Applied Physics Letters* 118, 112401 (2021).

National Research Priority: NSF–Quantum Leap

Fabrication of Stable, High-performance MIS Photoanodes for Solar Powered Water Oxidation

Stable, efficient photoelectrodes are a key component in solar powered electrolysis for green hydrogen production. To achieve high performance combined with stability, a metal-insulator-semiconductor (MIS) structure is often employed to protect the semiconductor absorber from corrosion in aqueous solution. However, the need for efficient transport of photogenerated carriers across the insulator, which usually requires very thin insulator layers, is often in conflict with the requirements for stability, which mandates use of thicker insulators. The resulting devices exhibit excellent onset potential, photocurrent density, and stability, and these results suggest outstanding potential for realization of cost-effective, high-performance photoelectrodes for green hydrogen production using renewable energy sources.



This photoelectrode enables efficient transport of photogenerated carriers from the semiconductor to the metal catalyst via a direct, localized physical connection while simultaneously enabling the use of thick, highly stable protective insulating layers.

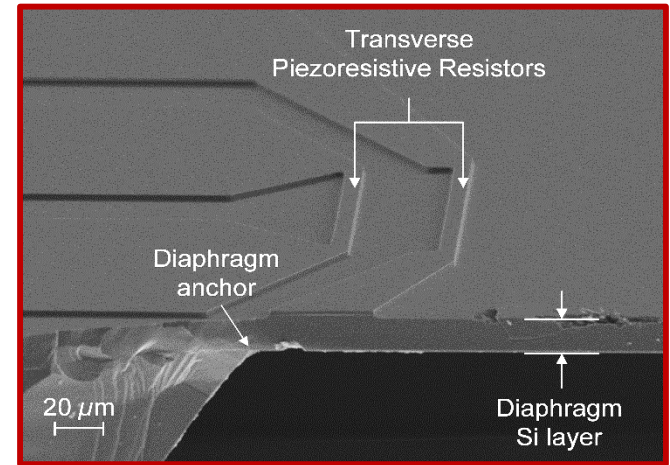
Sonil Li, Li Ji, Alex DePalma, Ed Yu, Electrical and Computer Engineering, University of Texas at Austin. Work performed at Texas Nanofabrication Facility.

This work was supported by NSF (DMR 1720595). *Nature Nanotechnology*, 12(1), (2021).

National Research Priority: DOE-Microelectronics

Infrasound Microphones Using Microfabricated Piezoresistive Silicon

Sources of infrasound include volcanos, earthquakes, meteorites, and large man-made explosions. Infrasound from such events can be detected on the opposite side of the globe, as these low frequency waves are only mildly attenuated. Infrasound monitoring is one of three critical technologies used to monitor for nuclear testing activity. Infrasound sensors were fabricated using special double layer SOI wafers (two epitaxial layers separated by two layers of SiO₂). Piezoresistors were etched into the top-most epitaxial layer, and a KOH etch through the backside releases the mechanical diaphragm. The devices were packaged and are presently under evaluation at a rigorous testing facility on Kirtland Airforce Base in Albuquerque, NM.



SEM micrograph of piezoresistive infrasound microphone.

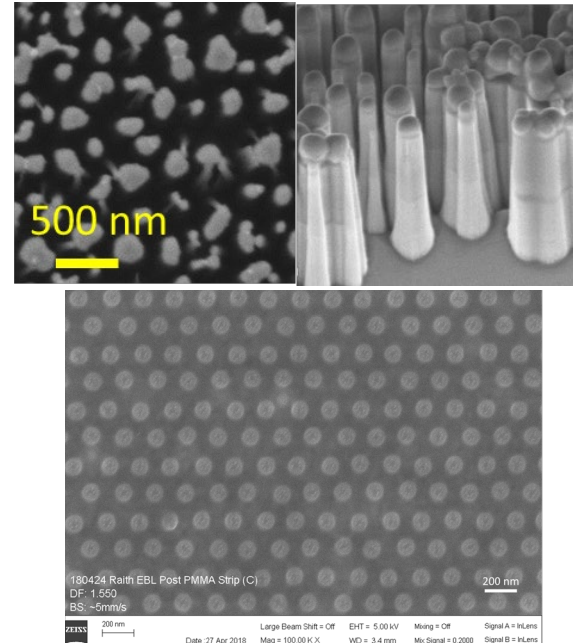
Neal Hall, Silicon Audio. Work performed at Texas Nanofabrication Facility.

This work was supported by DOE, National Nuclear Security Administration.

National Research Priority: DOE-Nuclear Security

Optical Metasurfaces

Optical metasurfaces are being made using Graphene-Based optical devices, flat lens and phase plate design, plasmonic resonators, and Anti-Reflective Surface Structures (Motheye). These are fabricated using electron beam lithography, nanoimprint lithography, and deep silicon reactive ion etching.



SEM micrograph of anti reflective surface structures, and graphene metasurface

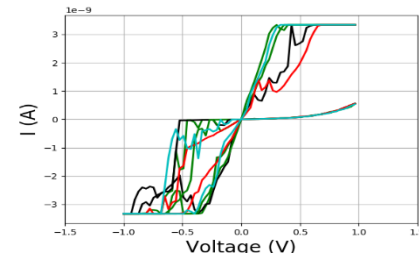
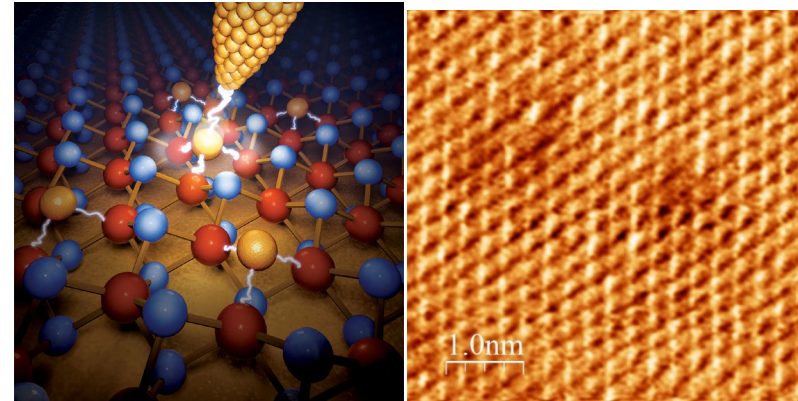
Steve Savoy, Nanohmics. Work performed at Texas Nanofabrication Facility.

This work was supported by NSF SBIR and STTR grants.

National Research Priority: NSF–Quantum Leap

Memristor Effect in Single-Defect MoS₂

Here we elucidate the origin of the switching mechanism in atomic sheets using monolayer MoS₂ as a model system. Atomistic imaging and spectroscopy reveal that metal substitution into a sulfur vacancy results in a non-volatile change in the resistance, which is corroborated by computational studies of defect structures and electronic states. These findings provide an atomistic understanding of non-volatile switching and open a new direction in precision defect engineering, down to a single defect, towards achieving the smallest memristor for applications in ultra-dense memory, neuromorphic computing and radio-frequency communication systems.



AFM micrograph of MoS₂ single layer defect used for memristive function.

SM Hus, R Ge, PA Chen, L Liang, GE Donnelly, W Ko, F Huang, Dej Akinwande, Electrical and Computer Engineering, University of Texas at Austin. Work performed at Texas Nanofabrication Facility.

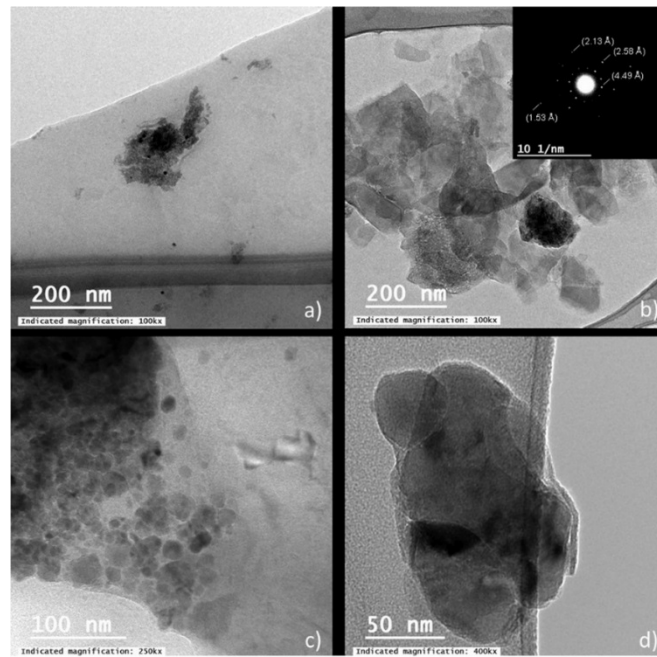
This work was supported by NSF Award # ECCS-1809017. *Nature Nanotechnology*, 16(1), 58-62 (2020).

National Research Priority: NSF–Quantum Leap

***Virginia Tech National Center for Earth and
Environmental Nanotechnology
Infrastructure (NanoEarth)***

Riparian soil carbon release promoted by nanocolloids & higher temperatures

Increasing temperatures in alpine regions accompanied by glacial retreat is occurring rapidly due to climate change. This may affect riparian soils by increasing weathering rates, resulting in greater organic carbon (OC) release to rivers via movement of iron-containing colloids and nanominerals. Increased concentrations of iron- or silicate-nanominerals would result in higher surface area for OC adsorption. To test the influence of temperature on OC leaching, mineral weathering and nanocolloid facilitated release of OC were examined through a series of controlled laboratory batch and column experiments using sediment from the banks of the Nisqually River, Mount Rainier in Washington State (USA). Results show that OC leaching rates for 20°C were two to three times greater than for 4°C. Further, the results suggest that nanocolloids are responsible for moving this increased OC load from these sediments. When hydrologically connected, OC is released from bank sediments to rivers faster than presently anticipated in fluvial environments experiencing climate change-induced glacial retreat. Further, a one-dimensional, finite-element computational model developed for this study estimates that a 1°C increase in temperature over a 90-d summer runoff period increases the OC release rate from sediments by 79%.



TEM images of nanomaterial for Day 8 from effluent out of columns: (a) illite + glass beads; (b) illite-S4; (c) S20; (d) illite-S20. (a), (b), and (c) are clusters of minerals, and (d) are individual plate-like minerals.

Rod, K. A., Smith, A. P., Leng, W., Colby, S., Kukkadapu, R. K., Bowden, M., Qafoku, O., Um, W., Hochella, M. F., Jr., Bailey, V. L., and Renslow, R. S. Work performed at NanoEarth.

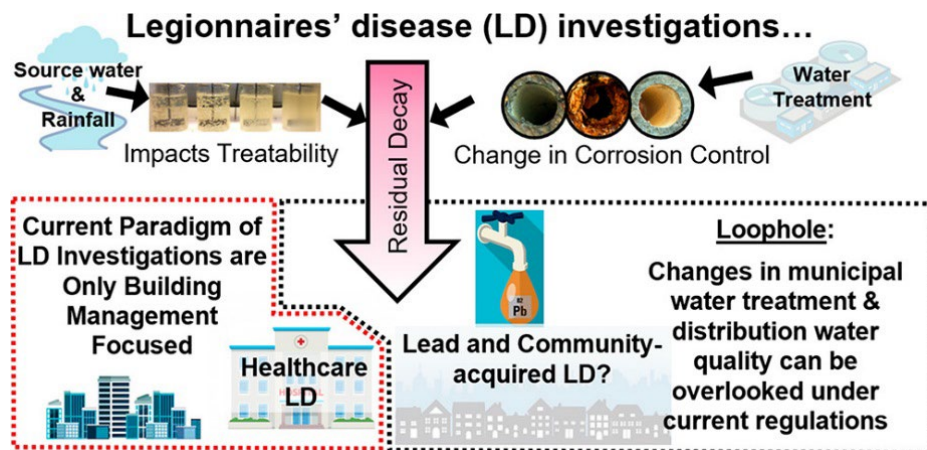
This work was supported by DE-AC05-76RLO 1830 and NSF ECCS 1542100. *Vadose Zone Journal*, 19(1), e20077.

National Research Priority: NSF–Understanding the Rules of Life

Legionella Contamination and the Municipal Water System

Fifty-eight people were sickened and 12 died from a Legionnaires' disease (LD) outbreak in Quincy, IL, in 2015. The outbreak was widely publicized and politicized and the official outbreak investigation identified deficiencies at the Illinois Veteran's Home (IVHQ) as the precipitating cause of the outbreak. However, we discovered in our analysis that the conclusions of the investigation did not account for four community-acquired cases that occurred concurrently with no IVHQ exposure. Notably, 3–6 months prior to the outbreak, we found that the primary disinfectant was changed and corrosion control was interrupted, causing a sustained decrease in disinfectant residuals throughout Quincy's distribution system. These municipal system deficiencies were not identified in prior investigations of the outbreak, but their impacts on public health outcomes are consistent with those of the 2014–2016 Flint

Water Crisis. However, they occurred in Quincy without any legal violations in the municipal water system or public acknowledgment of community-wide health risks. This study supports the critical need for improved data collection during changes in municipal water treatment. Additional regulatory and communication requirements can better protect public health from both LD and lead.



The current paradigm of Legionnaires' disease investigations allows changes in municipal water treatment and distribution water quality to be overlooked under current regulations.

Rhoads, W.J., Keane, T., Spencer, M.S., Pruden, A., & Edwards, M.E. Work performed at NanoEarth

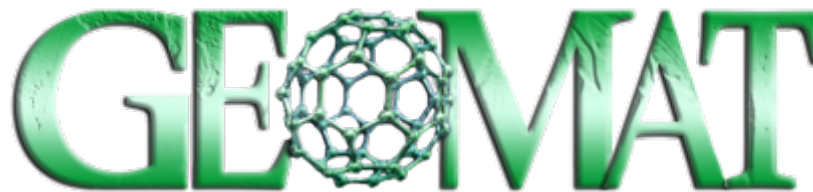
This work was supported by the State of Illinois; NSF CBET (1336650, 1556258, and 1706733); the Alfred P. Sloan Foundation Microbiology of the Built Environment Program; and the Science and Engineering of the Exosome (SEE) Center supported by the Institute for Critical Technology and Applied Science at Virginia Tech. *Environmental Science & Technology Letters*
<https://doi.org/10.1021/acs.estlett.0c00637>

National Research Priorities: NAE Grand Challenge—Providing Access to Clean Water

Developing a nano-enabled solution for separating oil and water

GeoMat is commercializing a multifunctional nanoparticle platform that has broad utility separating oil from water. The particles were developed by professor Lead at the University of South Carolina Center for Environmental Nanoscience & Risk. Professor Lead and his research team have published extensively on the technology (e.g., see Palchoudhury and Lead, 2014) and have been awarded various university-owned patents.

NanoEarth has been proud to leverage our unique “nanotechnology innovation ecosystem” to support the efforts of professor Lead and GeoMat as a partner on the team’s NSF I-Corps program and, most recently, their very first NSF SBIR award (\$256k)!



GeoMat LLC – a spin-out from the University of South Carolina’s Center for Environmental Nanoscience and Risk (CENR) (Jamie Lead, PI). Work performed at NanoEarth.

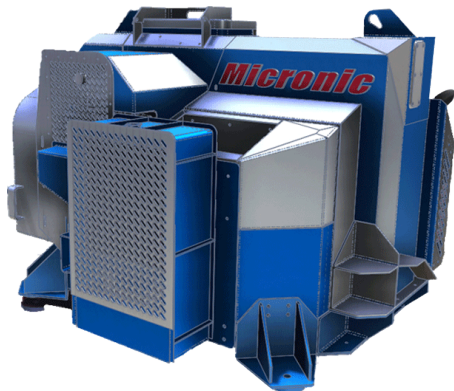
This work was supported by NSF SBIR IIP 2036258 and NSF ECCS 1542100.

National Research Priorities: NAE Grand Challenge—Providing Access to Clean Water

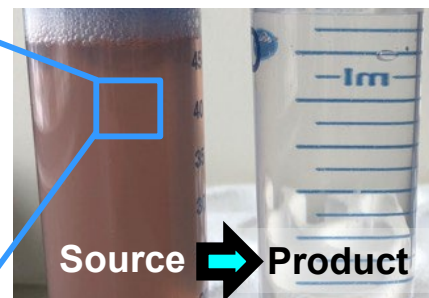
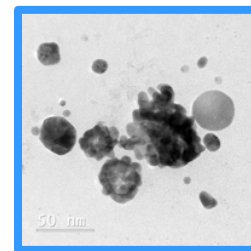
Developing a water purification solution that cleans water from virtually any source

The Center for Innovative Technology (CIT) and The Pearl Fund announced that CIT GAP Funds and The Pearl Fund L.P. led a **\$3 million** seed round investment in Micronic Technologies, Inc, with participation from CAV Angels. Located in a Southwest Virginia Opportunity Zone, Micronic Technologies is a developer of a breakthrough Zero Liquid Discharge (ZLD) water purification technology that reduces wastewater volume by 95% and removes over 99% of contaminants in a sustainable and cost-effective way that hasn't been achievable until now.

NanoEarth demonstrated the effectiveness of MicroEvap™ purification technology which resulted in an invention disclosure, multiple proposals including SBIR, and support in securing private investment.



**MicroEvap™
Technology**



Micronic Technologies – Southwest Virginia-based and woman-led, early stage clean technology company (Karen Sorber, CEO). Work was performed at NanoEarth.

This work was supported by NSF ECCS 1542100.

National Research Priorities: NAE Grand Challenge—Providing Access to Clean Water

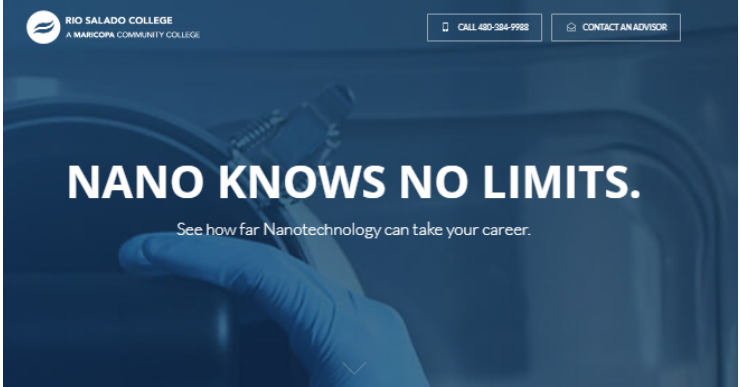
Education and Outreach

Supporting Micro and Nano Technicians through Hybrid Teaching Methods

Dr. Rick Vaughn, the STEM Program Chair at Rio Salado College (RSC) has been awarded a “New to ATE” proposal to the NSF Advanced Technological Education (ATE) program. The new award began in July 2021 and will enable RSC to (1) offer a six-course certificate, and an associate degree in Nanotechnology, (2) provide an accessible and affordable academic program for students to gain employable skills, (3) actively recruit students from under-represented and underserved groups, and (4) establish partnerships with industry and other partners to prepare students to fabricate and characterize materials for biological, textile, chemical, light, and electrical applications, all at the micro and nanometer scale. The advanced laboratory classes for RSC students are hosted by ASU core facilities under the NCI-SW umbrella.

Rok Vaugh, STEM Program Chair, Rio Salado College

<https://www.riosalado.edu/web/online/campaigns/nanotech/>



What is Nanotechnology?

Think small. Extremely small. Nanotechnology is where science, engineering and technology meet—at the nanoscale. With this study, nano technicians are able to manipulate individual atoms and molecules to change the properties of tools and products. And this science can be used in industries such as manufacturing, engineering, biology, chemistry, and more.

Learn Nano, Save Big

Apply for a [spring term scholarship](#) and up to **HALF** of your education could be on us.
Contact Rick Vaughn to learn more.



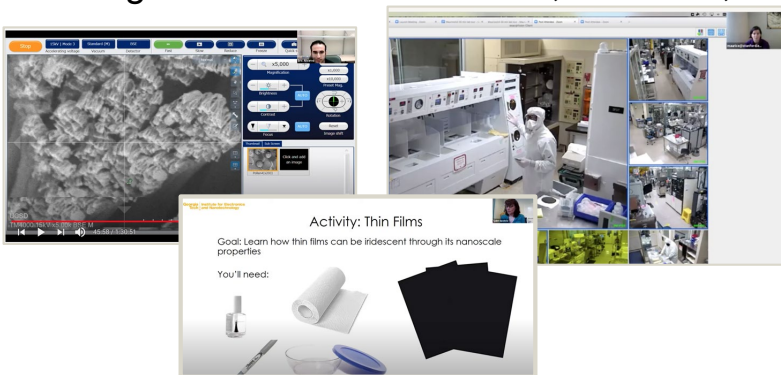
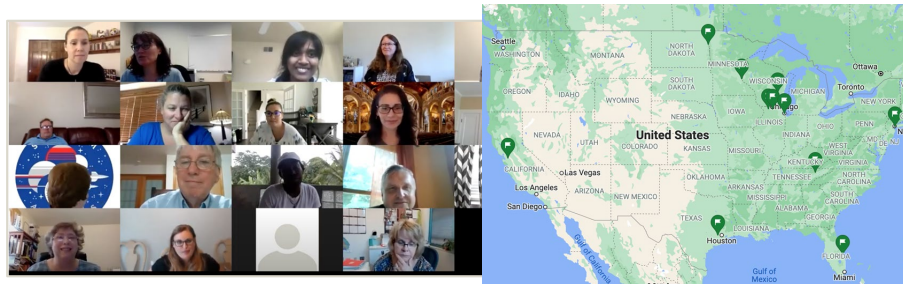
Rick Vaughn
Faculty Chair, STEM Initiatives
Rio Salado College
✉ rickvaughn@riosalado.edu
☎ (480) 817-8661

Rio Salado College began marketing the new AAS degree program to recruit students for Fall 2021

National Research Priority: NSF–NSF INCLUDES

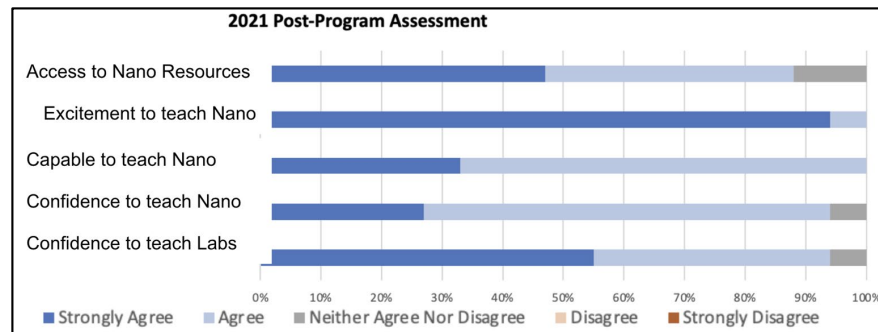
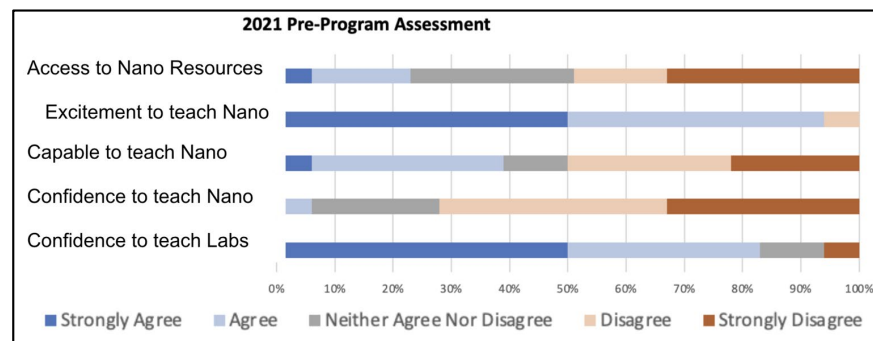
Nanoscience Summer Institute for Middle School Teachers was held virtually with SENIC

- Data shows learning is not impacted by virtual environment and utilizing hands-on kits and remote technology (external evaluator)
- Leveraged technology at multiple sites for virtual interactive tours
- 100% surveyed would recommend this to a colleague
- Utilizing NNCI resources - JSNN, Nanooze, SDNI



“This was by far the most informative and enjoyable summer course I have taken. I really feel this will make a difference in how my students look at the world.” - Daniel Giner- 8th grade science Katy TX

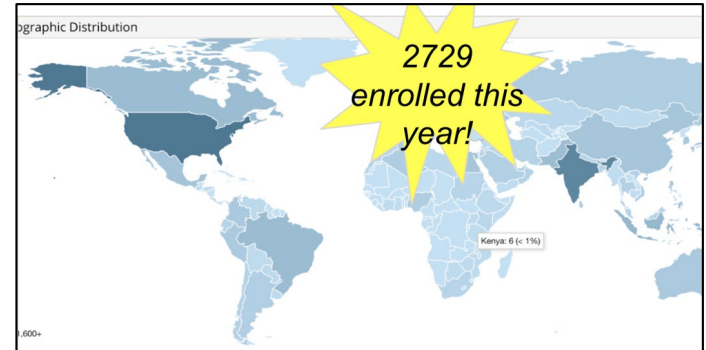
This work was supported by NSF Award # ECCS-2026822.



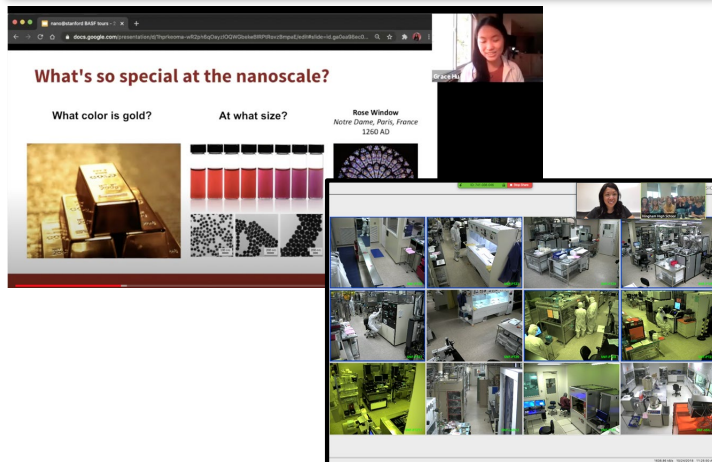
National Research Priority: White House FY2022, Administration R&D Budget
 Priorities-Build the S&T Workforce of the Future

K-12 Outreach and Technical Education

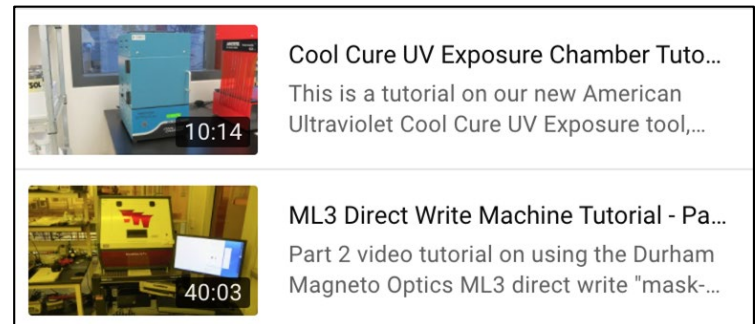
- 1962 students/ adults reached using remote tours, activities, & guest lectures
- Benefits: record programs to share out on YouTube channel (+555 subscribers with 60 K views), reach many students at once, low barrier to entry, currently improving accessibility



Virtual Classroom Visits, Tours, & Festivals



- Growing edX enrollment (5481 total from 119 countries) / certificate option being added
- Expand video development & increased view counts



This work was supported by NSF Award # ECCS-2026822.

National Research Priority: White House FY2022, Administration R&D Budget
Priorities-Build the S&T Workforce of the Future

Community College Internship Program

- Motivation - mutually beneficial for students' hands on experience and providing facility support, began 2019
- Past Work- supported 4 students from Foothill College, Cañada College*, College of San Mateo*
- Track career of interns - all went to 4-year colleges!
- Current Work - 4 interns hired from over 30 applications from Mission College* and West Valley College



This work was supported by NSF Award # ECCS-2026822.



PAID INTERNSHIPS

AT STANFORD NANOFACILITIES

Learn how things are made and seen at the micro- and nanoscale! The nanofacilities are used for cutting edge research, in areas including electronics, MEMS, optics, physics, biology/biotechnology, medicine, materials science, and chemistry.

Students will work in a cleanroom to collect and report data, and work with staff to troubleshoot any issues that arise. Duties may also include inventory support, chemical safety, technical support, or characterization of micro- and nano-fabrication equipment.

No prior background or experience is required. All training will be provided.

Job Details:

- Commitment of at least 8 hours per week (hours are flexible)
- Work least two quarters (Fall and Spring)
- Salary ~ \$18 per hour
- Potential to earn college credit
- Preferred - completion of intro chemistry/ physics

Apply NOW!
<https://bit.ly/nano-internship>

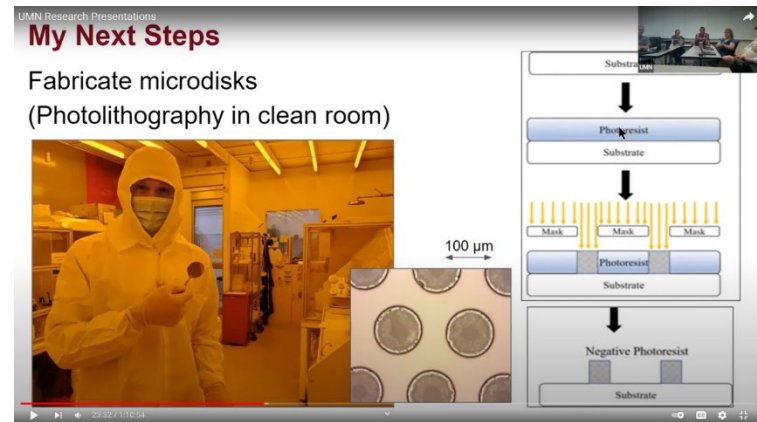
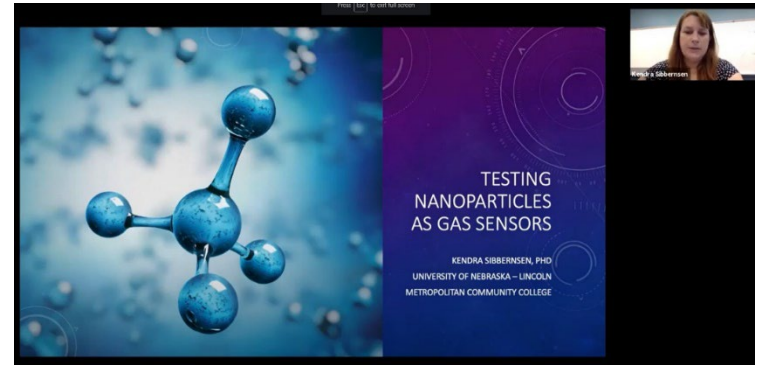
Visit <http://nanolabs.stanford.edu> to learn more
For inquiries, email dmduran@stanford.edu



National Research Priority: White House FY2022, Administration R&D Budget
Priorities-Build the S&T Workforce of the Future

Research Experiences for Teachers Across the NNCI

Awarded in spring 2020, the NSF-supported RET hosted the first cohort of educators in summer 2021. SENIC (lead), MINIC, NNF, and SHyNE welcomed 5 high school teachers or technical/community college faculty on their campuses for 6 weeks of hands-on research. As a networked program, everyone met virtual 1-2 times a week to share their research and receive feedback on their proposed original lessons. In addition to research, teachers participated in a nano-careers webinar series featuring industry speakers who are also users of site facilities. The educators will present on their experience and lessons at the 2022 annual National Science Teachers Association Meeting. Their lessons will also be posted on the NNCI's searchable database and nanoHUB, and the teachers are recording short videos intended to help their peers implement their lessons.

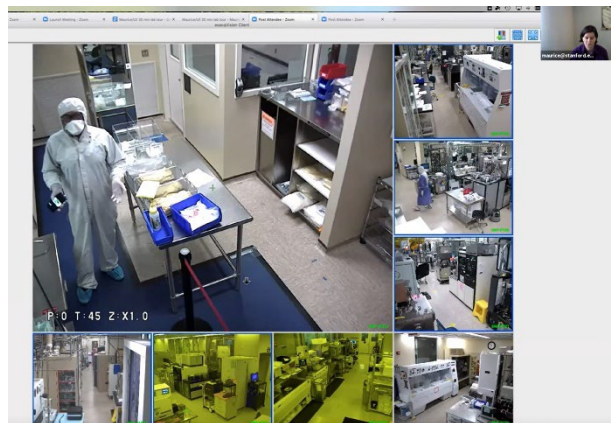


This work was supported by NSF RET (#1953418 at SENIC)

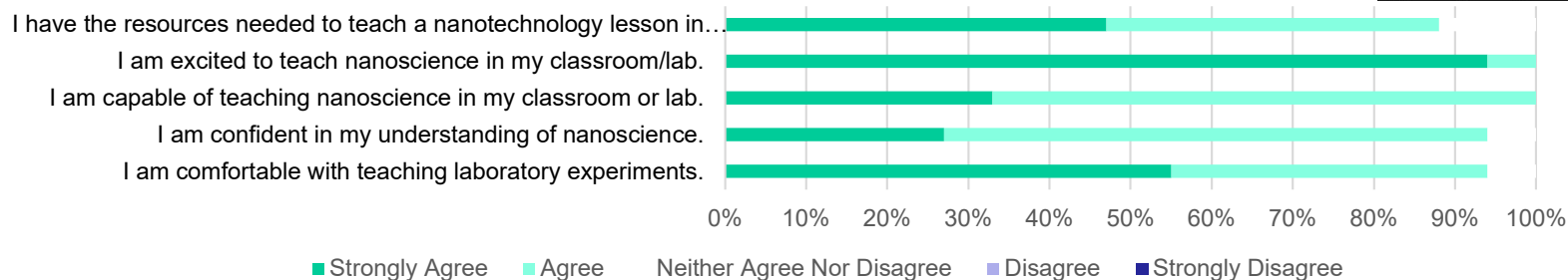
National Research Priority: NSF-INCLUDES

Nano Summer Institute for Middle School Teachers (NanoSIMST)

SENIC hosted a week-long virtual NanoSIMST in June 2021. Due to personnel changes at nano@Stanford, SENIC included their 15 teachers in the program. The 30 teachers (15 from NC, 15 from Stanford) learned about nanotechnology and careers, worked through hands-on demos, heard from experts, went on virtual lab tours, and developed their own ideas for implementing nanotechnology in their classrooms.



2021 Post-Program Assessment



This work was supported by the SENIC NNCI funding (NSF ECCS-2025462).

National Research Priority: NSF-INCLUDES

NanoEarth 2021 Virtual NTEC (NanoTechnology Entrepreneurship Challenge)

“Recognizing aspiring scientific entrepreneurs who wish to develop nanotechnology-based products for social good”

7 Week Plan – NSF I-Corps-like Experience

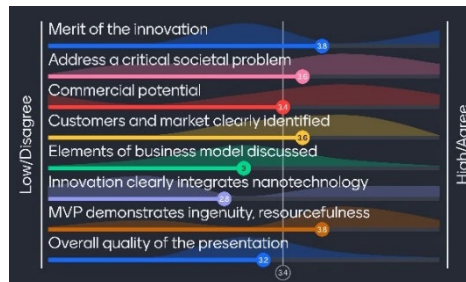
Week	MVP	Business Model Generation
1		Write your business thesis
2		Customer segments and value propositions
3		Channels and customer relationships
4		Revenue streams
5		Key resources, activities, and partnerships
6		Cost structure
7		*NTEC Launch Lunch

\$7,500 in awards made to 9 teams – 15 students & 11 faculty at 3 institutions

2021 Project Titles:

- Bee MycHotels (CCC)
- BIO-FET (VT)
- NanoSeed (VT)
- Passive urban air filter system (VT)
- Water vapor-based AC generator (VT)
- Carbon nanotube based solar cell (VT)
- Ultra-tall synthetic tree passive hydropower (VT)
- Hydrothermal liquefaction with nanoscale catalysts (NCAT)
- Nano coal fly ash: From waste to resource (NCAT)

Panel Scoring for Bee MycHotels



Entrepreneur Highlight: **Katy Ayers** Central Community College, Nebraska

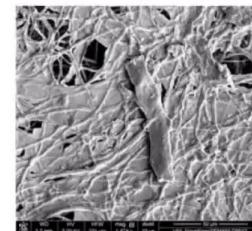
Bee MycHotels utilize a native fungal bio-composite material to grow nesting habitat for solitary bees and wasps. The native fungus was grown into untreated wood dust inside of specially designed molds.



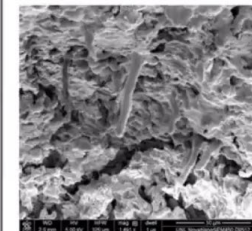
Industrial agriculture uses large polystyrene blocks for nesting habitat, but polystyrene is neither recyclable nor biodegradable. MycHotels provide farmers a natural bio-material to improve soil food webs in croplands while providing pollinator nesting cavities needed for production of crops



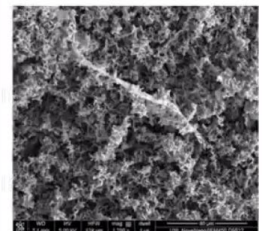
The NTEC project focus was to scrutinize the degradation process of Bee MycHotels as they are mounted outdoors. This work was completed in collaboration between NanoEarth and the Nebraska Nanoscale Facility (Terese Janovec & Steve Wignall).



Fresh Sample



2 years old – wetter conditions



2 years old – dryer conditions

National Research Priority: White House FY2022, Administration R&D Budget

Priorities-Build the S&T Workforce of the Future